Università degli Studi di Urbino Carlo Bo

Dipartimento di Scienze Biomolecolari (DISB)

Ph.D. PROGRAMME IN: Biomolecular and Health Sciences

CYCLE: XXXV

"Development of human monoclonal antibodies for the treatment of solid tumors resistant to the current pharmacological treatments and overexpressing the Carcinoembryonic Antigen-related Cell Adhesion Molecule 1 (CEACAM1)"

Thesis written with the financial contribution of Regione Marche (Progetto di Dottorato Innovativo a caratterizzazione Industriale)

ACADEMIC DISCIPLINE: BIO/10

Coordinator: Prof. Marco Bruno Luigi Rocchi

Supervisor: Prof. Mauro Magnani

Co-Supervisor: Prof. Paolo Mariani

External Co-Supervisor: Prof. John E. Shively

Co-Supervisor: Dr. Valentina Fiori

Ph.D. student: Michela Centonze

ACADEMIC YEAR

2021/2022

INDEX

ABSTRACT

Background: The role of Carcinoembryonic Antigen-related Cell Adhesion Molecule 1 (CEACAM1) as a recently characterized immune-checkpoint inhibitor as well as marker for tumor progression and metastasis development of several solid tumors, makes it an attractive target for Cancer Immunotherapy. Herein, we describe the development and characterization of DIA 12.3, a new fully human IgG1 antibody against CEACAM1, which derives from the previously developed anti-CEACAM1 single chain variable fragment (scFv) antibody, termed DIATHIS1. **Methods:** Bicistronic vectors were designed for IgG1 and IgG4 antibody expression and stable cell lines were developed for their production. *In vitro* assays were performed to evaluate the physico-chemical properties of the antibodies and their biological activity. In addition, the mutated mtN297A IgG1 was developed in order to reduce the effector functions of the antibody Fc region and, thus, to prevent excessive cytotoxicity. After antibody DOTAylation and radiolabeling with ^{64}Cu, PET experiments with NOD-SCID gamma (NSG) mice and hCEACAM1 or hCEA double transgenic mice were performed to evaluate the *in vivo* tumor targeting and biodistribution of ^{64}Cu-DOTAylated-DIA 12.3 antibody. **Results:** The current project was focused on the IgG1 antibody, since it showed better structural and functional performances compared to IgG4. More in detail, we found that DIA 12.3 antibody purified by Protein A Affinity Chromatography has a high-purity grade monomeric formulation, with structural as well as biological stability eight months after the purification and of storage at 4°C. ELISA assays revealed that DIA 12.3 is able to bind hCEACAM1 antigen with a linear activity and high affinity. Flow cytometry analyses demonstrated high antibody immunoreactivity with hCEACAM1 expressed on the cell surface membrane of human metastatic melanoma, bladder and colon cancer cell lines. Furthermore, cytotoxic assays displayed the capability of DIA 12.3 to enhance the Natural Killer (NK)-92 cell-mediated cytotoxicity against metastatic melanoma, bladder, colon and head&neck cancer cells. ELISA and flow cytometry assays showed that the N297A mutation does not affect the antibody binding ability, but it results in reduced stimulation of NK cell-mediated tumor killing, as expected. DIA 12.3 and mtN297A DIA 12.3 antibodies also show strong binding activity to CEACAM1 antigen on neutrophil cell surface, without inducing toxicity or triggering unnecessary activation of neutrophils. Biodistribution analyses revealed the specific localization of the radiolabeled DIA 12.3 antibody to hCEACAM1-positive xenograft in NSG mice. **Conclusion:** These findings highlight the potential of DIA 12.3 antibody as a candidate in Immunotherapy treatments of CEACAM1-expressing solid tumors and indicate the need for further *in vitro* and *in vivo* evaluation of DIA 12.3 pharmacokinetic and pharmacodynamic profile.

1. INTRODUCTION

1.1 The Human Carcinoembryonic Antigen (CEA) family

The Carcinoembryonic Antigen (CEA) family belongs to the glycosylated immunoglobulin superfamily (IgSF) (1). The human CEA family is encoded by 18 genes and 11 pseudogenes located on chromosome 19q13.2. These proteins are subdivided into the CEA-related cell-adhesion molecules (CEACAMs; Fig. 1.1) and the pregnancy-specific glycoproteins (PSGs) on the basis of protein homologies and developmental expression patterns. The structure of CEACAMs consists of one N-terminal immunoglobulin variable (IgV)-like domain, followed by a variable number of Ig constant (IgC)-like domains. While PSGs are secreted proteins, CEA family members can be secreted, glycosylphosphatidylinositol (GPI)-anchored or transmembrane proteins with a short or long cytoplasmic tail which can contain immunoreceptor tyrosine-based inhibition motifs (ITIMs), immunoreceptor tyrosine-based switch motifs (ITSMs) or immunoreceptor tyrosine-based inhibition motifs (ITAMs) (2). Figure 1.1 summarizes the structural organization of human CEACAMs, the number of known splice isoforms and the distribution of their orthologs in mammalian species (Fig.1.1, 3).

CEA family members have a wide tissue distribution. They are expressed in columnar epithelial cells of the colon, in mucous neck cells and mucous cells of the stomach, in squamous epithelial cells of the tongue, esophagus and cervix, in secretory epithelia of sweat glands and in prostatic epithelial cells (4). In addition to the expression in epithelia, CEACAM1 can be found also on granulocytes, lymphocytes and endothelial cells. CEACAM6 is expressed on granulocytes and monocytes, while CEACAM3 and CEACAM8 are found exclusively on granulocytes (4).

Different CEA family members play diverse functions according to the various signaling motifs within their cytoplasmic domains and the modes of membrane anchorage. In general, CEACAMs mediate cell–cell adhesion and they are critical modulators of several cellular processes in physiological as well as pathological contexts, ranging from the shaping of tissue architecture to the regulation of insulin homeostasis and T-cell proliferation. Furthermore, CEACAMs work as receptors for host-specific viruses and bacteria in mice and humans (5).

More in details, CEACAMs mediate intercellular binding by homophilic (CEACAM1, CEACAM5 and CEACAM6) and/or heterophilic (CEACAM1–CEACAM5, CEACAM5–CEACAM6 and CEACAM6–CEACAM8) interactions (4), which involve the extracellular domains (Fig.1.1) (6).

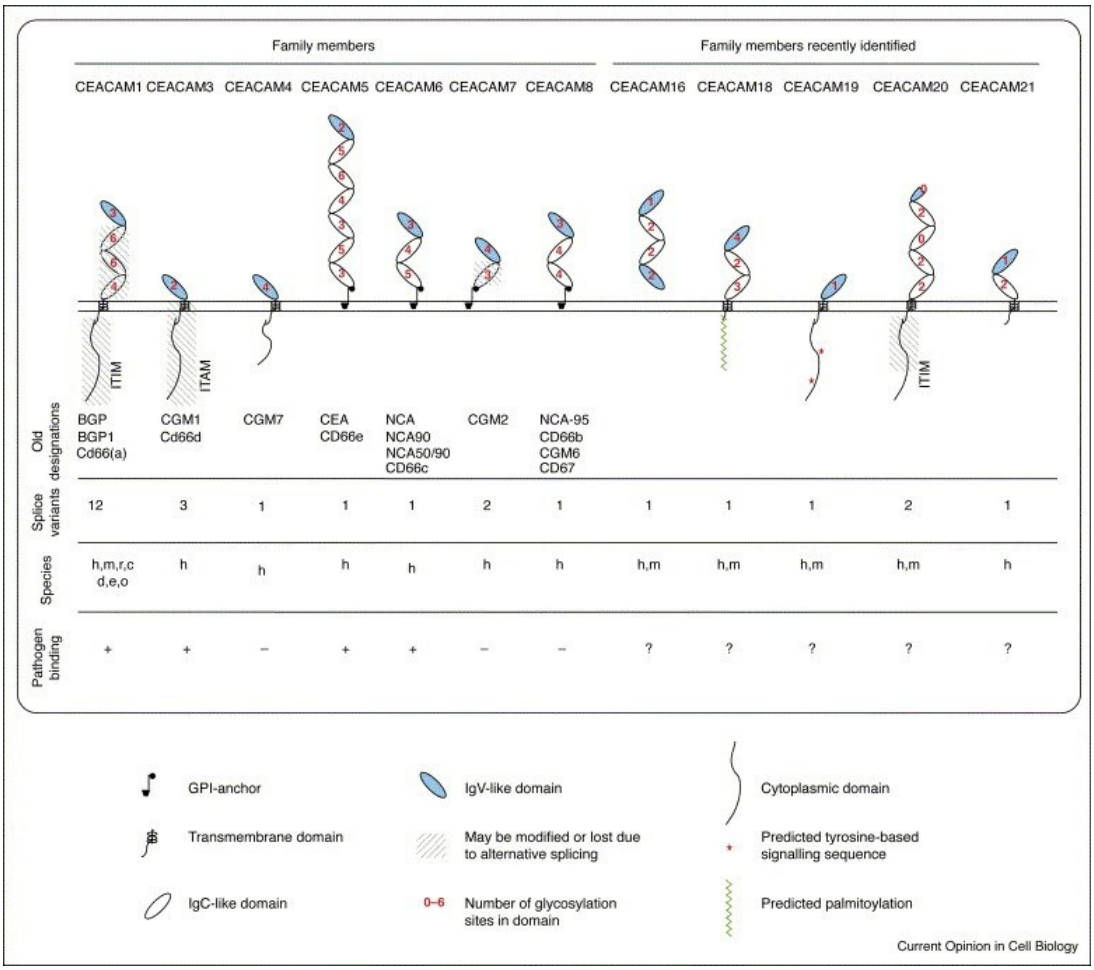

Fig. 1.1. Overview of the human CEA family members. *The known splice isoforms of the different CEA family members and the distribution of their orthologs in mammalian species are here represented. Species abbreviations: c, cow; d, dog; e, elephant; h, human; m, mouse; o, opossum; r, rat (3).*

1.2 Insights into CEACAM1

1.2.1 CEACAM1 expression, structure and splicing

Carcino Embryonic Antigen-related Cell Adhesion Molecule 1 (CEACAM1) is a unique member of the CEA family. It is the most well preserved CEA family member across species, with orthologues in mammal species (7) and it has the widest distribution in humans (8). In particolar, CEACAM1 is expressed by epithelial, endothelial, lymphocytes and myeloid cells (8). Amongst the human CEA family, CEACAM1 gene undergoes the most extensive alternative splicing, resulting in the production of 12 splice variants. All the variants contain the IgV-like domain (which is conserved among CEA-family members) followed by up to three IgC2-like domains (A1, B, A2) and/or Alu sequences (Alu), a transmembrane domain and a signaling cytoplasmic tail containing a long (L) or a short (S) domain (Fig. 1.2, 9).

Each splicing isoform differs from the others by the number of extracellular domains, the membrane anchorage and/or the length of the cytoplasmic tail, based on the inclusion or absence of exon 7,

respectively. For example, CEACAM1-4 is the isoform with four extracellular immunoglobulin like domains; CEACAM1-4L is the CEACAM1-4 isoform with a long cytoplasmic tail, while CEACAM1-4 with a short cytoplasmic tail is known as CEACAM1-4S (9). The differential splicing of exons encoding the cytoplasmic and transmembrane domains affects the type of cellular response induced by CEACAM1 binding. CEACAM1 isoforms with a long cytoplasmic tail, contains two ITIMs, generally involved in the transmission of inhibitory signals. By contrast, ITIM sequences are not present in CEACAM1 isoforms with short cytoplasmic tails, but they contain sequences able to bind tropomyosin and globular actin (10), indicating an interaction of CEACAM1 short isoforms with the cytoskeleton. The abundance of CEACAM1 expressed by the cells and the relative ratio of long to short isoforms are not static but can vary depending on the cell type, growth phase and activation status (11).

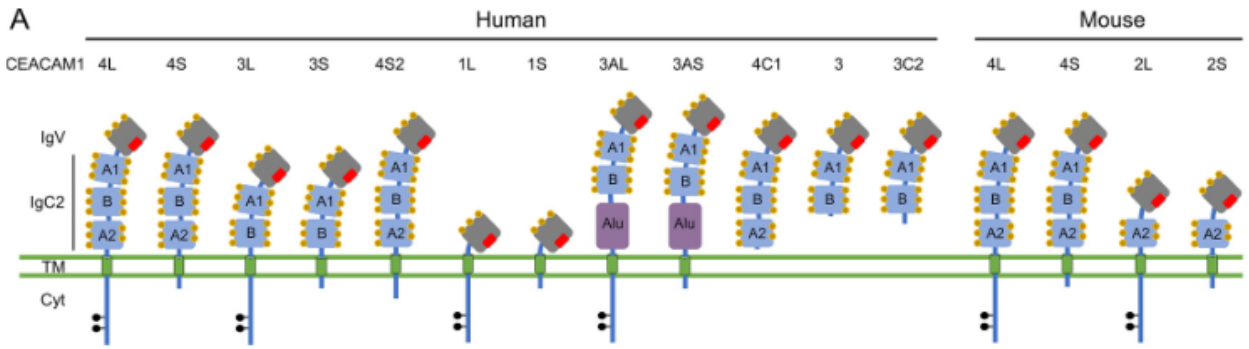

Fig. 1.2. Schematic representation of human and mouse CEACAM1 isoforms. *Each human isoform contain the N-terminal IgV domain, up to three IgC2 domains (A1, B, A2) and/or an Alu sequence (Alu), a transmembrane sequence and a short (S) or long (L) cytoplasmic tail. All the four mouse isoforms contain the N-terminal IgV domain, followed by one or three IgC2 domains, a transmembrane domain and a short or long ITIM-containing cytoplasmic tail. The IgV domain contains the homophilic and heterophilic binding surface indicated in red. The brown circles depict the glycosylation sites, while the ITIM tyrosines are represented by black circles (9).*

1.2.2 CEACAM1 homophilic and heterophilic interactions

The N-terminal IgV domain of CEACAM1 acts as the extracellular binding site and determines the CEACAM1's unique homophilic and heterophilic binding profile. In the hCEACAM1 IgV domain there are 108 amino acids organized in 9 beta strands (ABCC'C"DEFG) that fold inside the conserved IgV anti-parallel tertiary structure (12) of IgV-containing proteins, such as T cell receptor (TCR) (13), T cell inhibitory and mucin domain containing protein 3 (TIM-3) (14), and programmed cell death protein 1 (PD-1) (15). On the opposing site, ABED and GFCC'C" faces are linked by an internal salt bridge (R64 : D82). Furthermore, important is the protrusion of the CC' loop on hCEACAM1, where the side chains of key residue important for ligand binding, such as F29, Y34, V39, D40, R43, Q44 are exposed (9, Fig. 1.3).

Mutagenesis analysis of hCEACAM1 highlighted the critical role of the GFCC'C" interface, in particolar of the CC' loop (residues Y34, V39, D40, R43, Q44) (16), in determining the homodimerization of the hCEACAM1 IgV domain (17).

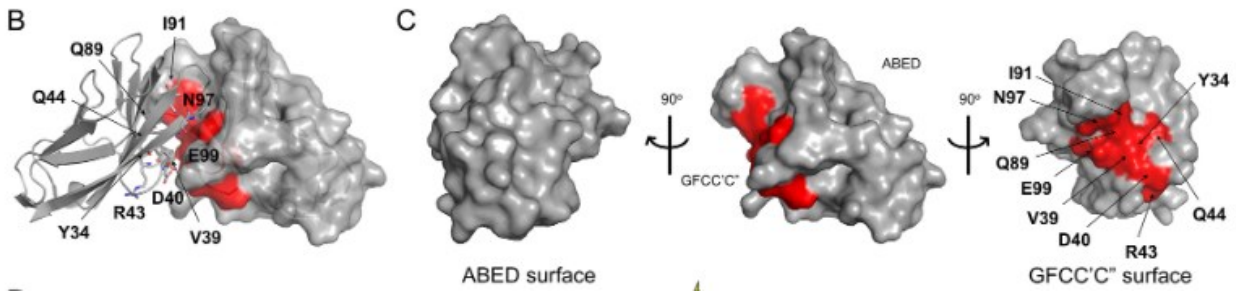

Fig. 1.3. Homodimeric structure of hCEACAM1 IgV. *B: Residues involved in the homophilic interactions between hCEACAM1 IgV and one of its ligands PDB ID 4QXW (left). C: Representation of the homophilic interacting residues within the GFCC'C" surface (9)*

1.2.3 CEACAM1 intracellular dimerization

CEACAM1 is mainly found as a cis-homodimer at the level of epithelial-cell surface (18). The dimeric form influences the ability of the receptor to recruit signaling molecules, such as SRC-family kinases and the SH2 domain-containing protein tyrosine phosphatase (SHP1) (19). Following CEACAM1 binding, the balance between monomeric and dimeric forms affects cellular responses (Fig. 4, 20). The dimeric state is dependent on the intracellular calcium ion (Ca^{2+}) concentration. At high Ca^{2+} concentration the binding of Ca^{2+} -loaded calmodulin to the cytoplasmic domain of both CEACAM1 short and long isoforms results in the dissolution of cis-dimers *in vitro* (21). The complex interplay between dimerization and differential CEACAM1 signaling under various cellular activation states, makes it difficult to assess the CEACAM1 functions (21).
Besides the formation of cis-dimers, CEACAM1 is also involved in trans-homophilic interactions (22). While CEACAM1 monomers can be involved in homophilic intercellular binding (23), it remains unclear whether cis-dimers must dissociate before mediate intercellular binding. The protein-protein intercellular interactions mediated by CEACAM1 are trans-homophilic interactions via N-terminal domains (23) (Fig. 1.4). The presence of multiple IgC2 domains seems to increase the affinity of homophilic binding (23). In addition, the capability of the receptor to be involved in intercellular binding is also governed by signals transmitted from the cytoplasmic domain, as suggested by different pharmacological agents which are known to affect CEACAM1 distribution in the cells (24).

The GFCC'C" face of IgV domains expressed by CEACAM1, CEACAM3, CEACAM5, CEACAM6 and CEACAM8 share more than 90% of similarity and they might interact with each other to form of GFCC'C"-mediated CEACAM family heterodimers (25). However, CEACAM5 IgV is the CEACAM family

member that shares the highest sequence homology with CEACAM1 IgV. Indeed, biochemical studies showed that only CEACAM5, commonly named CEA, binds to CEACAM1 with high affinity (25).
Differently from CEACAM1 and CEACAM5, CEACAM3 and CEACAM6 present two specific CC' loop sites, where substitutions at position 43 (R43S) and 44 (Q44L) reduce the potential heterophilic binding to CEACAM1 (26).
CEACAM8 shares an arginine at position 43 with CEACAM1, but it has a unique substitution at position 44 (Q44R) (25). The sequence variability in the CC' loop weakens both CEACAM1-CEACAM6 and CEACAM1-CEACAM8 heterophilic interactions, which result to be 100-fold weaker than CEACAM1 homophilic interactions (25).

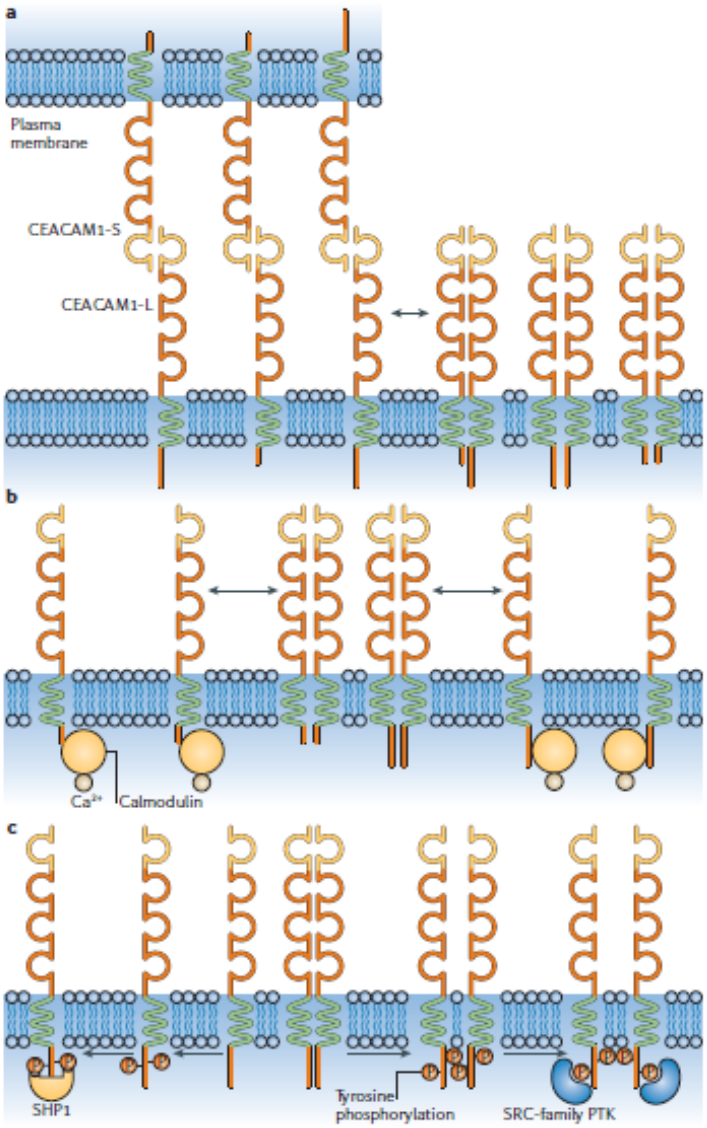

Fig. 1.4. Representation of monomeric, homodimeric and heterodimeric states of CEACAM1-L and CEACAM1-S. *A: Besides the intercellular binding mediated by the monomeric forms, it is possible that cis-dimers can also bind in trans. The balance between the monomeric and dimeric forms is influenced by the expression level of each isoform. B: The binding of CEACAM1 4S and CEACAM1 4L to* Ca^{2+} *-*

bound calmodulin results in the dissociation of CEACAM1 dimers. C: CEACAM1-L can be phosphorylated on the tyrosine residues in the two ITIMs within the cytoplasmic domain, resulting in the recruitment of the SH2-domain-containing protein tyrosine phosphatase 1 (SHP1). Although these phosphorylated tyrosine residues are spaced to allow the recruitment of SHP1, steric hindrance between the adjacent long cytoplasmic domains in CEACAM1-L homodimer is proposed instead to allow SRC-family protein tyrosine kinases (PTKs) to bind through their single SH2 domain (20).

1.3 The functions of CEACAM1 in the immune compartments

CEACAM1 modulates the innate and adaptive immune response and it has tumor-associated functions in many compartments of the immune system (fig. 1.5, 27). Especially studied in T and NK cells, CEACAM1 is a recently characterized inhibitory immune checkpoint that suppresses the signal transmission on immune cells via two ITIMs (28). Even if less investigated, CEACAM1 plays a functional role also in B lymphocytes (29) and in neutrophils (30).

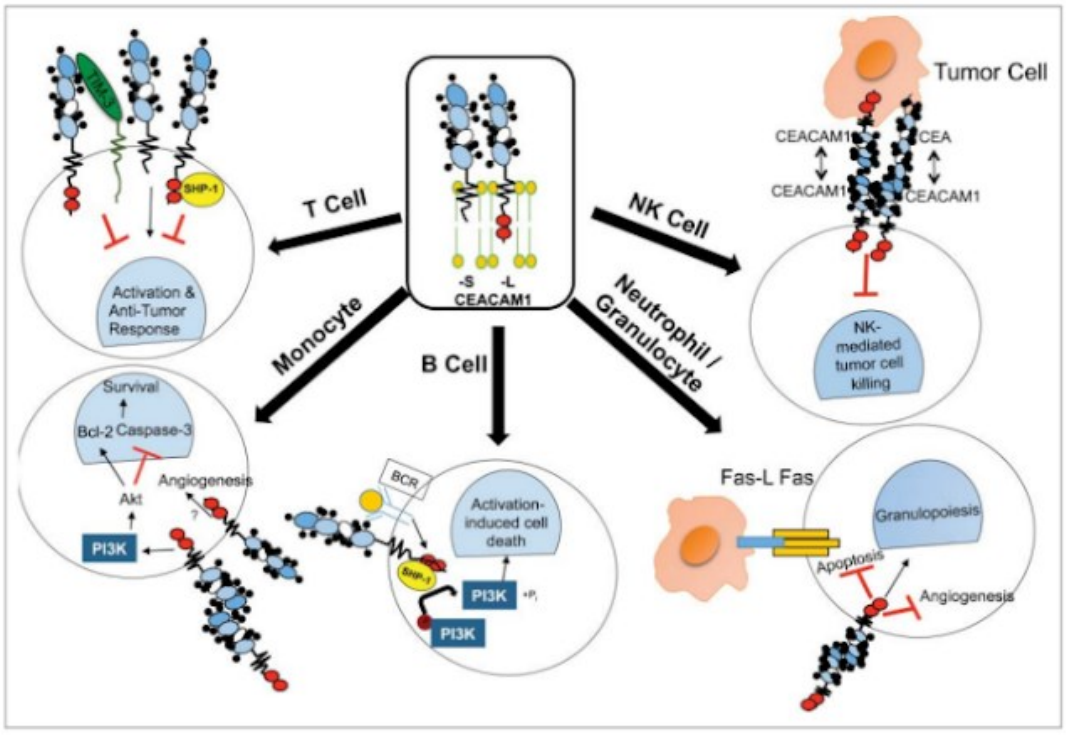

Fig. 1.5. Summary of CEACAM1 functions in immune cells: *In* ***T cells****, CEACAM1-L acts as inhibitory receptor by recruiting SHP-1 to the phosphorylated ITIMs of CEACAM1-L cytoplasmic domain. This leads to the change of the T cells activation threshold, resulting in decreased immunosurveillance in tumors. Opposite to CEACAM1-L, CEACAM1-S promotes T cell activation and regulatory functions. CEACAM1 also co-operates with TIM-3 expressed on the T cell surface, promoting the inhibition of T cell activation.* ***NK Cells****: the homophilic interactions between CEACAM1-L expressed on the surface of NK cells and CEACAM1 on tumor cells, block the NK-mediated tumor cell killing, independently of MHC class I status.* ***B cells****: upon the activation of the B cell receptor (BCR), CEACAM1-L on B cells is*

phosphorylated on the ITIM domain, resulting in the SHP-1 recruitment and dephosphorylation of PI3K, which stimulates the activation-induced cell death of B cells. ***Neutrophils/ granulocytes****: in monocytes the CEACAM1 homophilic binding results in the cell survival, since it activates PI3K, which in turn promotes the activation of Bcl-2 and inhibition of caspase-3. CEACAM1 expressed on the granulocyte surface promotes granulopoiesis and inhibits granulocyte-mediated angiogenesis and apoptosis (27)*

1.3.1 T cells

CEACAM1 is the only member of the CEACAM family to be expressed on T cell surface (31). While it is not expressed on resting T cells, CEACAM1 expression levels increase on activated T cells by IL-2 stimulation (31). Both the CEACAM1-S and CEACAM-L isoforms can be expressed at different ratio on T cells with opposite effects on their activation and functions, suggesting that T cell functions are regulated in a tunable fashion by CEACAM1-L and CEACAM1-S isoforms. However CEACAM1-L is more expressed on T cells than CEACAM1-S, except with the intestinal tissues where CEACAM1-S dominates over the CEACAM1-L expression (32).
While CEACAM1-S positively stimulates T cell activation and mediates regulatory activities (33), CEACAM1-L acts as an inhibitory receptor by downregulating T cell activation and functions (34). The CEACAM1-L isoform exerts its inhibitory function by the two cytoplasmic domain ITIMs, which are not present in CEACAM1-S (34). ITIMs in CEACAM1-L cytoplasmic domain are phosphorylated by a variety of Src-related tyrosine kinases, resulting in the recruitment of the tyrosine phosphatases SHP-1 and SHP-2, which de-phosphorylate several tyrosine residues within receptor tyrosine kinases or adaptor proteins expressed at the cell surface, leading to their inactivation (36).
More in detail, CEACAM1 is biochemically associated with the TCR/CDR complex (37), and it works as an immune checkpoint inhibitor of T cell signaling via ITIMs motifs, protecting T cells from prolonged activation (37). Following T cell activation, p56lck kinase phosphorylates the two ITIMs tyrosine residues, leading to the association with SHP-1 in the proximity of the T cell receptor (TCR) signaling complex (38). The recruited SHP-1 dephosphorylates the TCR CD3-ζ chain and TCR-associated protein kinase 70 kDa (ZAP-70), inhibiting the activation of the TCR signaling complex (Fig. 1.6, 20). The final result is the inhibition of different effector functions, including T cell proliferation, production of Th1 and Th2 cytokine and cytotoxicity (36).
On T cells CEACAM1 is co-expressed with TIM3, an heterophilic ligand of CEACAM1 (39). Together they work as activation-induced inhibitory molecules involved in T cell tolerance by inducing T cell exhaustion (40). CEACAM1-TIM3 biochemical interaction stimulates TIM3 inhibitory functions by facilitating TIM-3 maturation and expression on the T cell surface and, as consequence, TIM-3-mediated signaling. CEACAM1 can also interacts *in trans* with TIM3. This suggests that heterophilic interactions between TIM3 on T cells and CEACAM1 on tumor cells may result in T cell downregulation via TIM3 activation on T cells. PDL-1 is another heterophilic ligand with which CEACAM1 synergistically cooperates to induce an inhibitory effect on T cell functions (41). In a study conducted by Zhang *et al.,* tumor-infiltrating CD8+ T lymphocytes in colon cancer patients showed the maximal T cell exhaustion when TIM-3 and CEACAM1 are co-expressed, suggesting that CEACAM1

and TIM-3 are markers of high T cell exhaustion (42). Taken together, CEACAM1-L is an immune checkpoint inhibitor on T cells that shows promising results for cancer immunotherapy.

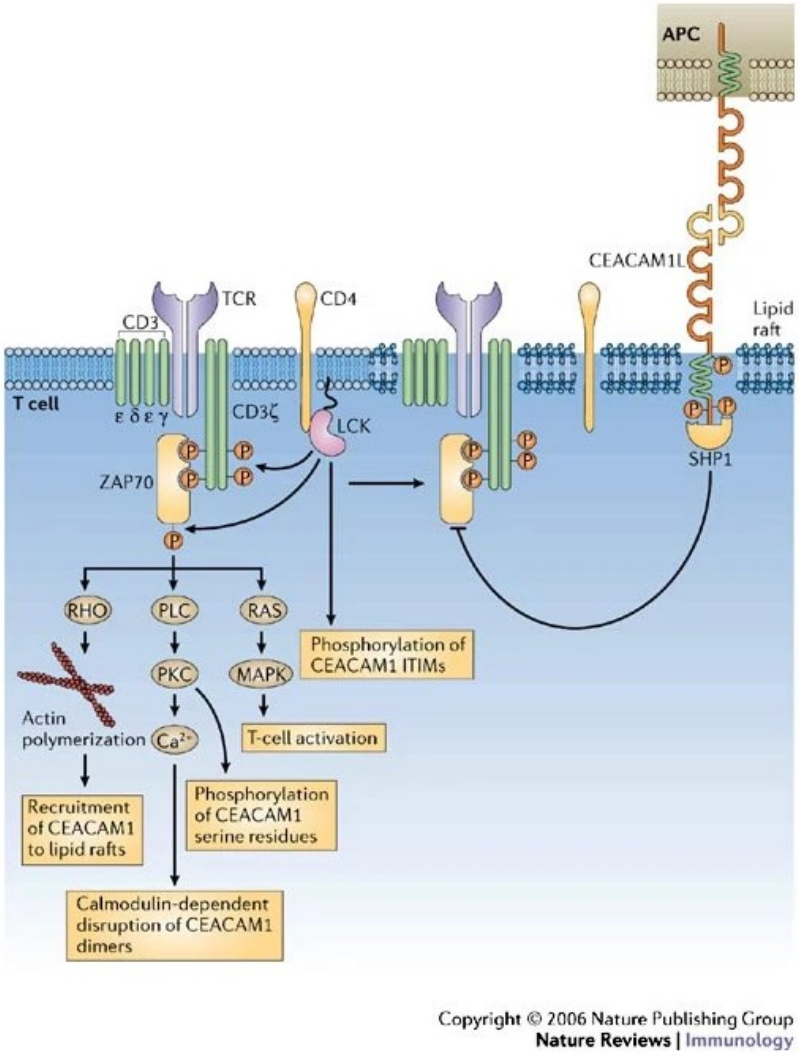

Fig. 1.6. CEACAM1-L on T cells: Following activation of the TCR/CD3 complex on T cells, the SRC-family protein tyrosine kinase phosphorylates tyrosine residues in the ITIMs of cis-dimers of CEACAM1-L, cytoplasmic domain of the CD3ζ and ZAP70. Recruitment of phosphorylated ZAP70 to the TCR–CD3 complex results in the activation of protein kinase C (PKC), which leads to the phosphorylation of serine residues of CEACAM1-L and to the calmodulin-dependent disruption of CEACAM1-L cis-dimers by intracellular calcium flux; activation of RHO GTPase promotes the actin-dependent cytoskeletal rearrangements and the subsequent recruitment of CEACAM1-L into lipid rafts. The trans homophilic interactions between the monomeric CEACAM1-L on T cell surface and monomeric CEACAM1 on the cell surface of an antigen-presenting cell (APC) leads to the recruitment of SHP1, that in turn dephosphorylates ZAP70, resulting in the inhibition of TCR–CD3 complex signaling. SHP1 dephosphorylates also CEACAM1-L, causing the AP2-mediated internalization of CEACAM1-L and, as consequence, blocking the inhibitory signaling (20).

1.3.2 Natural Killer (NK) Cells

Natural killer (NK) cells are immune cells involved in the innate defense against viral infections and tumor development, through their cytotoxic-mediated killing of virus-infected and tumor cells (43). NK cytotoxic action is determined by the balance between signaling mediated by surface activated receptors and inhibitor molecules (killer-cell immunoglobulin-like receptors, KIRS) (43). The inhibitor molecules recognize class I major histocompatibility complex (MHC) proteins expressed on the surface of opposing cells (43) and the inhibitory signal is mediated by the ITIMs located within the cytosolic domain of inhibitor receptors (43). The NK killing is restricted to cells that don't express the MHC on cell surface, while virus-infected or tumor cells express MHC proteins, and the interactions between MHC and KIR result in the inhibition of NK cell mediated cytotoxicity (44). CEACAM1 has been recently identified as an inhibitory co-receptor on NK cells which mediates inhibitory signaling independently from the MHC complexes (45). CEACAM1 is overexpressed on NK cells upon their activation by interleukin-2 (IL-2), IL-12 and IL-18 (46). It has been observed that CEACAM1 is overexpressed on the NK cell surface in patients with transporter associated with antigen processing (TAP2) deficiency. TAP2 protein mediates the loading of peptides onto MHC class I complexes and as consequence, the TAP2 deficient patients don't express surface MHC-peptide (47). When the MHC class I molecules are not exposed on the surface because of the lack of TAP-2, NK cell-mediated killing is activated. Thus, CEACAM1 overexpression on NK cells is a compensatory mechanism which confers protection against NK mediated cytotoxic activity and autoimmune disease (47). However, it has been observed that soluble CEACAM1 can block CEACAM1 homophilic interactions, enhancing NK-mediated cytotoxicity (48). Thus, the NK-mediated cell killing may be dependent on the ratio of membrane-bound and soluble CEACAM1 (48).

Furthermore, tumor cells that lack the MHC protein expression rely on the interaction with CEACAM1 on NK cells to escape from NK mediated tumor killing (45). This has been confirmed by the observation that CEACAM1 and CEACAM5 expressed on melanoma cells are involved in homophilic and heterophilic interactions, respectively, with CEACAM1 expressed on NK cells, leading to the inhibition of the NK-mediated cytotoxic activity (49). Importantly, mutagenesis studies revealed that R43 and Q44 found on the GFCC'C" surface are two crucial residues that mediate the inhibitory functions of CEACAM1-L on NK cells (50).

NKG2D is one of the activating receptors on NK cells which recognizes specific stress-inducible activating ligands (51). NKG2D binds the adapter molecule DAP10 in human and mouse cells (52). The formation of the NKG2D-DAP10 receptor complex results in the recruitment of the growth factor receptor binding protein 2 (Grb2), a guanine nucleotide exchange factor Vav1, and the p85 subunit of the phosphatidylinositide kinase (PI3K), leading to the transduction signaling that triggers anti-tumor cytotoxic responses (53). However, previous studies have shown that CEACAM1 expressed on tumor cells inhibits the NK-mediated immune surveillance (54) (Fig. 1.7, 55). Following the *in trans* homophilic CEACAM1 interactions, CEACAM1 on NK cell surface dimerizes and physically associates with the NKG2D activating receptor, leading to the SHP-1 mediated dephosphorylation of the guanine nucleotide exchange factor Vav1. This results in the inhibition of NKG2Ds ability to induce the cytolysis of CEACAM1-expressing target cells (56). Another mechanism through which tumor cells evade the NK cell-mediated killing is by downregulating the expression of NKG2D ligands (NKG2DL)

on tumor cell surface (56). Studies revealed that tumor cells increase NKG2DL surface expression in response to CEACAM1 silencing. In addition, Markel and his group (57) provided evidences that the homophilic interactions between CEACAM1 on tumor cells and CEACAM1 on NK cells via the N-terminal domain are a mechanism exploited by melanoma cells to escape from NK cell–mediated killing independently of MHC class I recognition (57). Upon activation, NK cells express the TIM-3 which cooperates with CEACAM1. More in detail, CEACAM1 regulates TIM-3 mediated tolerance and exhaustion (58). Moreover, it has been observed that the blockage of both CEACAM1 and TIM-3 in murine colon cancer model increases the antitumor response compared to the administration of single inhibitors (58).

Taken all together, these findings reveal that CEACAM1 expression enables tumor cells to escape from NK-mediated killing.

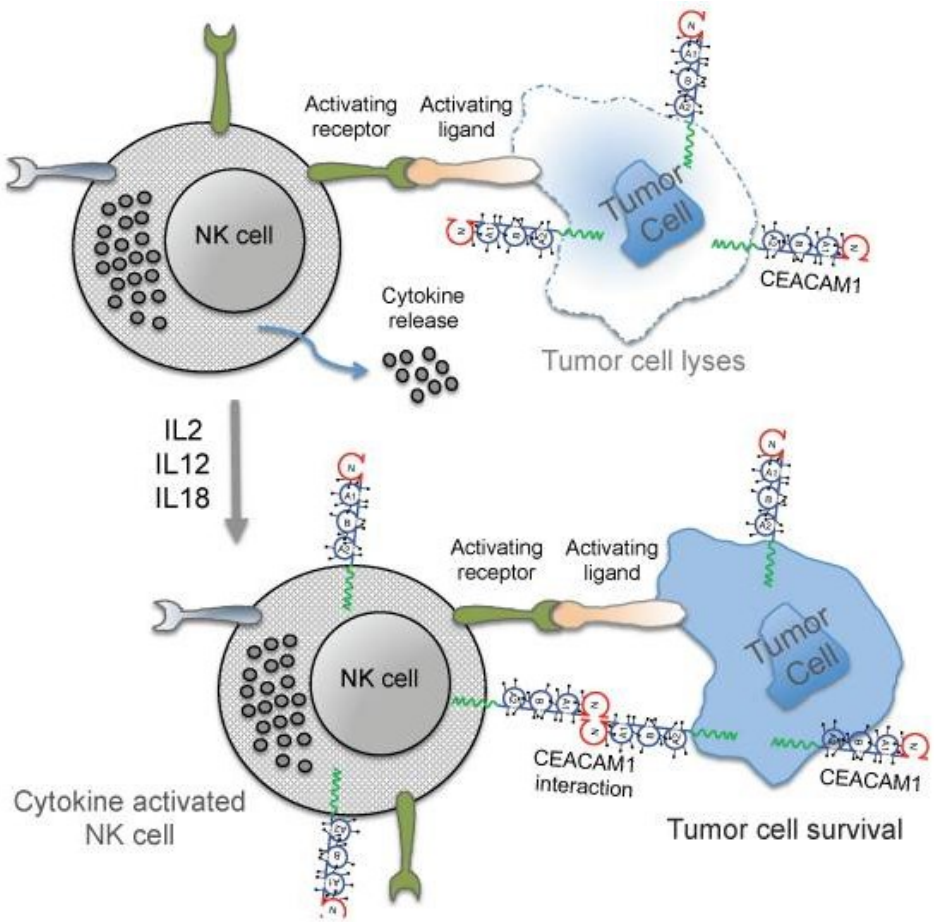

Fig. 1.7. CEACAM1 effects on NK cell - mediated cytotoxicity against tumor cells. *The binding between the activating receptors on NK cells with activating ligands on malignant cells triggers the NK-mediated cytotoxic activity, resulting in the cytokines release and cell lysis. CEACAM1 expressed upon cytokines stimulation of NK cells, interacts with CEACAM1 on tumor cells, blocking the cytolytic function of NK cells (55).*

1.3.3 Neutrophils

1.3.3.1 CEA family in neutrophils

Neutrophils are the most abundant innate immune cells in bone marrow as well as peripheral blood and they play a key role in the first line of defense against infections. Despite their short-half life of 6-20 hours to avoid needless tissue damage, neutrophils outnumber mononuclear leukocytes in inflammatory sites by 2 orders of magnitude, highlighting their major influence on the local and systemic long-term immune response (59).

CEACAM1, CEACAM3, CEACAM6 and CEACAM8 modulate neutrophil responses to bacterial pathogens. While CEACAM3 is constitutively expressed on human neutrophils, CEACAM1, CEACAM6 and CEACAM8 are expressed at low levels on resting neutrophils. Following neutrophil activation, these members are transported from intracellular granules to the cell surface (60). CEACAM3 has a major role in activating neutrophils in response to the bacterial pathogens: following ligation by bacterial pathogens, it acts as an activating receptor via ITAMs, leading to bacterial internalization and killing (61). CEACAM3 expression mediates neutrophil activation and results in neutrophil degranulation and oxidative burst (61). However it has been observed that CEACAM3 also regulates the long-term cytokine release, enhancing the overall inflammatory response in bacterial infection by the subsequent attraction of additional immune cells (62).

Despite the major role of CEACAM3 in the human neutrophil response against bacteria, CEACAM1 also mediates pathogen binding and promotes phagocytosis without significantly activating neutrophils (63).

Among the other members, CEACAM1 is abundantly expressed on neutrophils and it is frequently used as receptor for Gram-negative pathogens, by mediathing the inhibition of the host immune response (64). It has been observed that CEACAM1 activation upon ligand binding leads to the increasing of the phosphorylation and activation of SHP1 and ERK1/2, causing the blockage of caspase 3-mediated pathways. This results in the delay of the spontaneous and Fas ligand-induced apoptosis of neutrophils in rats (65). These findings suggest that CEACAM1 activation may prolong the neutrophil half-life and consequently the neutrophil functions during the inflammatory reaction. On the other hand, CEACAM1 inhibition can promote neutrophil apoptosis (65).

Furthermore CEACAM1 is a negative regulator of neutrophil granulopoiesis (66). Granulocyte-colony stimulating factor receptor (G-CSFR) is an essential regulator of granulopoiesis and binding of the ligand G-CSF to G-CSFR results in the phosphorylation of signal transducer and activator of transcription (STAT3), that in turn promotes neutrophil production. CEACAM1 acts as a co-inhibitory receptor of G-CSFR via ITIM and SHP-1, leading to downregulation of STAT3 activation. As a consequence, it has been observed that CEACAM1 -/- mice developed neutrophilia because of the elevated G-CSFR-Stat3 signaling (66).

Shively and his group showed that CEACAM1 also downregulates the neutrophil production of interleukin-1B (IL-1B) induced by IL-6 and LPS (67). LPS Gram-negative bacteria express lipopolysaccharide (LPS), an endotoxin that interacts with toll-like receptor-4 (TLR4) on neutrophils. LPS stimulation leads to phosphorylation of CEACAM1 on ITIMs, followed by recruitment of SHP-1 that prevents the activation of syk kinase, a critical mediator in IL-B1 production. As a result, the IL-

B1 production is inhibited. On the contrary, an hyper production of IL-1b was observed in neutrophils negative for CEACAM1 expression. These findings suggest that while CEACAM1 normally regulates the inflammatory response at the site of infection preventing hyper-inflammation, in the case of Gram Negative pathogens which bind to neutrophils, inflammation is further attenuated, favoring the infectious process (67).

1.3.3.2 Dual role of neutrophils in cancer

Neutrophils have a dual role in diseases, since they exert both defensive and harmful functions (68). Infact, besides their anti-pathogen and tissue regenerating functions, neutrophils are involved in different pathogenesis (68). The complex and controversial role of neutrophils in cancer initiation, growth and metastasis, relies on their cell plasticity and potential ability to undergo cell reprogramming (Fig. 1.8, 68).
On one hand neutrophils have inhibitory effects on cancer. They exert anticancer cytotoxic effects by producing Reactive Oxygen Species (ROS), such as H_2O_2 and NO, resulting in the inhibition of cancer growth (68). ADCC is another mechanism by which neutrophils kill cancer cells and it is mediated by the neutrophil expression of FcϒR receptors (69, 70). It has been observed that treatments with anti-CD52 mAb (alemtuzumab) and anti-CD20 mAb (rituximab) in mouse lymphomas have reduced efficacy when neutrophils are depleted (71). Furthermore, neutrophils produce chemokines that recruit T- and NK cells to indirectly kill cancer cells (72). Neutrophils are also involved in the metastasis development and in fact, it has been observed that neutrophil depletion facilitates metastasis (85). At early tumor stages, neutrophils acquire the characteristics of the antigen-presenting cells (APCs), allowing the stimulation of T cell proliferation that protects against the formation of tumor metastasis (73). Primary tumor cells secrete CCL2 cytokine and G-CSF that activate the cytotoxic functions of neutrophils. Studies showed that neutrophils migrate from primary breast tumor sites into the lung where they exert inhibitory effects on the arrival and colonization of metastatic cancer cells (74). Moreover, neutrophil expression of thrombospondin 1, IL-1β and the receptor tyrosine protein kinase MET, blocks cancer cell mesenchymal-to-epithelial transition, resulting in the inhibition of metastasis development (75).

However, mature neutrophils can be reprogrammed by tumor microenvironment to shift their anticancer properties to cancer-promoting ones (76). Neutrophil reprogramming may explain the heterogeneity of neutrophil subsets found in cancer patients. Studies revealed that mature neutrophils are reprogrammed into multipotent progenitors in the presence of a chemical cocktail (77), which support cancer growth and metastasis development. In fact, a high number of neutrophils in the peripheral blood of cancer patients has been observed and the neutrophil-to-lymphocyte ratio (NLR) has been shown to be a tumor prognostic marker which correlates with poor prognosis in several solid malignancies (78). Neutrophils provide a link between inflammation and cancer: they are a crucial component of inflammation which plays an important role in promoting cancer initiation (79). Neutrophils recruited to inflammatory sites drive oncogenic transformation through different mechanisms. Neutrophil release of genotoxin DNA substances, like ROS and reactive nitrogen species

(RNS), increases DNA instability (80). Furthermore, a shift of neutrophil functions to immunosuppression facilitates cancer development. In this context, arginase 1 (ARG-1) released by neutrophils depletes arginine in T cells, causing the inhibition of CD3-mediated T cell activation and proliferation. In addition, the expression of the H+ pumping ATPase on neutrophil cell surface, causes cancer acidosis which may lead to immune escape, by inhibiting the activity of T cells and NK cells. Furthermore, neutrophil-mediated recruitment of macrophages and Tregs in the tumor initiation site, contributes to create an immunosuppressive environment that helps the cancer progression (81). Neutrophils exert the tumor promoting properties also in the process of metastasis development, from the origin of the premetastatic niche to the growth of metastases. Before the arrival of cancer cells, neutrophils accumulate in distant organs where they form the premetastatic niche (68). Aggregation of neutrophils have been observed in the lungs prior to the development of metastasis in mouse models of melanoma and breast cancer, and it was associated with pulmonary metastasis development in both cases (82). Furthermore it has been observed that neutrophils also mediate the formation of premetastatic niche in ovarian cancer metastasis (83). In the early stages of metastasis, neutrophils release angiogenic factors such as MMP-9, which degradates the extracellular matrix that, in turn, releases the VEGF, resulting in the acceleration of angiogenesis (84). Neutrophils also direct cancer cells to endothelial cells, allowing cancer cells to enter and be guided into the bloodstream (72). This occurs through the release of cathepsin G, a neutrophil-derived serine protease, which is able to promote cell migration, enhances E-cadherin-mediated intercellular adhesion and cancer cell aggregation, promoting the entry of cancer cell into blood vessels (85). Furthermore, neutrophil extracellular traps (NETs) released by activated neutrophils have been observed to participate in the development of cancer metastasis. NETs are large extracellular complexes composed of chromatin, cytosolic and granule proteins (86). NETs are able to trap circulating cancer cells (CTCs), helping them to reach and promote their adhesion to distant sites (87). The interaction between neutrophils and CTCs promotes cell cycle progression and enhances the metastatic potential of CTCs (88). Several studies showed that ROS produced by neutrophils stimulate NETs production, and the direct interaction between NETs and cancer cells activates neutrophils, facilitates the migration of cancer cells, promotes the anchoring of cancer cells to endothelial cells, and promotes the extravasation of cancer cells from blood vessels (89, 90, 91).
Mass spectrometry analyses revealed that among the NETs associated proteins, CEACAM1 is the most promising candidate involved in capturing cancer cells and promoting NET-induced metastasis. In fact, CEACAM1 expressed on NETs helps the adhesion and migration of colon carcinoma cells *in vitro* and *in vivo,* and it enhances *in vivo* metastasis development. These results have been confirmed by Rayes et al. who demonstrated that the blockage of CEACAM1 decreases adhesion, migration, and metastasis of colon carcinoma cells, identifying CEACAM1 as a potential marker and target for novel therapeutics aimed to inhibit the pro-metastatic interactions between NETs and cancer cells (92).

Taken all together, neutrophils represent a promising target immune cell population for anticancer therapy. However, neutrophils' controversial role in cancer due to their plasticity, requires further investigation and should be considered in cancer therapy.

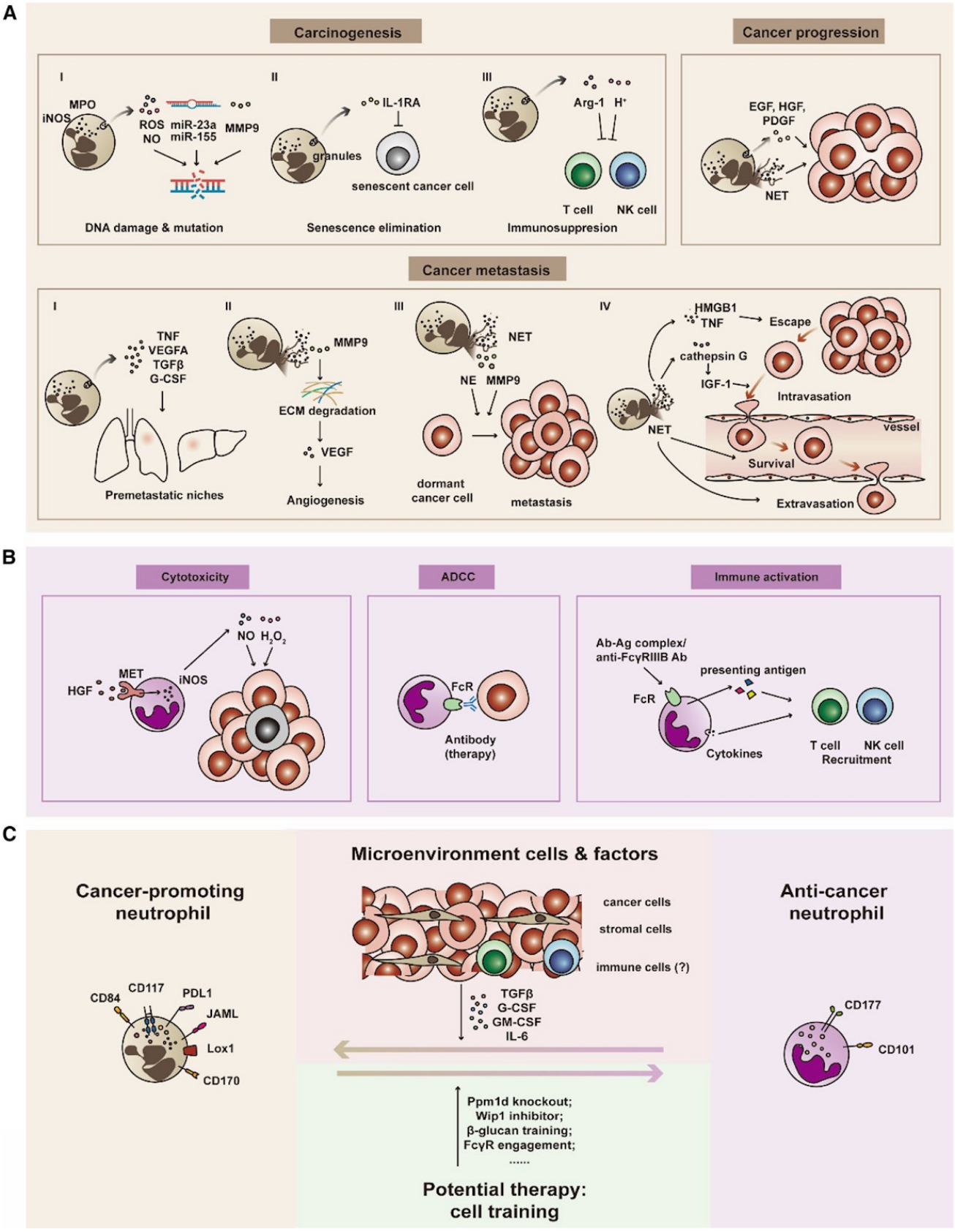

Fig. 1.8. Dual role of neutrophils due to their plasticity in cancer. A) Neutrophils with cancerogenic effects: 1) Neutrophils can promote cancer initiation by producing ROS, NO, microRNAs and MMP9, which are responsible to induce DNA damage and gene mutation. Furthermore, neutrophils eliminate

senescence through IL-1RA. They also mediate immunosuppression by releasing Arg-1 that inhibits CD3-mediated T cell activation and proliferation, and by creating an acidic environment that makes T and NK cells inactive against cancer cells. 2) Neutrophils release cytokines and NETs, thus stimulating cancer cell progression. 3) Neutrophils promote metastasis development by releasing cytokines that allow the formation of the premetastatic niche in distant organs. MMP9 released by neutrophils induces angiogenesis by promoting the VEGF production from degraded ECM. Neutrophils produce HMGB1 and TNF, which help cancer cells to migrate toward blood vessels. Cathepsin G is released by neutrophils and it induces intravasation through the activation of IGF-1. NETs interact with cancer cells, allowing their survival in the peripheral blood and facilitating their extravasation. In addition, MMP9 and NE within NETs contribute to the metastasis formation by waking up dormant cancer cells in distant organs.

B) Neutrophils with anti-cancer properties. *1) Neutrophils produce H_2O_2 and NO to exert antitumor cytotoxic effects. Furthermore, neutrophils kill cancer cells by ADCC triggered by antibody therapy. Cancer cells are indirectly killed by leukocytes recruited by neutrophil-released chemokines.* ***C) Neutrophil reprogramming:*** *during cancer progression, cancer cells and stromal cells release various cytokines that may be responsible for the conversion of neutrophils' properties from anti-cancer into pro-cancer ones (68).*

1.4 The multipurpose targeting of CEACAM1 in cancer therapy

Besides the previously described functions in various compartments of the immune system, CEACAM1 is an attractive target for cancer immunotherapy also because it has established functions in several solid tumors. Infact, CEACAM1 is a therapeutic target for cancer treatment and CM24, an anti-CEACAM1 monoclonal antibody, is being testing in ongoing phase I/II clinical study for the treatment of advanced solid tumors in combination with nivolumab (NCT04731467). In contrast to the decreased expression at the early tumor stages, CEACAM1 is overexpressed at the metastatic stages of several solid tumors (Fig. 1.9, 93), including melanoma (94), bladder cancer (95), pancreatic cancer (96), colon cancer (97) and Non Small Cell lung cancer (NSCLC) (98). CEACAM1 overexpression positively correlates with tumor progression, angiogenesis, metastasis development and overall survival, making CEACAM1 an important tumor biomarker (Fig. 9) (93). Moreover, CEACAM1's role in promoting tumor progression is further supported by the interplay between CEACAM1 and the immune cells as previously seen.

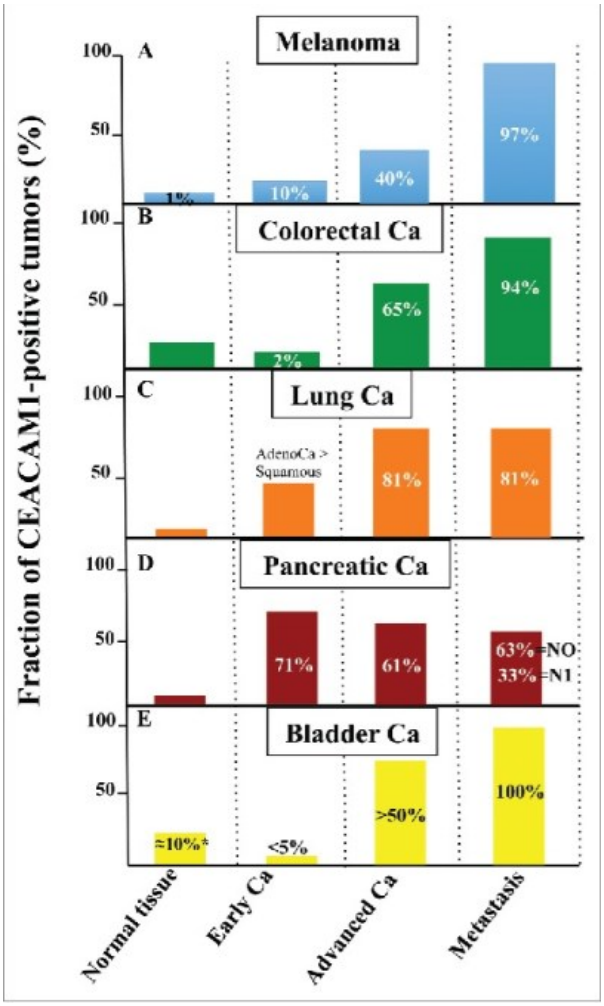

Fig. 1.9. CEACAM1 expression in different types of solid cancers. *The graph shows the expression of CEACAM1 in normal tissues, early stages of carcinomas, advanced carcinomas and metastatic stages for melanoma (A), colorectal (B), lung (C), pancreatic (D) and bladder (E) cancers. The numbers within the columns represent the percentages of patient samples positive for CEACAM1 expression (93).*

Like previously described, it has been observed that the homophilic interactions between CEACAM1 expressed on tumor cells and CEACAM1 on NK cells inhibit NK-mediated killing independently of MHC class I recognition and also interfere with the production of the interferon-γ (IFN-γ) by NK cells and tumor-infiltrating lymphocytes (TILs) (45, 49). These findings are confirmed by *in vivo* studies: in mouse cancer model, CEACAM1 silencing results in the upregulation of NK cell activating ligands expressed on tumor cell surface (99). Thus, a monoclonal antibody specifically targeting CEACAM1 would lead not only to the direct inhibition of CEACAM1 overexpressing tumor cells, but also to the rescue of the immune system activation, resulting in the increased anti-tumor response (93). Such an antibody would represent a powerful therapy to treat local as well as metastatic tumor (93).

1.4.1 CEACAM1 in Melanoma

Normally, CEACAM1 is not expressed on melanocytes (100). However, Egawa et al. observed an increased expression of the CEA protein family on acquired and congenital melanocytic nevi (101). Immunohistochemical studies performed by Gambichler's group revealed that CEACAM1 expression progressively increases from benign nevi to dysplastic nevi and even more to melanomas (102). In metastatic melanoma, 89% of lesions express CEACAM1 and the expression positively correlates with tumor progression (103). Several studies demonstrated the prognostic value of serum levels of soluble CEACAM1 in melanoma diagnosis and progression, suggesting that it could be a useful prognostic and predictive tumor marker (104). Higher CEACAM1 levels in the blood correlate with decreased patient survival and failure response to immunotherapy (105).
Besides its role as prognostic biomarker, the relationship between CEACAM1 overexpressing tumor cells and immune cells is well established in melanoma patients, where a high number of circulating NK and CD8+ cells overexpress CEACAM1 (106). *In vitro* studies on a mouse melanoma cell line demonstrates that the CEACAM1 4-L isoform downregulates the expression levels of NKG2D ligands on cell surface (107). In line with these results, *in vitro* studies of melanoma cells co-incubated with tumor-infiltrating lymphocytes (TILLs) revealed that surviving melanoma cells acquired resistance against TIL-mediated anti-tumor response by increasing the CEACAM1 expression on their cell surface (108). *In vivo* studies showed that the efficacy of TIL cell transfer therapy has limits in melanoma patients due to the homophilic CEACAM1 interactions between melanoma and TILs cells that result in the reduction of TILs' functions (108). A therapy able to specifically target CEACAM1 could represent a powerful tool to restore the anti-tumor immune system response. Infact, the increased expression of CEACAM1 at the advanced stages of melanoma and its relationship with the immune system compartments, together with the established success of the immunotherapies in metastatic melanoma, highlight the need of anti-CEACAM1 monoclonal antibodies to treat metastatic melanoma patients (105). One example is MRG1, a murine IgG1 anti-CEACAM1 monoclonal antibody developed by Markel's group, which was shown to act as potent inhibitor of CEACAM1 homophilic interactions and to enhance the T cell response against melanoma cells *in vitro* as well as in SCID/NOD mice bearing human melanoma xenografts (109).

1.4.2 CEACAM1 in Colorectal cancer (CRC)

The first studies of CEACAM1 were conducted in the colorectal cancer (CRC)(110). However CEACAM1's role in CRC remains controversial. It was initially identified as a tumor suppressor, since it was found to be downregulated in the early stages of CRC (111). CEACAM1 downregulation has been reported in more than 85% of early stages of colorectal adenomas and carcinomas (112). By contrast, specific anti-CEACAM1 antibodies showed high binding to high-grade adenocarcinomas and metastatic CRC tissues (113). In addition, the increased CEACAM1 expression at the advanced stages of CRC positively correlates with invasiveness and metastatic spread (114). However, the correlation between CEACAM1 and tumor invasiveness has not been observed in other studies (115).

Consistent with the observation that CEACAM1 expression increases the tumor aggressiveness and downregulates the immune system anti-tumor response, Huang YH's group demonstrated that CEACAM1-deficient mice exhibited protection from colorectal neoplasia (116). These results are confirmed by the findings that CEACAM1, together with TIM3, is higher expressed on circulating CD8+ T cells and TILs from CRC patients compared with normal tissues (117). Furthermore, double-positive (CEACAM1+TIM3+) T cells within CRC tumors showed a significant decrease in IFNγ production (117). Therefore, anti-CEACAM1 monoclonal antibodies should be considered as therapeutic agents also for metastatic CRC patients, because of the direct effect on tumor cells as well as the capability to block the inhibition of immune cell functions in CRC. To date, CC4 and WL5 are promising novel murine anti-CEACAM1 mAbs that showed reactivity to colon cancer cells and capability to enhance the immune cell-mediated cytotoxicity (118, 119).

1.4.3 CEACAM1 in bladder and prostate cancer

Immunohistochemical studies carried out by Ferrer's group revealed that CEACAM1 is highly expressed on epithelial cells from the luminal surface of transitional epithelium in non-malignant bladder tissues (120). By contrast, tumor cells became negative for CEACAM1 expression at the early tumor stages, while the endothelial cells of immature blood vessels growing into the epithelial layer containing tumor cells were found to express CEACAM1 (120). CEACAM1 is still overexpressed by the endothelial cells of blood vessels associated with the tumor mass also in the invasive bladder cancer, suggesting that CEACAM1 inhibition could have anti-angiogenic effects in this tumor (120). In conclusion, these studies suggest that concomitantly with a downregulation of CEACAM1 in bladder cancer cells, its expression appears to be upregulated in endothelial cells of tumor-associated blood vessels (120). However, differently from endothelial cells, epithelial cells remain CEACAM1 negative, correlating with high expression of VEGF-C (120). Infact, when CEACAM1 is silenced, an increase in the blood vessel formation was observed. On the other hand, a reduction in tumor growth was recorded in several bladder cancer cell lines upon CEACAM1 overexpression (120).
Similar findings were observed in prostate intraepithelial neoplasia by Tilki's group (121). In fact, epithelial dysplastic cells were found with lower CEACAM1 expression levels, while it was upregulated in adjacent endothelial cells, concomitantly with an increased expression of VEGF-A, -C, and -D. This suggests that CEACAM1 expression by endothelial cells may promote angiogenesis (121). Ergün and coworkers confirmed these results by demonstrating that the change in CEACAM1 expression stimulates proangiogenic activities of fibroblasts which are factor-dependent, including neocapillary formation, proliferation and chemotaxis, leading to the activation of angiogenesis (122). They observed high levels of CEACAM1 during the angiogenic activation not only at the endothelial cell surface level but also in the supernatant, suggesting a possible release of soluble CEACAM1 protein into body fluids during the activation of the angiogenesis (122). Based on these findings, western blot analyses performed by Tilki's group on 135 urinary samples, lead to the conclusion that higher urinary levels of CEACAM1 are associated with advanced stages of urinary bladder carcinoma (123). These evidences highlight the potential role of CEACAM1 as a biomarker also in bladder cancer.

In conclusion, these data suggest that the downregulation of CEACAM1 in the dysplastic epithelium is one of the earliest events occurring during the switch from non-invasive to invasive and vascularized tumor (124). Also, these findings support the previous hypothesis of CEACAM1's role as tumor suppressor in the normal epithelia (125). On the other hand, CEACAM1 downregulation by epithelial cells results in the increase of the expression of proangiogenic factors (126) which in turn triggers the endothelial CEACAM1 upregulation (120), promoting invasiveness and metastasis development.

1.5 An overview of Cancer Immunotherapy

Tumor cells can escape the attack of the immune system through different mechanisms, such as by down-regulating the expression of tumor antigens, overexpressing proteins that allow immunity escape, recruiting immune regulatory cells or by releasing immune inhibitory factors (127).
In recent decades, Cancer Immunotherapy has attracted attention as promising therapeutic approach to treat various tumors, such as melanoma, NSCLC, breast cancer, colorectal cancer and pancreatic cancer (128). Immunotherapy is the biotherapy that sensitizes the patient's immune system to fight cancer with increased selectivity and reduced side effects (129). By stimulating the patient's antitumor immune response, immune cells can play a crucial role in tumor surveillance and clearance. Firmly established as a pillar of cancer care which has improved patients survival and quality of life, Immunotherapy is the prevalent cancer treatment in recent years and ongoing clinical trials (130). Cancer Immunotherapy has several advantages over non-specific cancer therapy methods, such as chemotherapy, radiotherapy and surgery. Infact, tumor-targeting immune cells can reach distant areas from the primary tumor site, such as metastasis and cancer stem cells, which are impossible to reach by surgery. Furthermore, the specificity in tumor targeting by immune cells allows to reduce the side effects, which instead represent an important drawback of chemotherapy and radiotherapy (131). There are different Cancer Immunotherapy approaches to enhance the immune system response against cancer: adoptive cell therapy, cancer vaccines, immuno-modulators and monoclonal antibodies (Fig. 1.10, 132).

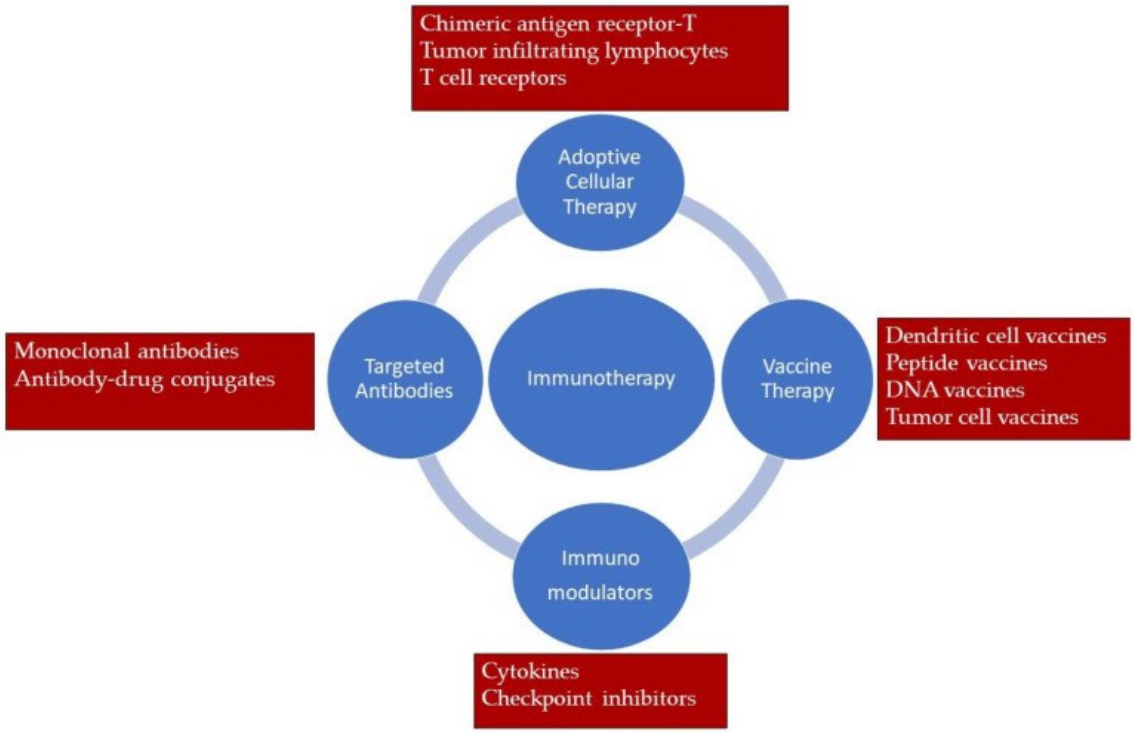

Fig. 1.10. Immunotherapy approaches for cancer treatment (132)

Adoptive cell therapy (ACT) is a rapidly growing area of clinical investigation consisting in removing patients' or donors' immunological effector cells, growing and modifying them to overexpress genes involved in tumor treatment, and reinfusing the modified cells into the patient (132). There are currently three different types of ACT: ACT with tumor-infiltrating lymphocytes (TIL), ACT using genetically engineered T cell receptor (TCR) gene therapy and ACT with chimeric antigen receptor (CAR) modified T cells (132). While TIL therapy involves expansion of a heterogeneous population of T cells found in the patient's tumor, CAR T cells and TCRs involve expansion of a genetically modified T-cell specifically against tumor antigens (132). Although the use of other immune cell types such as NK cells is also an area of current research, efforts are still required to overcome obstacles and make this an effective anti-cancer therapy (132). Despite the successful results in hematologic malignancies (134), the role of ACT in solid tumors is growing but it is still in its early stage.

Cancer vaccines are used as an approach to prevent or treat cancer. The most used type is peptide-based vaccines, which contain immunogenic epitopes derived from tumor-associated antigens (135). The final goal of therapeutic cancer vaccines is to stimulate antitumor T cells by immunizing patients against tumor-associated antigens, destroy the tumor and prevent relapse (135). Vaccines are usually administered with dendritic cells (DCs), which are used as adjuvants to increase the effectiveness thanks to their ability to initiate and support immune response (135). With the growing knowledge on the structure of tumor-associated antigens, the interest in cancer vaccines is increasing. The most observed clinical benefit of therapeutic cancer vaccines is the prolonged survival (136). However, the lack of cancer eradication could be mainly explained by the suboptimal vaccine design and the immunosuppressive tumor microenvironment (137).

Immuno-modulators can be distinguished in cytokines and immune checkpoint inhibitors. Cytokines are important regulators of innate and adaptive immunity. They regulate proliferation, differentiation, effector functions, and the survival of leukocytes and mediate the communication among immune system cells. In light of their functions, cytokines have been exploited in the treatment of cancer (138). Interleukin-2 (IL-2) has been approved for the treatment of advanced melanoma and metastatic renal cancer. Interferon-alpha (IFN-α) is used to treat patients with cell leukemia, follicular lymphoma, chronic myeloid leukemia and acquired immune deficiency syndrome (AIDS)-related Kaposi sarcoma (139). The efficacy treatment of other cytokines, including IL-7, IL-12, IL-15, IL-18, IL-21, have been studied in clinical trials (138). However, combinatorial treatments of cytokines with anti-cancer monoclonal antibodies are being investigated in clinical trials to further stimulate the antitumor immune responses (139). Immune checkpoint inhibitors (ICIs) are a novel class of monoclonal antibodies that target immune checkpoint receptors, such as CTLA-4, PD-1, LAG-3, TIM-3 or inhibitory ligands, such as PD-L1, expressed on immune cells and tumor cells. By stimulating the immune system to elicit an anti-tumor response, ICIs have improved the treatment of a wide range of cancers, including metastatic melanoma, non-small lung cancer and renal cell carcinoma (140).

Antibody-based immunotherapeutics have revolutionized cancer therapy, enabling the treatment of previously untreatable types of cancer (166). They are the most approved cancer immunotherapy methods and the number of mAbs receiving approval from the FDA and entering in the clinic is increasing (141). Table 1.1 shows the FDA approved mAbs used in cancer therapy and the antigens against which they are directed (142). The role of mAbs and ICIs is further discussed more in detail below.

Table 1. FDA-approved monoclonal antibodies for cancer.

Name	Antigen	Format	Indications (Year of First Approval) [1]
Unconjugated Antibodies			
Atezolizumab	PD-L1	Humanized IgG1	Bladder, Non-small cell lung (2016), and Triple-negative breast (2019) cancers (2019)
Avelumab	PD-L1	Human IgG1	Urothelial Carcinoma (2017) and Merkel Cell Carcinoma (2017)
Bevacizumab	VEGF	Humanized IgG1	Colorectal (2004), Non-small cell lung (2006), Renal (2009), Glioblastoma (2009), and Ovarian (2018) Cancers
Cemiplimab	PD-1	Human IgG4	Cutaneous squamous-cell carcinoma (2018)
Cetuximab	EGFR	Chimeric IgG1	Colorectal cancer (2004) and Head and neck squamous cell carcinoma (2006)
Daratumumab	CD38	Human IgG1	Multiple Myeloma (2015)
Dinutuximab	GD2	Chimeric IgG1	Neuroblastoma (2015)
Durvalumab	PD-L1	Human IgG1	Bladder Cancer (2017)
Elotuzumab	SLAMF7	Humanized IgG1	Multiple Myeloma (2015)
Ipilimumab	CTLA-4	Human IgG1	Melanoma (2011) and Renal cell carcinoma (2018)
Isatuximab	CD38	Chimeric IgG1	Multiple Myeloma (2020)
Mogamulizumab	CCR4	Humanized IgG1	Cutaneous T-cell lymphoma (2018)
Necitumumab	EGFR	Human IgG1	Non-small cell lung cancer (2015)
Nivolumab	PD-1	Human IgG4	Melanoma (2014), Lung (2015), and Renal (2018) cancers
Obinutuzumab	CD20	Humanized IgG2	Chronic lymphocytic leukemia (2013)
Ofatumumab	CD20	Human IgG1	Chronic lymphocytic leukemia (2014)
Olaratumab	PDGFRα	Human IgG1	Sarcoma (2016)
Panitumumab	EGFR	Human IgG2	Colorectal Cancer (2006)
Pembrolizumab	PD-1	Humanized IgG4	Melanoma (2014), Various (2015-)
Pertuzumab	HER2	Humanized IgG1	Breast cancer (2012)
Ramucirumab	VEGFR2	Human IgG1	Gastric cancer (2014)
Rituximab	CD20	Chimeric IgG1	B-Cell Lymphoma (1997)
Trastuzumab	HER2	Humanized IgG1	Breast cancer (1998)
Gemtuzumab ozogamicin	CD33	Humanized ADC	Acute myeloid leukemia (2000)
Brentuximab vedotin	CD30	Chimeric ADC	Hodgkin's lymphoma and Anaplastic large-cell lymphoma (2011)
Trastuzumab emtansine	HER2	Humanized ADC	Breast cancer (2013)
Inotuzumab ozogamicin	CD22	Humanized ADC	Acute lymphoblastic leukemia (2017)
Polatuzumab vedotin	CD79B	Humanized ADC	B-Cell Lymphoma (2019)
Enfortumab vedotin	Nectin-4	Human ADC	Bladder cancer (2019)
Trastuzumab deruxtecan	HER2	Humanized ADC	Breast cancer (2019)
Sacituzumab govitecan	TROP2	Humanized ADC	Triple negative breast cancer (2020)
Moxetumomab pasudotox	CD22	Mouse ADC	Hairy-cell leukemia (2018)
Ibritumomab tiuxetan	CD20	Mouse IgG1-Y90 or In111	Non-Hodgkin's lymphoma (2002)
Iodine (I131) tositumomab	CD20	Mouse IgG2-I131	Non-Hodgkin's lymphoma (2003)
Blinatumomab	CD19, CD3	Mouse BiTE	Acute lymphoblastic leukemia (2014)

[1] Indications and year of first approval for each antibody were accessed using the FDA drug database [57].

Table 1.1. mAbs approved by FDA for cancer treatment according to the year of approval (142).

1.5.1 Monoclonal antibody-based Immunotherapy: antibody structure and mechanisms of action

The intact antibody molecule consists of two heavy chains and two light chains which are paired together by disulfide bonds (Fig. 1.11, 143). Each light chain consists of one variable domain (vL) and one constant domain (cL), while the heavy chains have one variable domain (vH) and a different number of constant domains (cH) (144). From a functional point of view, the antibody structure can be divided into three functional subunits, two Fragment antigen binding domains (Fabs) and the crystallizable fragment (Fc). The two Fabs are linked to the Fc by the hinge region that confers conformational flexibility to the Fabs with respect to the Fc. Both the two Fabs contain identical antigen-binding sites, and they are responsible for the binding of the antibody to specific target antigens. The variable region of the Fab is composed of a pair of vH and vL. In contrast, the Fc region binds to a variety of receptor molecules expressed on the effector cells, governing the effector function profile (144).

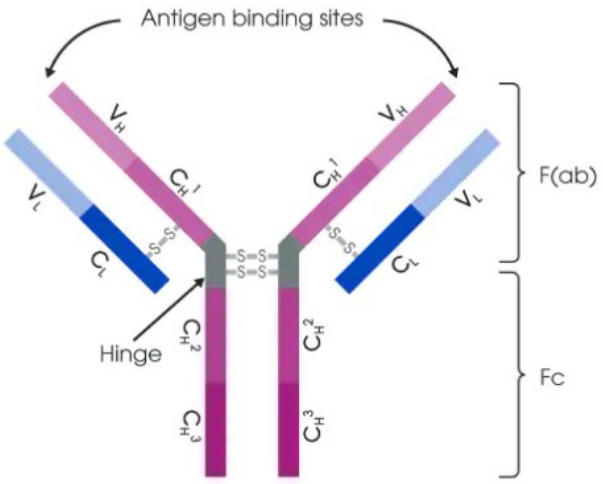

Fig. 1.11. Scheme of full intact antibody structure. *vH, heavy chain variable domain; vL, light chain variable domain; cH, heavy chain constant domain; cL, light chain constant domain (143).*

Since the beginning of their development, mAbs were focused on targeting tumor-associated antigens (TAAs) to directly kill tumor cells (145). Infact, mAbs specifically against TAAs which are important for the growth, survival and invasiveness of the tumor, represent a specific treatment tool able to induce tumor cell death through various mechanisms (Fig. 1.12, 146). mAbs directly kill tumor cells by binding and blocking growth factor receptors, resulting in the inactivation of signal pathways involved in the cancer cell proliferation, or they can act as vector bearing toxic drugs or radioisotopes to deliver toxic payloads (147). The indirect mechanisms involve the components of the host immune system and they rely on the affinity of the antibody Fab region to specifically target the antigen, as well as the ability of the Fc region to recruit components of the host immune system (148). The indirect mechanisms can be distinguished in: complement-mediated cytotoxicity (CDC) that requires the complement activation, antibody-dependent cellular phagocytosis (ADCP) that facilitates tumor cell phagocytosis by macrophages, and antibody dependent cell-mediated cytotoxicity (ADCC) (148).

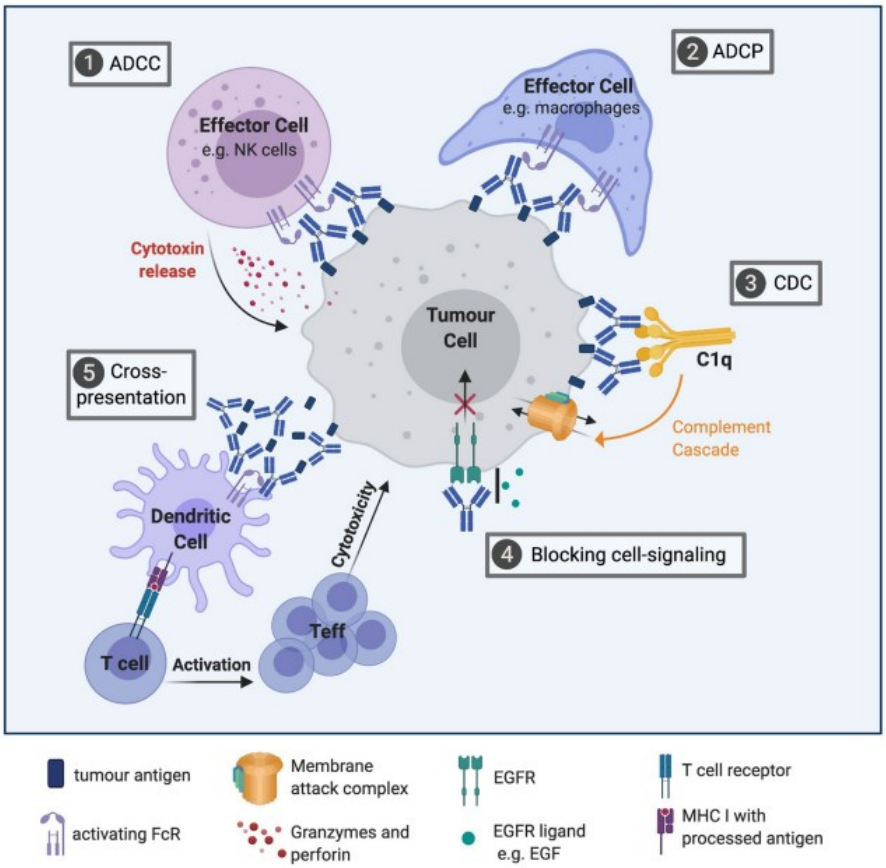

Fig. 1.12. Mechanisms of action of antibodies against tumor antigens. *Antibodies mediate tumor cell-killing via different mechanisms: (1) antibody-dependent cell-mediated cytotoxicity (ADCC); (2) antibody dependent cell-mediated phagocytosis (ADCP); (3) complement-dependent cytotoxicity (CDC), (4) blockage of signaling pathways in tumor cells and (5) formation of immune complexes, resulting in the tumor antigen cross-presentation by dendritic cells (DCs) (146).*

ADCC is the main mechanism of action of many mAbs with strong affinity to the Fc receptors (FcR) expressed on effector cells (149). In the ADCC process, antibodies act as a bridge that links the effector cell to a target cell: they first opsonize the target cell by binding specific antigens on target cell surface via their Fab, while through their Fc portions they bind to the Fc receptors (FcR) on effector cells. Once the recruited effector cells have been activated, they can induce the killing of target cells via nonphagocytic mechanisms, through three key mechanisms: release of cytotoxic granules, Fas signaling and production of reactive oxygen species (149).
NK cells, monocytes, macrophages, neutrophils, eosinophils, and dendritic cells are FcγR receptors expressing immune cells and, thus, they are capable of inducing the ADCC (150).
FcγRs are the most important FcR class involved in tumor cell clearance by myeloid cells and they can be distinguished in activating FcγRI (CD64), FcγRIIA (CD32A), FcγRIIIA (CD16A) which transduce activating signals through ITAMs, and inhibitory FcγRIIB (CD32B) and FcγRIIIB (CD16B) receptors, which instead deliver inhibitory signals through ITIMs (151). FcγRI is expressed by macrophages, DCs, neutrophils and eosinophils (152), while FcγRIIIA is expressed by NK cells, DCs, macrophages and mast cells, and it is required for NK cell-mediated ADCC (152). FcγRIIB can be found on myeloid and B cells,

while FcγRIIIB is exclusively expressed on human neutrophils (150). Upon the antibody binding to the effector cell, tyrosine within the ITAMs on the FcR receptors are phosphorylated by cellular src kinases. Following activation, the effector cells polarize and exocytose their cytotoxic granules in calcium-dependent manner (153). Perforin and Granzyme are two key components of the granules which are released during ADCC to induce cell death. Perforine creates pores within the target cell membrane, facilitating the entry of the granzyme B and other cytolytic substances released by effector cells into the target cells, resulting in DNA fragmentation and apoptosis of the target cell (Fig. 1.13, 154). Another mechanism through which effector cells mediate target cell death is by upregulating Fas ligand expression, aimed to cause apoptosis in the target via Fas signaling (155).
Examples of mAbs whose mechanism of action relies on ADCC include rituximab, trastuzumab, cetuximab and pertuzumab (156).

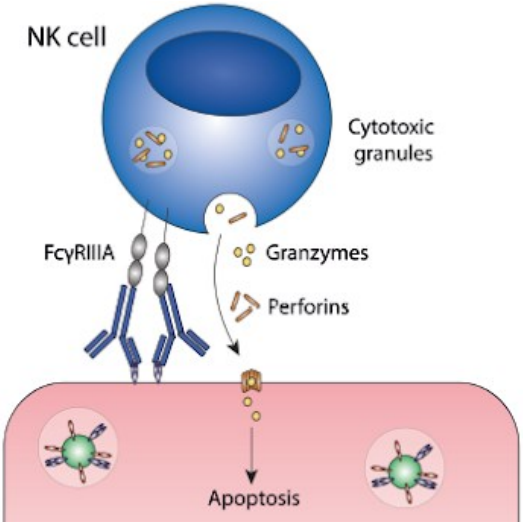

Fig. 1.13. NK cell-mediated ADCC to kill target cells. *The Fab fragment of a mAb binds to the antigen on the target cell, while the Fc portion interacts with the FcγRIIIA expressed on the NK cell. Following the antibody binding, Syk/src family kinases phosphorylate the ITAMs in the FcγRIIIA receptor, resulting in the release of cytotoxic granules containing granzymes and perforins. By creating pores in the target cell surface, perforins help granzymes to enter into the target cells, triggering the apoptosis of the target cell (154).*

Despite the promising development of antibodies targeting TAAs, in recent years, an important shift toward immunomodulatory antibodies which target non-tumor cells in the TME instead of cancer cells has been recorded (157). The first clinical used antibody targeting the TME was specifically against VEGF, aiming to block tumor angiogenesis (158). An important breakthrough in antibody therapy are the ICI antibodies, which target immune checkpoint inhibitors on immune cells to reactivate them to kill tumor cells. T cells are the major immune effector cells that mediate anti-tumor immunity, and PD-1/PD-L1 and CTLA-4 inhibitory receptors on patients' T cells represent the target against which the most recently developed ICIs antibodies are directed (159).

T cell activation requires the recognition of a specific MHC-presented antigenic peptide by the T cell receptor TCR and a co-stimulatory signal from a co-receptor expressed on the target cell (160). T cell activation is blocked when the only TCR signal is present. Other types of suppressive signals on T cells are mediated through the inhibitory receptors CTLA-4 and PD-1 on T cells that bind B71/2 and PD-L1 ligands, respectively, on antigen presenting cells (APCs). However, to inhibit anti-tumor T cell response, cancer cells express B71/2 and PD-L1 ligands. Therefore, antibodies blocking the inhibitory receptors on T cells or their ligands on tumor cells can kill tumor cells by enhancing the tumor-specific T cell response (161).
Research is now focused on expanding the use of ICIs to treat different cancers in combinations with other immunotherapies and to develop immunomodulatory antibodies targeting other known T cell suppression pathways (162).

1.5.2 Antibody subtypes for tumor Immunotherapy

In the evolution of antibody repertoires, while highly variable Fabs are emerging, the sets of constant heavy chains are limited (163). The type of heavy chains define the five human antibody isotypes: IgA, IgD, IgE, IgG, and IgM, and it governs the antibody functional and pharmacokinetics properties (Fig. 1.14, 164). Furthermore, antibody isotypes differ in the glycosylation patterns and, in particolar, in the amounts of N-glycosylation. While all IgG isotypes are N-glycosylated at position N297, which is hidden within the protein, other isotypes are N-glycosylated in different more exposed sites (165). In addition, the length of the hinge region, the number and orientation of disulfide bonds vary among isotypes, resulting in variable flexibility between the two Fab arms and between Fab and Fc regions (165). These differences in the hinge region affect the antibody binding to Fc receptors, and thus, the Fc-mediated effector functions, as well as particular sets of effector functions mediated by the variable antigen binding (166). Infact, the limited scenery of the constant heavy chains endows the variable antigen binding regions with particular sets of effector functions (165).

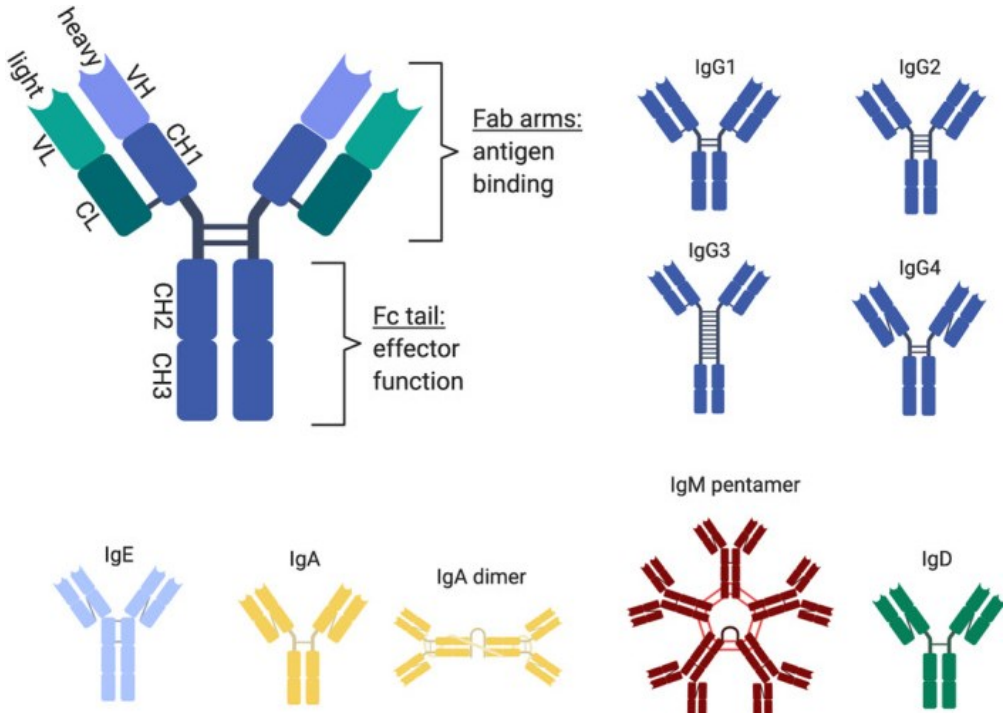

Fig. 1.14. Structure of antibody isotypes*. Human antibodies can be classified into five different isotypes: IgG, IgA, IgM, IgE and IgD. IgG and IgA can be further divided into the subclasses IgG1, IgG2, IgG3, IgG4, and IgA1 and IgA2, respectively. All isotypes have a similar overall structural organization. While the light chain contains one variable domain and one constant domain, the heavy chain contains one variable domain and a different number of the constant domain: IgG, IgA and IgD contain three constant domains (cH1–3), while IgE and IgM four (cH1–4). All the antibodies of the same isotype/subclass contain the identical constant domains (164).*

As previously described, the anti-tumor effects of mAbs and their treatment efficacy rely on different mechanisms of actions, which in turn involve both the Fab arm and Fc-mediated effector functions (165). Therefore, the choice of the optimal antibody isotype for therapeutic applications is dictated by the intended mechanism of action and is a critical point for the therapeutic success of mAbs (165). Currently, many mAbs show therapeutic efficacy in the clinic only in subsets of patients, confirming that the optimal isotype selection and the Fc optimization during the antibody development may be crucial to improve the patient outcome (164).

The IgG class represents the most commonly used mAb-based cancer immunotherapy in clinic, due to its longer half-life and stability into the bloodstream (167). IgG class can be further subdivided into IgG1, IgG2, IgG3, IgG4 subclasses. Up to now, most of the approved mAbs in cancer treatment are of IgG1 isotype (Table 1.2, 168). From *in vitro* experiments, IgG1 showed higher capability than other isotypes to induce mononuclear cell-mediated ADCC (169). Both IgG1 and IgG3 are highly activating with strong Fc-mediated effector functions, due to their capability to bind to all FcRs, but to the activating ones with higher affinity (170). However, IgG3 is not selected as therapeutic mAb because its longer hinge region and polymorphic nature are responsible for the increasing risk of unstability and immunogenicity (171). Most of the effector functions mediated by IgG1 occur via FcγRIIIA

expressed on macrophages and NK cells, resulting in the triggering of ADCC and ADCP (172). On the contrary, IgG2 has limited effector functions, due to its overall poor binding to most FcRs. Also IgG4 is considered a poorly activating isotype because it binds to most activating FcRs and to the inhibitory FcγRIIB receptor with similar affinity (170).

Targeted drugs	IgG subclass	Target	Indications	Mechanism of action	Refs
Rituximab (Rituxan)	IgG1	CD20	NHL	ADCC/CDC	[2]
Trastuzumab (Herceptin)	IgG1	Her2	Breast cancer	Growth signal blocking; ADCC	[3, 4]
Cetuximab (Erbitux)	IgG1	EGFR	mCRC	Growth signal blocking; ADCC	[5]
Bevacizumab	IgG1	VEGF	Solid tumors	Angiogenesis inhibition	[6]
Panitumumab (Vectibix)	IgG2	EGFR	mCRC	Growth signal blocking	[7]
Ofatumumab (Arzerra)	IgG1	CD20	CLL	ADCC/CDC	[8]
Alemtuzumab (Campath)	IgG1	CD52	CLL	ADCC/CDC	[9]
Denosumab (Xgeva)	IgG1	RANKL	Bone tumor	Growth signal blocking	[10]
Ipilimumab (Yervoy)	IgG1	CTLA-4	Solid tumors	Depleting Treg cells	[11, 12]
Pertuzumab (Perjeta)	IgG1	Her2	Breast cancer	Growth signal blocking	[13]
Obinutuzumab (Gazyva)	IgG1	CD20	CLL	ADCC; apoptosis induction	[14]
Ramucirumab (Cyramza)	IgG1	VEGFR2	Solid tumors	Angiogenesis inhibition	[15]
Pembrolizumab (Keytruda)	IgG4	PD-1	Solid tumors	Neutralizing inhibitory signal in T cells	[16]
Nivolumab (Opdivo)	IgG4	PD-1	Solid tumors	Neutralizing inhibitory signal in T cells	[17]
Dinutuximab (Unituxin)	IgG1	GD2	Neuroblastoma	ADCC/CDC	[18]
Daratumumab (Darzalex)	IgG1	CD38	Multiple myeloma	ADCC/CDC; apoptosis induction	[19]
Elotuzumab (Empliciti)	IgG1	SLAMF7	Multiple myeloma	ADCC,direct activation of NK cells	[20]
Atezolizumab (Tecentriq)	IgG1	PD-L1	Solid tumors	Neutralizing inhibitory signal in T cells	[21]
Avelumab (Bavencio)	IgG1	PD-L1	Solid tumors	Neutralizing inhibitory signal in T cells; ADCC	[22]
Durvalumab (Imfinzi)	IgG1	PD-L1	Solid tumors	Neutralizing inhibitory signal in T cells	[21]
Mogamulizumab (Poteligeo)	IgG1	CCR4	CTCL	ADCC	[23]
Cemiplimab (Libtayo)	IgG4	PD-1	Solid tumors	Neutralizing inhibitory signal in T cells	[24]

Table 1.2. List of approved mAbs for cancer therapy and their isotypes/subclasses (168)

Human IgG antibodies also show favorable biotechnological characteristics. In fact, they can be expressed at high protein yield in transfected cells, purified by protein A affinity Chromatography, and can be stored in specific formulations to increase the stability. These features allow to obtain optimal therapeutic agents in compliance with the Good Manufacturing Practice (GMP) (173).
The choice of IgG subclasses strongly depends on the nature of the target. In case of therapeutic mAbs targeting antigen expressed on tumor cells, IgG1 should be the primary antibody format, especially when the Fc-mediated effector function is the main mechanism of action to kill tumor cells (168). Carefully strategies have to be considered to select the isotype in the case of targets expressed by immune cells, in order to avoid to kill them (168). For targets on normal effector immune cells, like PD-1 which is expressed on CD8 T lymphocytes, IgG4 should be the first choice, since it has weak affinity to all FcγRs and, thus, it will not trigger detectable Fc-mediated effector functions able to eliminate the PD-1-expressing CD8 T lymphocytes (168). For this reason, all the currently approved antibodies targeting PD-1 are in the IgG4 format. On the contrary, IgG1 should be preferred to target ICPs expressed in immunosuppressive cells, such as Treg, in order to deplete them via ADCC/ADCP (174). The approved Ipilimumab is an IgG1 antibody targeting CTLA-4, which is expressed on Treg, thus enabling the elimination of Treg from TME (174). As an alternative, some mutations can be introduce in the Fc portion of IgG1 antibodies to reduce their affinity for the FcγRs. In particular,

N297A mutation was among the first one to be described in order to reduce the antibody effector functions, such as ADCC (175).

1.5.3 Targeting CEACAM1: DIATHIS, a human antibody fragment

Advances in molecular biology and genetic engineering techniques have enabled the development of various antibody fragments with potential applications in Cancer Immunotherapy and with different pharmacological properties, such as single-chain variable fragments. The scFv is composed of the variable regions of the heavy and light chains of the intact immunoglobulins, paired by a peptide linker of 10-25 amino acids (Fig. 1.15, 176).

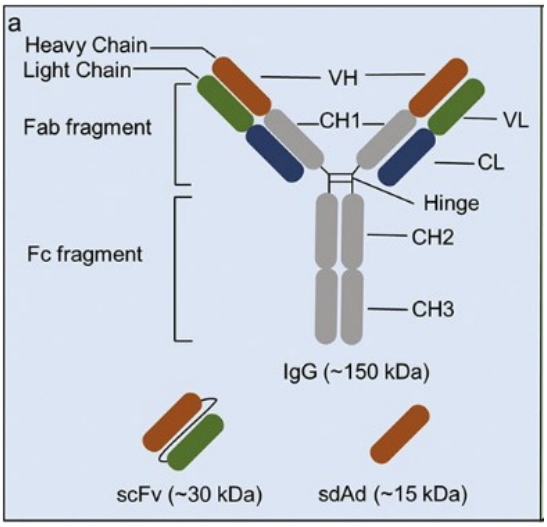

Fig. 1.15. Comparison of the structures of antibody and antibody fragments. *As already seen, the full-length antibody consists of two Fab fragments and one Fc fragment. In contrast, the scFv and the single-domain antibody (sdAd) contain only the antigen-binding domains. The scFv is composed of the vH vL regions, while the sdAd contains only the vH region (176).*

ScFv antibodies show altered physico-chemical features. Due to their smaller size (approximately 25-30 kDa) compared to the full lenght immunoglobulin (150 kDa), scFv antibodies show higher ability of intratumor penetration, providing better opportunities for solid tumor treatment. Also, their short circulation time in the bloodstream makes them suitable for tumor imaging with low background signals. Furthermore, given the lack of Fc fragments, scFvs do not trigger ADCC, ADCP and CDC, and, thus, they are mainly used in anti-tumor immunotherapy to block immune checkpoints targets (176).
In light of the structural advantages of scFv fragments, DIATHEVA s.r.l., in collaboration with the Istituto Superiore di Sanità, developed a human antibody targeting CEACAM1 in the scFv format, called DIATHIS1 (177). scFv DIATHIS1 was originated from the human scFvE8 antibody, which in turn was first isolated from a human scFv displayed phage library (178) by bio-panning approach against the CEA family antigens and then subjected to the affinity maturation process as previously described

(179). DIATHIS showed binding activity to CEACAM1/3/5 antigen expressed on the surface of melanoma cells, by immunofluorescence and flow cytometry studies (177). In addition, co-incubation experiments of effector NK cells with melanoma cells treated with the antibody revealed that DIATHIS enhances the NK cell-mediated cytotoxicity against melanoma cells (180).

However, besides the better penetration into solid tumor tissues, the structure of the scFv is responsible for several drawbacks. Antibody fragments lack the Fc domain, which is important to stabilize full-size antibodies. Compared to the parental mAbs, the scFv fragments show lower thermostability and a higher tendency to aggregate, therefore increasing the risk of immunogenicity (181).

Furthermore, given their size and the lack of the Fc fragment, scFvs have a very short half life (0.5-30h) (182). The rapid renal clearance represents a drawback for therapeutic applications and can entail the need for more frequent and higher doses into patients, resulting in lower efficacy and higher costs. On the contrary, mAbs size (150 kDa) exceed the renal clearance threshold (~70kDa), avoiding them from being eliminated through the kidneys and increasing their serum half-lives (21-24 days). Moreover, the antibody retention in the bloodstream is further increased by the interaction of the Fc portion of IgGs with the neonatal Fc receptor (FcRn) expressed on the surface of several cell types, including vascular endothelium cells, monocytes and macrophages as well as with barrier sites such as the glomerular filter in the kidneys (183). In fact, FcRn plays a crucial role in IgG homeostasis. Most serum proteins undergo pinocytosis and gradual acidification in endosomes, with subsequent fusion with lysosomes and hydrolysis. Differently, upon binding of IgGs to FcRn at low pH, FcRn acts as a protective carrier that transports IgG away from the lysosome and back to the cell surface, where the IgGs dissociate at neutral pH (184).

Considering all these findings, this PhD project was driven by the main goal to convert DIATHIS1 into the fully intact format, aiming to bypass the limits linked to the scFv format and to develop a therapeutic agent with superior pharmacodynamic and pharmacokinetic profiles.

2. OBJECTIVES

This project was aimed to:

1) Develope human cell lines for the stable production of fully human intact anti-CEACAM1 mAbs;

2) Perform comparative structural and functional analyses of anti-CEACAM1 IgG1 and IgG4 antibodies to select the best antibody subclass as therapeutic agent;

3) Characterize the final human antibody-producing cell line;

4) Adapt the cell line to the growth in suspension;

5) Evaluate the *in vitro* antibody efficacy;

6) Assess the *in vivo* binding properties of the antibody in NSG and Tg(CEACAM1)-Tg(CEA) transgenic mice.

3. MATERIALS AND METHODS

3.1 Cells

HEK293 cells, metastatic bladder cancer cell lines (TCC-SUP and 5637) and Natural Killer (NK)-92 cells were from DSMZ (Germany). Metastatic melanoma cell line (MelC), originating from human metastatic melanoma specimens, was obtained from the Department of Therapeutic Research and Medicines Evaluation, Pharmacogenetics (ISS Rome, Italy). Metastatic colon cancer cell line (HT29) was obtained from Mario Negri Institute of Milan (Italy). Human breast cancer (MDA-MB-231) cell line was from ATCC. Murine breast cancer (E0771) cell line was obtained from professor Saul Priceman (Beckman Research Institute, City of Hope, Duarte, California). Murine bladder cancer (MB49) cell line was from professor Hua Wu (Beckman Research Institute, City of Hope, Duarte, California). HEK 293 cells were cultured in DMEM medium supplemented with 10% of inactivated fetal serum bovine (FBS, Sigma), 1mM L-glutamine (Carlo Erba), glucose and 1mM non-essential amino acids (Gibco). MelC and 5637 cells were cultured in RPMI 640 medium supplemented with 10% of FBS and 1mM L-glutamine. TCC-SUP cells were cultivated in DMEM medium with 20% of FBS and 1mM L-glutamine. NK-92 cells require the presence of IL-2 (75 IU/ml, R&D system) for their in vitro growing in α MEM medium supplemented with 10% FBS and 2mM L-glutamine. HT29 cells were cultivated in McCoy's medium with 10% FBS and 1mM L-glutamine. MDA-MB-231, E0771 and MB49 cells were cultured in DMEM medium (Corning) supplemented with 10% of FBS (Sigma) and 1X GlutaMAX (Corning). All cells were grown at 37 °C in a 5% CO2 humidified incubator and with 1X antibiotic-antimycotic solution (Corning).

3.2 Construction of the bicistronic vector for the antibody expression

The encoding gene sequences of scFv Diathis Light Chain (LC), IgG1 Heavy Chain (HC) and IgG4 HC were cloned into three separate pcDNA 3.1 (-) vectors (Genscript). In particular, the designed hinge region-encoding gene sequence of the IgG4 antibody contains the S228P mutation to abolish the Fab-arm exchange process. For both IgG1 and IgG4 subclasses, the bicistronic vector for the simultaneous expression of the HC and LC genes was constructed as follow: the expression cassette bearing the CMV promoter, LC encoding gene and the polyA chain was amplified by PCR with the primer CMV BglII Fw, containing the sequence of the BglII restriction site, and the primer BGH PA NruI Rev, bearing the NruI restriction site sequence. The amplified expression cassette of the LC gene as well as the pcDNA 3.1 (-) vector bearing the IgG1 or IgG4 HC encoding gene, were digested by BglII (10U/µl) and NruI (10U/µl) restriction enzymes (Thermo Fisher) for 2,5 hours at room temperature (RT). The digested insert and vector were mixed and ligated by T4 ligase (10U/µl, Thermo Fisher) for 1 hour at RT. The ligation reaction was then transformed in E. coli DH5α competent cells.

In vitro mutagenesis of the developed bicistronic vector for the IgG1 antibody expression was performed by using the GenArt Site-Directed Mutagenesis System (Thermo Fisher), according to the the manufacturer's instructions. Briefly, primers were designed to introduce the N297A substitution in the Fc region of the wild type IgG1-expression plasmid. PCR was performed on the plasmid DNA (20ng/ml) using the AccuPrime™ Pfx DNA Polymerase supplied by the kit. The PCR product was then transformed in E. coli DH5α competent cells. High Resolution Melt (HRM) analyses were performed to screen the mutant transformed competent cell colonies. The insertion of the desired mutation was confirmed by sequencing.

3.3 Development of the antibody-producing stable cell line

Human Embryonic Kidney (HEK) 293 cells were used for the stable cell transfection to generate the IgG1 and IgG4 antibody-producing cell lines. The day before transfection, HEK293 cells were seeded at the final density of $10x10^5$ cell/ml in DMEM medium in wells of a 6 multiwell plate. The bicistronic vector was linearized by enzymatic digestion with ScaI (10U/µl, Thermo Fisher) for 4 hours at 37°C. The digested product was purified by the QIAquick PCR Purification kit (QIAgen). 1 µg of linearized DNA was mixed with basic DMEM medium and gene cellin (EuroBio). The mixture was incubated 15 minutes at RT to enable the formation of DNA-liposomes complexes and then gently added drop by drop to each well. 48 hours after the transfection, 0,5 µg/ml of the selection antibiotic G418 (Roche) was added to the transfected cell culture medium. Following two weeks of antibiotic selection, 100 µl of surnatant collected from each cellular pools were screened by ELISA assays against the human recombinant N-terminal + A1 constant Ig-like domains of CEACAM1 antigen (DIATHEVA s.r.l.). The cellular pool with the highest absorbance value was diluted by limiting dilution method in DMEM with 0,5 µg/ml G418 in three 96 multiwell plates, in order to theoretically seed 0.5 cell into each well. After 15 days of G418 selective pressure, 100 µl of supernatant collected from each grown clone were tested by ELISA assay, to identify the highest antibody-producing clone. The selected clone was in turn subjected to the single cell cloning, and following two weeks of antibiotic selection, the final best performing sub-clone was selected by ELISA test.

3.4 ELISA assay

96-well plates (High Binding, Thermo Fisher) were coated with 100 µl/well of 1 µg/ml of human N-terminal + A1 domain fragment of CEACAM1 antigen diluted in PBS1X and incubated at 37°C for 16–17 hours. Plates were washed five times with PBS1X containing 0,05% v/v of Tween-20 (TPBS) and then blocked with 150 µl/well of PBS1X containing 1% w/v of bovine serum albumin (PBSB) for 1 hour at 37°C. Upon five TPBS washes, coated plates were stored at 4°C. Coated plates were equilibrated at RT the day of the assay. 100 µl of each surnatant collected from the cellular transfected pools were added to the wells of CEACAM1 antigen-coated 96-well plate. For the antibody titration, the antibody was diluted in PBSB and 100 µl/well of serial antibody dilutions ranging from 100 µg/ml to 0,00038 µg/ml were added to the coated antigen. The plate was incubated for 90 minutes at 37°C. Following

five TPBS washes, 100 µl/well of mouse anti-Human Fc antibody (Meridian) diluted 1:500 in PBSB were added to the wells and incubated 1 hour at 37°C. 30 minutes after the addition of 100 µl/well of ABTS substrate (Surmodics), the absorbance values were recorded at 405 nm on a microplate reader.

3.5 Antibody purification by Protein A Affinity Chromatography

The stable cell clone expressing the antibody was maintained in culture for 9 days starting from an initial density of $2.5x10^5$ cells/ml. The first two days the incubator was set at 37°C, and the other seven at 30°C. Then, cell supernatants were collected and centrifuged at 1660 x g for 20 minutes using a centrifuge (Thermo Scientific). Protein A Affinity Chromatography was used for the antibody purification. 1 ml MabSelect PrismA protein A resin (Cytiva) was equilibrated with five column volumes (CV) of 0.1M phosphate buffer with 5 mM EDTA pH 7.8. Cell supernatant was diluted 1:2 in phosphate buffer with 10mM EDTA pH 7.8. The diluted supernatant was loaded into the column and at 1ml/min flow rate. Column was washed with different buffers in the following order: 5mM EDTA phosphate buffer, 5mM EDTA phosphate buffer with 0.65M NaCl pH 7.8, 5mM EDTA phosphate buffer with 0.65M NaCl and 5% (v/v) IPA, pH 7.8. The antibody was eluted in 0.1 M Sodium citrate, 0.15M NaCl and 2% (v/v) glycerol (pH 3). The antibody was neutralized with 2M Tris and its concentration was determined by recording the absorbance value at 280 nm. A buffer exchange with PBS was performed by using a centrifugal filter with a cut-off of 30kDa (Merck Millipore).

3.6 Reducing and non reducing SDS-PAGE

5 µg of the antibodies were diluted in Sample Buffer with or without β-mercaptoethanol to analyze the antibody at the reducing and non reducing conditions, respectively. Samples were boiled for 5 minutes, loaded on a 10% of polyacrylamide gel and ran at 100 V. The samples were visualized by staining with Coomassie brilliant blue.

3.7 Size Exclusion- High Performance Liquid Chromatography (SEC-HPLC)

Size Exclusion-High Performance Liquid Chromatography (SEC-HPLC) was used to evaluate the antibody structure. SEC was performed with the HPLC Jasco LC-4000 system using a TSK Gel G3000SW_{xL}L x I.D. column equilibrated with 0.1mol/L Na_2SO_4 + 0.05% NaN3 in 0.1mol/L Phosphate buffer, pH 6.7 at a flow rate of 0.5-1 ml/min. 100 µl of purified antibodies were injected into the column and the measurement of the absorbance at 280nm was used to detect the antibody. In order to estimate the antibody molecular wight, the system was calibrating by proteins of known molecular weight to build a standard curve: BSA 67,000 Da, Ovalbumin 43,000 Da, Ribonuclease 13,700 Da,

Aprotinin 6,512 Da, Vitamin B12 1,355 Da. Results were analyzed by using the software ChromNAV Ver.2-Spectra Manager.

3.8 Endotoxin level assessment

Limulus amebocyte lysate (LAL) gel clot assay was used to semiquantitatively determine the l endotoxin level contained within the purified antibody formulation by following the manual's instructions. Briefly, dilutions of the antibody in endofree water were prepared and 1ml of each dilution was added to separate tubes containing the Limulus Amebocyte Lysate. The tubes were incubated 30 minutes at 37°C without lids. After incubation, each tube was inverted 180°C. The antibody sample was considered negative for the presence of the endotoxins in case there was no formation of a solid clot after the tube inversion.

3.9 Adaptation of adherent cells to the suspension growth

The antibody producing stable cell line was adaptated to the growth in suspension in serum-free chemically defined medium (CDM4HEK, Cytiva). To do so, a sequential method was applied, which consists in gradually switching the cells from the serum-supplemented medium into the serum free medium (SFM) in several steps:

Passage	% serum supplemented medium (DMEM)	% serum-free medium (CDM4HEK)
1	75	25
2	50	50
3	25	75
4	12,5	87,5
5	6,25	93,75
6	3,125	96,87
7	1,56	98,43
8	0,78	99,22

At each step, cells were counted by Trypan Blue Exclusion method and seeded to the final density of $5x10^5$ cell/ml in the proper combination of media. Cells were kept in the same media conditions at least for 2 passages. Cells were passaged to the following step only if >90% of viability was recorded. Starting from the passage in 25:75 serum supplemented:SFM, cells were put on the orbital shaker at 100 rpm at 37°C to facilitate the adaptation process. To ensure a complete cell adaptation, cells were carried for 6-7 passages in 100% SFM medium.

3.10 Development of stable hCEACAM1 or hCEA-expressing murine bladder cancer and murine breast cancer cell lines

3.10.1 Transfection of murine bladder and breast cancer cells

Murine bladder cancer (MB49) and murine breast cancer (E0771) cells were transfected with plasmids by using the Lipofectamine 3000 Transfection Reagent kit (Thermo Fisher Scientific), according to the manufacturer's instructions. The day before transfection, cells were plated at the final density of $1x10^5$ cell/well in DMEM medium in wells of a 24-well plate. 1 µg of hCEACAM1 or 1µg of hCEA expression plasmids (Beckman Research Institute, City of Hope, Duarte, California) and 2 µl of P3000 reagent were diluted in 50 µl of DMEM. 0,75µl of lipofectamine 3000 were diluted in 25 µl of DMEM. 25 µl of each dilution mixture were mixed together 1:1 and the final volume was incubated 15 minutes at RT. 50 µl of the final mixture were added drop by drop into each well. 72 hours after the transfection, the selective antibiotic Geneticin (Gibco) was added to the transfected MB49 and E0771 cells at the final concentration of 1 µg/ml or 0.5 µg/ml, respectively.

3.10.2 Flow cytometry analysis for the screening of the transfected cellular pools

Following two weeks of antibiotic selective pressure, the cellular transfected pools were screened by flow cytometry analysis. For each pool, $5x10^5$ cell/ml were washed with PBS and centrifuged at 310 x g for 5 minutes. Cells were resuspended in 100 µl of PBS and incubated with or without 5µl of aCC1 (anti-hCEACAM1 antibody, R&D) or aCEA (anti-hCEA antibody, R&D) 30 minutes on ice. After the staining, cells were washed and resuspended in 500 µl of PBS. Samples were analyzed into the Flow Cytometer (BD LSRFortessa X-20) by recording a total of 10,000 events.

The pools with the highest percentage of hCEACAM1 or hCEA expressing cells were cultured in DMEM with Geneticin. When reached the confluence in T25 flasks, cells were FACS sorted. $2x10^6$ cell/ml were harverested, washed and stained with 5 µl of CC1 or aCEA antibodies. Samples were then washed, resuspended in 1ml of PBS and sorted by the cell sorter (BD FACSAria FUSION). After purity assessment, sorted cells were expanded in DMEM with Geneticin.

3.11 *In vitro* efficacy studies

3.11.1 Evaluation of DIA 12.3 binding activity by flow cytometry analysis

Flow cytometry analyses were carried out to test the reactivity of the antibody against human CEACAM1 antigen expressed on the surface of tumor cells, including metastatic melC, HT29, TCCSUP and 5637 cancer cells. The day prior to the flow cytometry test, tumor cells were plated at the final density of $5x10^5$ cell/ml in 3 ml/well of their medium in wells of a 6 multi-well plate. The day of the

assay, the media was aspirated from each well, cells were washed twice with PBS1X and incubated for 90 minutes at 37°C alone or with the antibodies diluted in PBS1X with 1% w/v of BSA. Following the treatment, cells were collected in FACS tubes, washed with 3 ml/tube of PBS1X and centrifuged for 8 minutes at 260 x g. Supernatants were aspirated and cells were resuspended again in 3 ml of PBS1X for a second wash. Cells were then resuspended in 500 µl of PBS1X containing 0.5% w/v of BSA and 1:1000 (v/v) diluted FITC goat anti-Human Fc secondary antibody (Abcam) and incubated for 1 hour at 37°C. After the staining, samples were washed, resuspended in PBS and analyzed with a Flow Cytometer (Becton-Dickinson, NJ).

3.11.2 Lactate Dehydrogenase (LDH) cytotoxicity assay to assess NK cell-mediated cytotoxicity

To evaluate the capability of the antibody to affect the NK-92 cell cytotoxicity against tumor cells, we performed LDH-Glo™ Cytotoxicity Assays (Promega). This assay is a bioluminescence method that quantifies the enzymatic activity of the lactate dehydrogenase (LDH), a widely used marker of cytotoxicity, which is released in the cell culture surnatants upon cell membrane destruction. Target tumor cells were harverested, washed and resuspended at the final density of $2x10^5$ cells/mL in basic DMEM with 5% v/v of FBS. Target cells were incubated alone or in the presence of the anti-CEACAM1 antibodies for 30 minutes at RT. Meanwhile, NK-92 cells were firstly diluted at $2x10^6$ cell/ml in basic RPMI medium with 5% v/v of FBS and then serially diluted ranging routinely from $1x10^5$ to $1x10^3$ cells. 50 µl/well of each NK-92 cell suspension dilution were seeded in 96 white walled assay plates, in triplicate. Following the antibody treatment, 50 µl/well of the target cell suspension were then added to the effector NK-92 cells at increasing effector/target cell ratio ranging from 1:1 to 10:1 in triplicate. Positive controls were used by adding 2 µl/well of TritonX-100 to determine the maximum LDH release, while triplicate wells without cells were set up to serve as negative control to determine the culture medium background. The plate was incubated for 4 hours at 37°C. 5 µl of supernatants from each well were collected and diluted in 95µl of LDH Storage buffer. The diluted samples were then stored at -20°C and the day of the assay they were further diluted in the LDH Storage Buffer to fit the linear range of the assay. 50µl of the diluted samples were transferred into a 96-well opaque, non transparent assay plate. 50 µl of the LDH Detection Reagent were then added in each well and the plate was incubated at RT for 60 minutes. Luminescence was recorded from 30 to 60 minutes after the addition of the LDH reaction agent. The % of cytotoxicity was calculated as follows:

100 × (Experimental LDH Release – Medium Background) / (Maximum LDH Release Control – Medium Background).

3.11.3 Human Neutrophil isolation and enrichment

Fresh blood samples were obtained from healthy donors at City of Hope Blood Donor Center (Duarte, California). The blood was mixed with an equal volume of 0,9% NaCl (Cytiva) with 3% of dextran and incubated 20 minutes at RT to allow the differential sedimentation of red blood cells (RBCs). The

leukocyte-rich and RBC poor plasma layer was saved and centrifuged 10 min at 250 x g at 5°C. The cell pellet was resuspended in a volume of 0,9% NaCl equal to the starting volume of blood. The cell suspension was then layered above 10 ml of Hypaque-1077 (Sigma) and centrifuged 40 minutes at 400 x g at 20°C, with no brake. After the aspiration of the top and the hypaque layers, the RBC/neutrophil pellet was subjected to the hypotonic lysis in 10 ml of cold 0,2% NaCl for 20 seconds to remove the remaining RBCs. The isotonicity was restored by adding 10 ml of ice-cold 1,6% NaCl. Cells were then centrifuged 6 minutes at 250 x g at 5°C and the pellet was resuspended in ice-cold PBS. The isolated sample was enriched with neutrophils by using the EasySep Human Neutrophil Isolation kit (StemCell). Briefly, the cell suspension was resuspended to a final concentration of 5 $x10^7$ cell/ml in PBS + 2% FBS and 1mM EDTA. Human Neutrophil Enrichment Cocktail was added to the tube at 50 µl/ml and incubated at 4°C for 5 minutes. Following the addition of Nanoparticles at 40 µl/ml cells, the cell suspension was further incubated at 4°C for 3 minutes. The recommended medium was added to bring the suspension to a total volume of 2,5ml and the tube was then placed into the magnet for 5 minutes. The suspension was poured off into a new tube. In this way the magnetically labeled unwanted cells remained bound inside the original tube, held by the magnetic field. The purity of the enriched neutrophil population was assessed by flow cytometry using the APC-conjugated mouse monoclonal antibody against CD66b (Biolegend). In total, 10,000 events were recorded.

3.11.4 Apoptosis detection of neutrophils

FITC Annexin V Apoptosis Detection kit with Propidium Iodide (PI) (Biolegend) was used for the apoptosis detection of neutrophils upon the incubation with or without 10 µg/ml of DIA 12.3 antibody in RPMI at 37°C, at the following time points: 0, 1, 2, 16, 18 and 20 hours. After the antibody treatment, neutrophils were washed with PBS and resuspended in Annexin Binding Buffer at the final concentration of $1x10^6$ cell/ml. 100µl of cell suspension were incubated with 5µl of FITC Annexin V and 10µl of Propidium Iodide Solution 15 minutes at RT in the dark. After the addition of 400 µl of Annexin V Binding Buffer to each tube, the samples were analyzed by flow cytometry with proper machine settings. In total, 10,000 events were recorded per each time point.

3.11.5 Detection of neutrophil-released NO_2^-

Isolated neutrophils were harverested, washed, counted and resuspended at the density of $2x10^6$ cell/ml in RPMI medium. Neutrophils were then serially diluted to $1x10^6$ cell/ml and $2x10^5$ cell/ml. Tumor cells were harverest, counted and resuspended at the final density of $2x10^5$ cell/ml in RPMI medium. 50µl of neutrophil suspension were seeded with 50µl of tumor cell suspension in the wells of a 96-multiwell plate at the following effector:target cell ratios, in duplicate: 10:1, 5:1, 1:1. For each effector:target cell ratio, three different treatment conditions were tested:

- Neutrophils pre-treated with or without 10 µg/ml of DIA 12.3 for 30 minutes at 37°C and then co-incubated with hCEACAM1-expressing MDA-MB-231 cells for 4 hours at 37°C;
- hCEACAM1-expressing MDA-MB-231 cells pre-treated with or without 10 µg/ml of DIA 12.3 for 30 minutes at 37°C and then co-incubated with neutrophils for 4 hours at 37°C;
- Neutrophils and hCEACAM1-expressing MDA-MB-231 cells were co-treated with or without 10 µg/ml of DIA 12.3 for 4 hours at 37°C.

Following the treatment, the Griess Reagent System (Promega) was used to detect NO_2- produced and released by neutrophils into the cell culture medium.

In order to accurately quantify the NO_2^- levels in the experimental samples, a nitrate standard reference curve was prepared by performing 6 serial twofold dilutions (50 µl/well) of a 100 µM nitrite solution. 50 µl of the Sulfanilamide Solution were added to the wells containing 50 µl of each experimental sample in duplicate and 50 µl of the dilution series for the Nitrite Standard reference curve. The plate was incubated 10 minutes at RT, protected from the light. 50 µl of NED Solution were dispensed to all the wells and the plate was again incubated for 10 minutes at RT in the dark. The absorbance values from each well were recorded at 520nm within 30 minutes in a plate reader.

3.12 *Ex vivo* studies

3.12.1 Extraction of immune cells from hCEACAM1 Knockout and hCEACAM1 Transgenic mice

CEACAM1 Knockout (KO) and Tg(hCEACAM1) mice were anesthetized and dissected to collect a 2mm approx. piece of the spleen and the blood by cardiac puncture. Blood samples were lysed to remove RBCs, by mixing the samples with sterile water five times. The lysis reaction was neutralized by adding PBS2X. The cell suspension was centrifuged at 350 x g for 5 minutes and the pellet was resuspended in PBS. The spleen was placed into the cell strainer previously rinsed with 2.5 ml of PBS. The spleen was mashed by using the plunger base of a syringe. PBS was poured on the filter until the spleen was completely mashed. The suspension was then centrifuged at 350 x g for 5 minutes and the pellet was resuspended in Red Blood Cell Lyses Buffer (Sigma). After 5 minutes of incubation at RT, the lyses reaction was stopped with PBS and the cell suspension was spinned down at 350 x g for 5 minutes. The final pellet was resuspended in PBS.

3.12.2 Enrichment of murine neutrophils

Neutrophils from the collected murine blood sample were enriched by using the Mouse Neutrophil Enrichment Kit (Stemcell). The cell suspension was resuspended to a final concentration of $5x10^7$

cell/ml in PBS + 2% FBS and 1mM EDTA. After the addition of 50 µl/ml of Normal Rat serum and 50 µl/ml of Mouse Enrichment cocktail, cells were incubated at 4°C for 15 minutes. Cells were then centrifuged at 300 x g for 10 minutes and the pellet was resuspended in the recommended medium with 50 µl/ml of Biotin Selection Cocktail. After 15 minutes of incubation at 4°C, 150 µl/ml of D Magnetic Particles were added and the suspension was incubated at 4°C for 10 minutes. The recommended medium was added to bring the cell suspension to a final volume of 2,5 ml and the tube was then placed into the magnet for 3 minutes. The cell suspension was poured off into a new tube. In this way the magnetically labeled unwanted cells remained attached to the tube, held by the magnetic field.

3.12.3 hCEACAM1 expression studies by flow cytometry

100µl of lysed blood, enriched neutrophil and spleen cell suspension deriving from the CEACAM1 KO mouse and Tg(hCEACAM1) mouse were separetely stained with three mixtures of antibodies:

-antiCD19-FITC, antiCD11b-PE, antiCD3-Pecy7, antiLy6G-BV605 (all Biolegend), DIA 12.3;

-antiCD19-FITC, antiCD11b-PE, antiCD3-Pecy7, antiLy6G-BV605, aCC1 (R&D);

-antiCD19-FITC, antiCD11b-PE, antiCD3-Pecy7, antiLy6G-BV605.

Following 30 minutes of incubation on ice, cells were washed with PBS and incubated with anti-human Fc antibody (1:2000, R&D) for other 30 minutes on ice. A total of 10,000 events were acquired in the live gate on the flow cytometer.

3.13 *In vivo* studies

3.13.1 Animal experiments

Animal studies were performed in accordance protocol 91037 approved by the City of Hope Institutional Animal Care and Use Committee, in accordance with the National Institute of Health Office of Laboratory Animal Welfare guidelines.

3.13.2 NSG mice

$5x10^6$ cell/ml of human breast cancer cells from parental, hCEACAM1 and hCEA-expressing MDA-MB-231 cell lines were harverested, washed twice with PBS and resuspended in 250µl of PBS and 250µl of matrigel (Corning). For each cell line, 50µl of cell suspension (500 000 cells) were injected into the mammary fat pad of eight week-old NOD.Cg-Prkdc scid Il2rg tm1Wjl/SzJ (NSG) female mice (Jackson Laboratory) (n=3), previously anhestetized with isoflurane.

3.13.3 Transgenic mice

Double transgenic mice expressing hCEACAM1 and hCEA antigens were developed by Dr. Shively's group (185). $4x10^6$ cell/ml of murine bladder cancer cells from parental, hCEACAM1 and hCEA-expressing MB49 cell lines were harverested, washed twice with PBS and resuspended in 360µl of PBS and 40µl of matrigel. For each cell line, 50µl of cell suspension (500 000 cells) were subcutaneously injected into eight week-old transgenic male mice (n=1 for parental cells, n=2 for hCEACAM1+ or hCEA+ MB49 cell lines), previously anesthetized with isoflurane.

3.13.4 Antibody conjugation to DOTA molecule and radiolabeling

20-fold excess of DOTA-NHS (220 nmol, Macrocyclics, TX) in 4.5µl of H_2O was added to 1.65mg (11 nmol) of Dia 12.3 antibody in 2.5 ml of PBS1X, and the pH was adjusted to 7.36 with 0.1N NaOH. The reaction solution was rotated at the RT under Argon overnight. Then the reaction mixture was dialyzed against the PBS1X buffer with five times and sterile filtered. Dota conjugation was confirmed by Instant Thin Layer Chromatogram (ITLC) performed by the Radiopharmacy Department at City of Hope. 100 µg of DOTA-DIA 12.3 was radiolabeled with 1 mCi or 10 mCi of $^{64}CuCl_2$ in 0.1 M HCl at pH 4.5 by adjusting the pH with 0.2, ammonium acetate. The product was purified by Size-Exclusion Chromatography by the Radiopharmacy Department at City of Hope.

3.13.5 PET Imaging and Biodistribution studies

Three weeks after the MDA-MB-231 cell injection, tumor-bearing NSG mice were injected into the tail vein with a single intravenous dose in the range of 113-120 µCi of 6,4 µg/mouse of ^{64}Cu-DOTA-labeled DIA 12.3 in 1% human serum albumin–buffered saline, after receiving a single intraperitoneal injection of 1 mg in 0.1ml of PBS of intravenous immunoglobulin (IVIG) 2 hours beforehand. In the second PET experiment with NSG mice, DOTA-DIA 12.3 was radiolabeled with 10 mCi of $^{64}CuCl_2$ in 0.1 M HCl at pH 4.5. 6,4 µg/mouse of ^{64}Cu-DOTA-labeled DIA 12.3 with 100 µCi of product per 10 µg + 30 µg/mouse of unlabeled DIA 12.3 antibody were injected in NSG mice. Two weeks after the MB49 cell injection, tumor-bearing Tg(hCEA)-Tg(hCEACAM1) mice were injected into the tail vein with a single intravenous dose in the range of 113-120µCi of 6,4 µg/mouse of ^{64}Cu-DOTA-labeled DIA 12.3 + 30 µg/mouse of unlabeled DIA 12.3 antibody in 1% human serum albumin–buffered saline. Shortly before scanning, mice were anesthetized with isoflurane and then imaged in a prone position on a GNET PET/CT scanner (SOFIE BIOSCIENCES) at various time points post injection (4, 24 and 44-48 hours post injection). Images were reconstructed as previously described (186) by using AMIDE software. Immediately after completion of the final scan, mice were sacrificed and dissected for biodistribution analyses. The tumor and various major organs (blood, liver, spleen, kidneys, lungs and carcass) were excised, weighted and assayed for radioactivity using an automatic calibrated gamma counter (Wizard). The percentage of injected activity dose per gram of tissue (%ID/g) was calculated for each specimen.

4. RESULTS AND DISCUSSION

4.1 Development of the antibody-producing stable cell line

In this project, DIATHIS1, a human anti-CEACAM1 antibody previously developed by DIATHEVA s.r.l., in collaboration with the Istituto Superiore della Sanità (Rome, Italy), in the single chain variable fragment format (scFv), was converted into a fully intact IgG1 and IgG4 antibodies, aiming to circumvent the scFv fragment limits due to their small size and the lack of the Fc fragment. For this aim, a bicistronic vector for the simultaneous expression of the Light Chain (LC) and the IgG1 or IgG4 Heavy Chain (HC) encoding genes, was created as illustrated in the scheme (Fig. 4.1). In the final construct, the expression of the heavy as well as the light chain was driven by the CMV promoter. The N-terminal portion of the two genes was fused with a peptide signal sequence (SP) that enabled the exportation of the antibody in the culture medium. The vector contained the neomycin resistance gene allowing the selection of positive clones with the addition of G418 to the culture media.

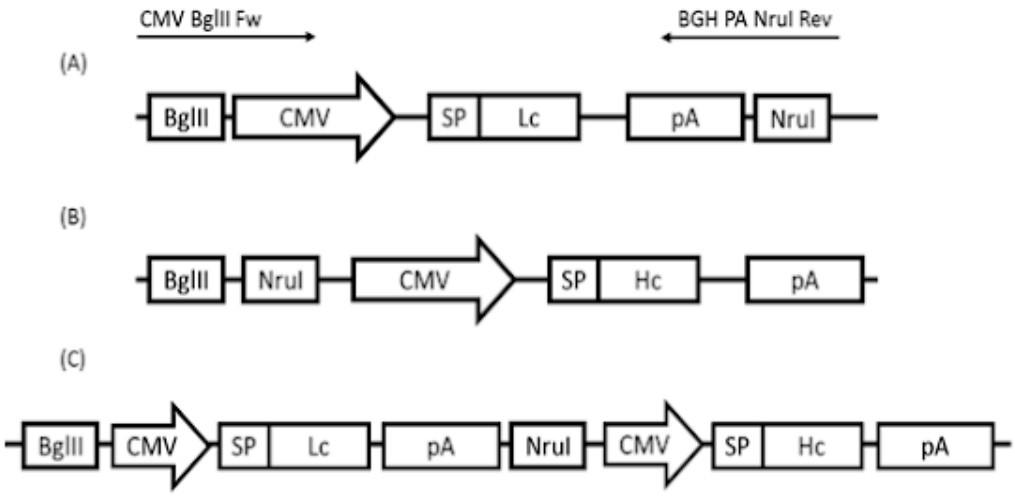

Fig. 4.1. Schematic representation of the bicistronic vector for the IgG antibodies expression: three separate pcDNA 3.1 (-) vectors were used to clone the encoding gene sequences of scFvDiathis LC, IgG1 and IgG4 HC. (A) The expression cassette bearing the CMV promoter, scFvDIATHIS1 LC encoding gene and the polyA chain, was amplified by PCR in order to add the sequence of BglII and NruI restriction sites, upstream and downstream the LC gene, respectively. The PCR product and the vector bearing the IgG1 or IgG4 HC encoding gene were both digested by BglII and Nru restriction enzymes. The digestion was followed by the ligation reaction to finally develop the bicistronic vectors for the simultaneous expression of the LC and the HC.

Once confirmed by sequencing the correct sequences of the genes encoding the full lenght IgG1 and IgG4 antibodies, the vectors were used for the stable transfection of the HEK293 cells. After two weeks of antibiotic selective pressure, the harvested cellular pools were tested with an ELISA assay for the antibody titer against the N-terminal + A1 domain fragment of CEACAM1 antigen (Fig. 4.2a).

The highest antibody-producing cellular pools were subjected to limiting dilution cloning. The highest expressing clones among the 24 IgG1-producing clones and 19 IgG4-producing clones were identify (Fig. 4.2b). The selected clones were subcloned by limiting dilution and the ELISA screening allowed to identify the #12.3 and #2.1 as final stable cell lines for the production of IgG1 and IgG4 antibodies, respectively (Fig. 4.2c).

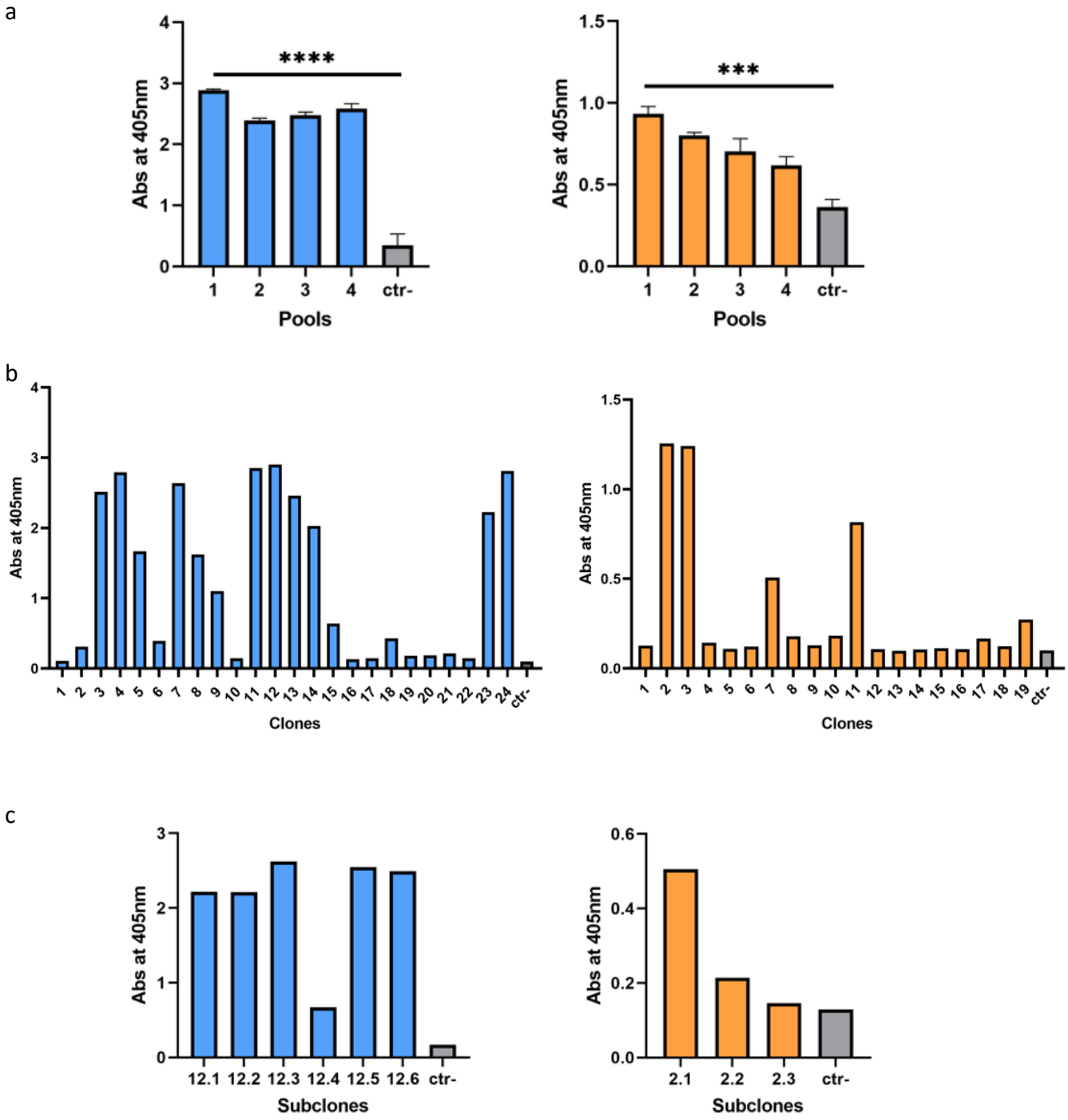

Fig. 4.2. Development of stable cell lines expressing anti-CEACAM1 IgG1 and IgG4 antibodies. The barplots show the absorbance values obtained by ELISA assays on 100 µl of the supernatants collected

from the transfected cellular pools (a), clones (b) and subclones (c) for the production of the IgG1 (blue) and IgG4 (orange) antibodies.

4.2 Structural and biological comparison between IgG1 and IgG4 anti-CEACAM1 antibodies

For preliminary studies, IgG1 and IgG4 antibodies were purified by Protein A Affinity Chromatography from 250 ml of supernatant collected respectively from the HEK293 cell subclone #12.3 and #2.1. The protein yield obtained for the IgG1 antibody (10,48 mg per 1L of surnatant) was about 10 fold higher compared to IgG4 (1,9 mg/L).

Structural analysis on fresh purified antibodies by SEC-HPLC revealed that both the subclasses had a monomeric conformation with a high purity degree, with a lack of molecular aggregates (Fig. 4.3). SDS-PAGE under reducing conditions confirmed the correct molecular size of two bands corresponding to the heavy and the light chains, for both IgG1 and IgG4 antibodies (Fig. 4.4). Despite the structural integrity highlighted by SEC-HPLC analysis, the SDS-PAGE under non reduced conditions revealed the presence of additional species of the antibodies for both the subclasses, such as dimers of the heavy chains, suggesting the incomplete formation of H-L disulfide bonds. These findings suggested that the optimization of the purification protocol is needed to increase the purity of the final purified product.

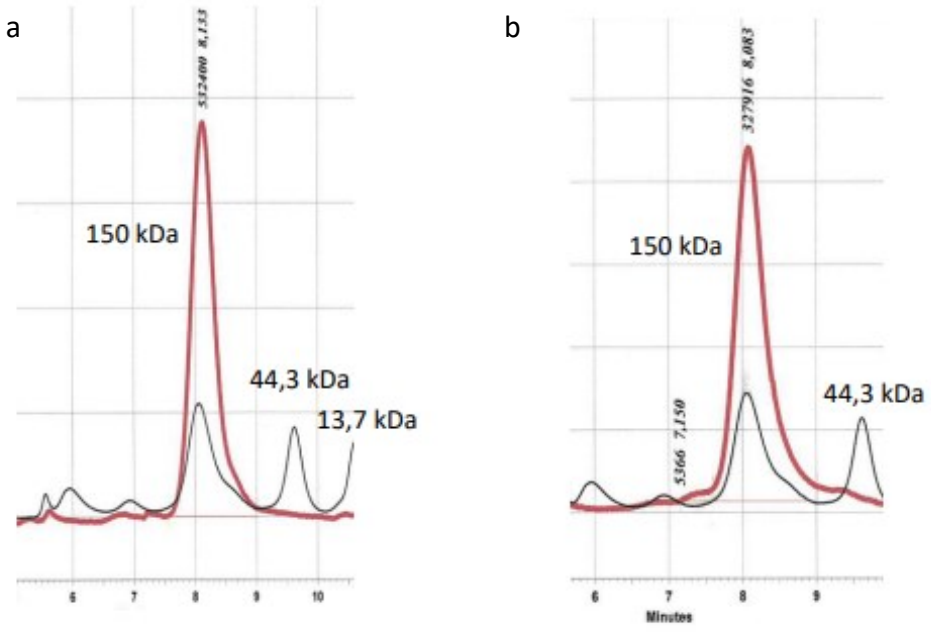

Fig. 4.3. SEC-HPLC analysis of IgG1 and IgG4 antibodies*. Chromatograms were obtained by using TSKgel G30 00SWxl resin in isocratic condition. The molecular weights were calculated based on a standard curve obtained by calibrating the system with molecules of known molecular weight:*

thyroglobulin 660 kDa, gamma-globulin 150 kDa, ovalbumin 44.3 kDa, ribonuclease A 43.7 kDa, 4-aminobenzoic acid 13.71 kDa.

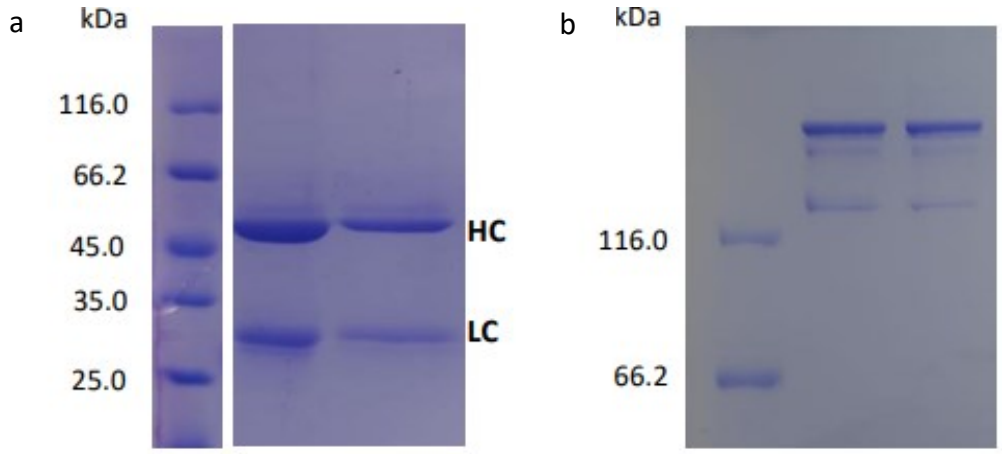

Fig. 4.4. SDS-PAGE analysis of purified IgG1 and IgG4 antibodies. *5µg of purified antibodies were loaded on a 10% polyacrylamide gel and analyzed by SDS-PAGE under reducing (a) and non reducing conditions (b). Order of loading samples: MW marker, IgG1, IgG4.*

However, IgG1 antibody showed higher structural stability than IgG4, after eight months of storage at 4°C. In fact, differently from IgG1, IgG4 antibody showed the presence of a band with a molecular weight higher than the band corresponding to the heavy chain, in non reduced SDS-PAGE analysis performed eight months after the purification (Fig. 4.5). Furthermore, IgG4 formed aggregates that precipitated and were visible by eyes (data not shown).

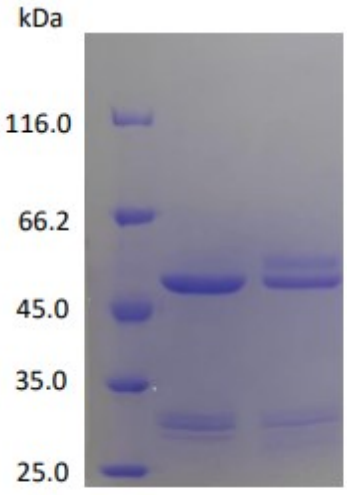

Fig. 4.5. SDS-PAGE analysis of IgG1 and IgG4 antibodies eight months after the purification. *5µg of IgG1 and IgG4 antibodies stored at 4°C were analyzed on 10% polyacrylamide gel. Order of loading samples: marker, IgG1, IgG4.*

These results are in line with previous findings showing that IgG4 has lower thermostability than IgG1 and that more likely undergoes aggregation and thermal denaturation, due in part to differences in the disulfide bond network between the heavy chain and the light chain of IgG1 and IgG4 (187, 188). Although the two subclasses share high degree of amino acidic sequence similarity in the constant region of both heavy chain and light chain, they show differences in the hinge region in terms of length and flexibility. In fact, IgG4 has a hinge region shorter and with lower flexibility than IgG1. Furthermore, it is known that IgG4 undergoes to a process called Fab-arm exchange, where a half molecule (composed by one heavy and one light chain) dissociates and interacts with an other half molecule to form a full antibody (187, 188). To prevent this problem, the known S228P mutation was inserted in the hinge region of the anti-CEACAM1 IgG4, since it has been reported to be able to abolish the Fab-arm exchange. However, the observed IgG4 instability and tendency to form aggregates during months after the purification, may be also due to a partial reduction of the Fab-arm exchange. In fact, studies revealed that the reverse mutation P228S (the corresponding residue found in IgG1) in IgG1 did not induce Fab-arm exchange, suggesting that this dynamic process does not exclusively depend on the hinge region (188).

To evaluate the binding activity, serial dilutions of the IgG1 and IgG4 antibodies ranging from 100 µg/ml to 0,00038 µg/ml were tested by ELISA titration assay on 96 multi-well plates coated with 1 µg/ml human N-terminal + A1 domain fragment of CEACAM1 antigen. Results showed that both IgG1 and IgG4 antibodies bound the antigen in a dose-dependent manner, but IgG1 showed a higher binding activity compared to IgG4 at equal doses. (Fig. 4.6).

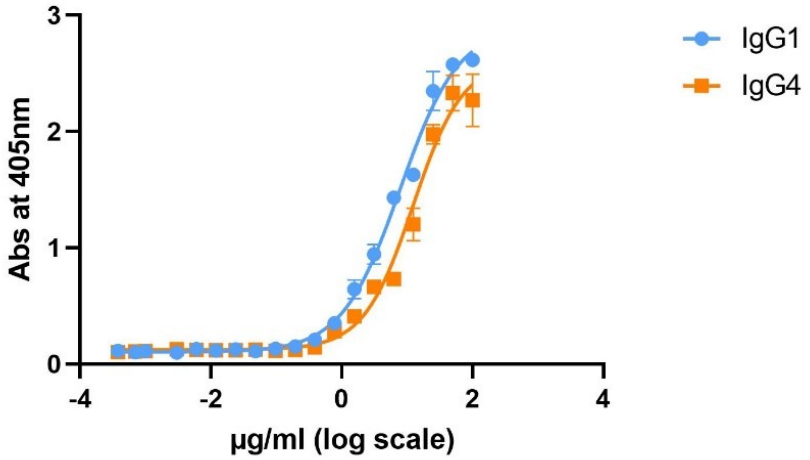

Fig. 4.6. Antibody titration by ELISA assay. *The binding activity of serial dilutions of purified IgG1 and IgG4 to N-terminal + A1 domain of human CEACAM1 antigen was tested by ELISA titration assay. The concentration values were log-transformed before performing the nonlinear regression on GraphPad Prism. Absorbance values are presented as mean +/- S.D of duplicate measurements.*

Flow cytometry analyses were performed to assess the ability of the two antibody subclasses to recognize and bind CEACAM1 antigen naturally expressed on the surface of metastatic melanoma (MelC) and colon cancer cells (HT29). The results showed that IgG1 antibody was more immunoreactive than IgG4 against CEACAM1 on the tumor cell surface. In fact, at equal doses and for all the tested doses, the percentages of cells bound by IgG1 and the values of the Mean Fluorescence Intensity (MFI) were higher than IgG4, suggesting the higher affinity of IgG1 to the target (Fig. 4.7).

a

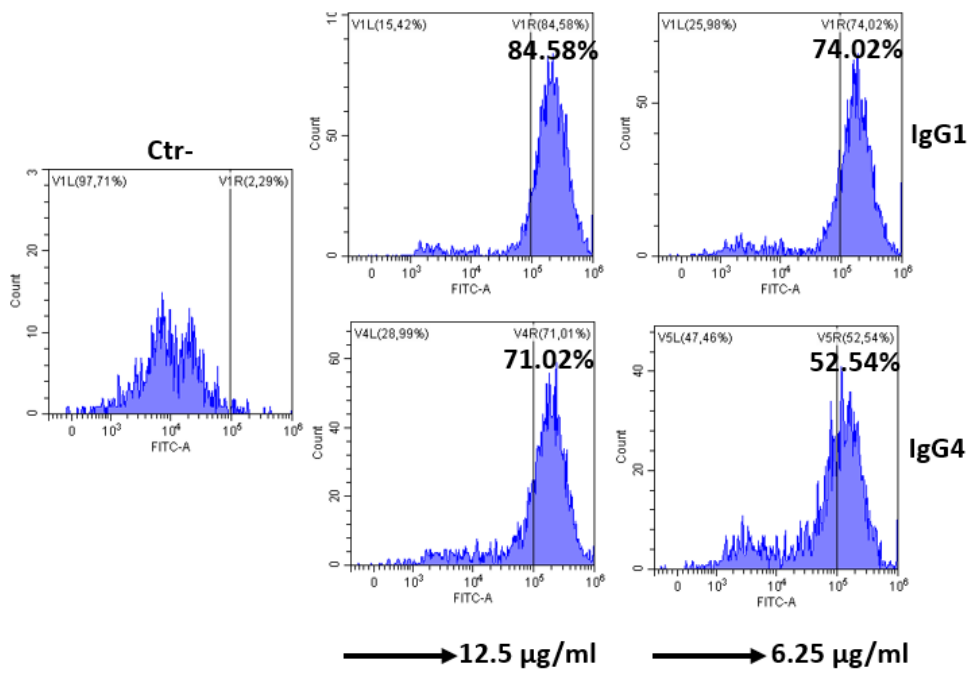

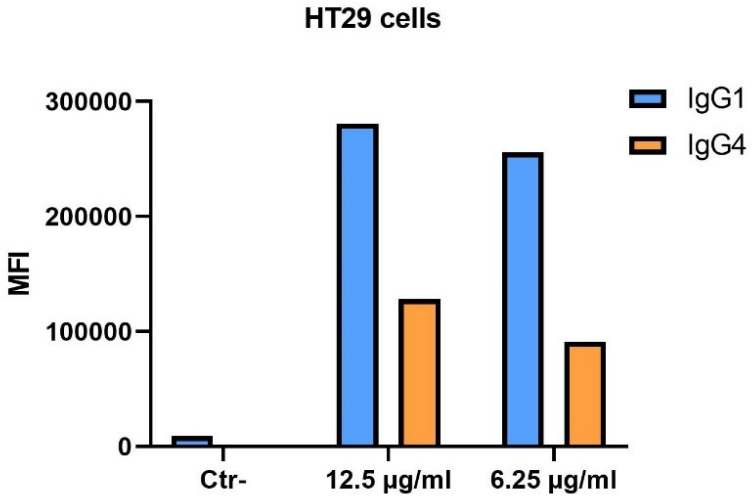

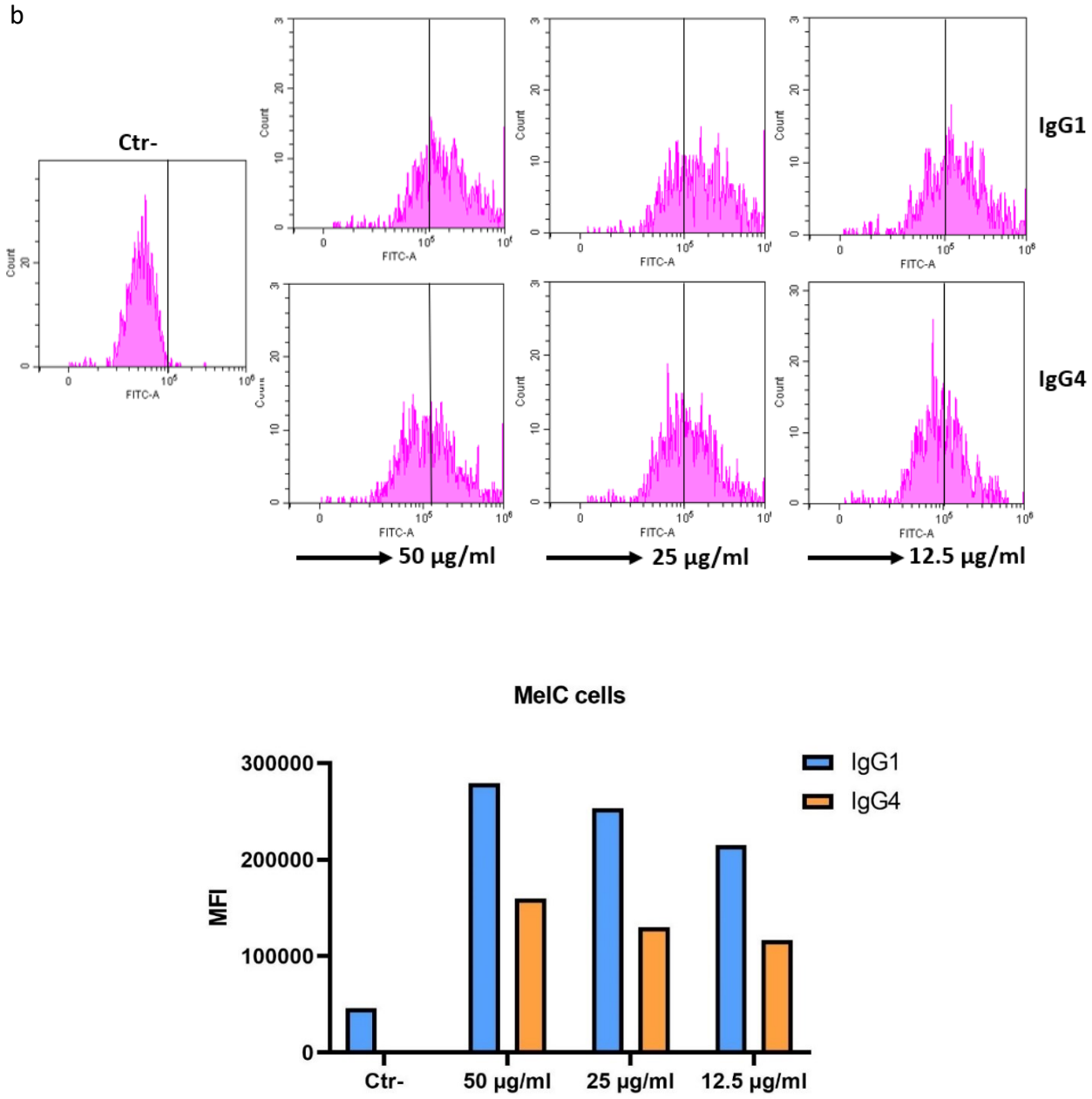

Fig. 4.7. Assessment of the IgG1 and IgG4 reactivity on tumor cells by flow cytometry analysis. Different doses of the antibodies were tested for the binding to human CEACAM1 antigen naturally expressed on the cell surface of advanced colon adenocarcinoma cells (HT29) (a) and metastatic melanoma cancer cells (MelC) (b). For both the tumor cell lines, the MFI values are represented in the bar graphs.

The stability of the biological activity for the two antibodies was evaluated eight months after the purification by ELISA titration (Fig. 4.8). Results highlighted that the storage at 4°C did not affect the functional stability, since IgG1 as well as IgG4 antibodies preserved a similar binding activity to CEACAM1 antigen.

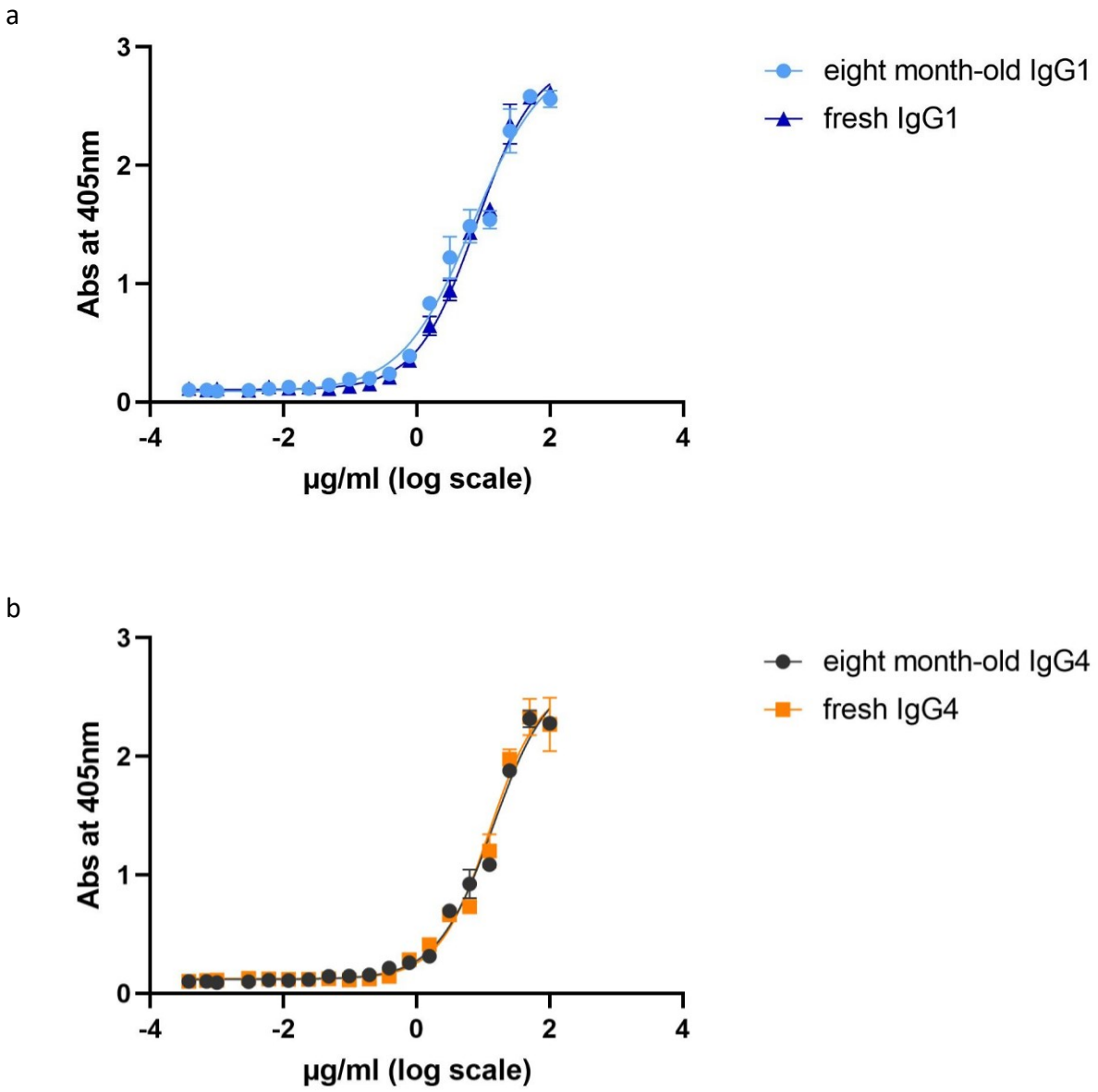

Fig. 4.8. Evaluation of the biological stability of IgG1 and IgG4 by ELISA titration assay. *The binding activity of the IgG1 (a) and IgG4 (b) was assessed after eight months of storage at 4°C. Absorbance values are presented as mean +/- S.D of measures in duplicate.*

These preliminary results highlighted the superior performance of IgG1 antibody compared to IgG4. In fact, the same purification protocol by protein A affinity Chromatography, allowed to obtain IgG1 at a higher protein yield than IgG4 antibody. Furthermore, IgG1 antibody showed higher binding activity to the target and better structural as well as biological stability. These pre-results represent features that make the IgG1 antibody a better therapeutic agent and for this reason IgG1 was selected as the antibody subclass for the following studies of this project. From now on, the anti-CEACAM1 IgG1 antibody will be referred with the name of its producing subclone (#12.3), DIA 12.3.

4.3 Optimization of the antibody production protocol

Endotoxins are lipopolysaccharides (LPS) present on the outer membrane of gram-negative bacteria. Following cell lysis, they are released into the circulation (189). Commonly found in the environment, endotoxin represents the most significant pyrogen in parenteral drugs and medical devices. If present in the bloodstream they may cause septic reactions with a variety of symptoms such as fever, hypotension, nausea and shock (189), while high concentrations can lead to serious collateral effects. The acceptable level of endotoxin contamination in injectable drug products has been established by FDA to be 5 EU/Kg/hr (190).

In order to purify a final product suitable for future therapeutic applications, the purification process has been optimized to reduce the endotoxin contamination. All the glassware were treated with 1M NaOH for 2 hours. After washes with GMP water, the glassware was incubated at 250°C for 1 hour. All the purification buffers were prepared with GMP water and sterile filtered using filters with a 0.22µm pore size. Furthermore, to increase the purity of the antibody and further reduce the contamination with endotoxins, the purification protocol during the protein A chromatography was implemented with several washing steps. After the samples loading, the column was washed with phosphate buffer added with 0.65M NaCl, followed by another washing steps with phosphate buffer with 0.65 NaCl and 5% (v/v) Isopropanol (IPA). Prior to the antibody elution with sodium citrate at pH 3.0, an additional washing step with 0.1M sodium citrate at pH 5.0 was added to eliminate mAb fragments or unfolded mAbs that bind to protein A with lower affinity (Fig. 4.9). This protocol resulted in a purified antibody with a purity determined by SDS-PAGE and SEC-HPLC ≥ of 95% and with a reduced endotoxin level in the final product lower than 10 EU/ml.

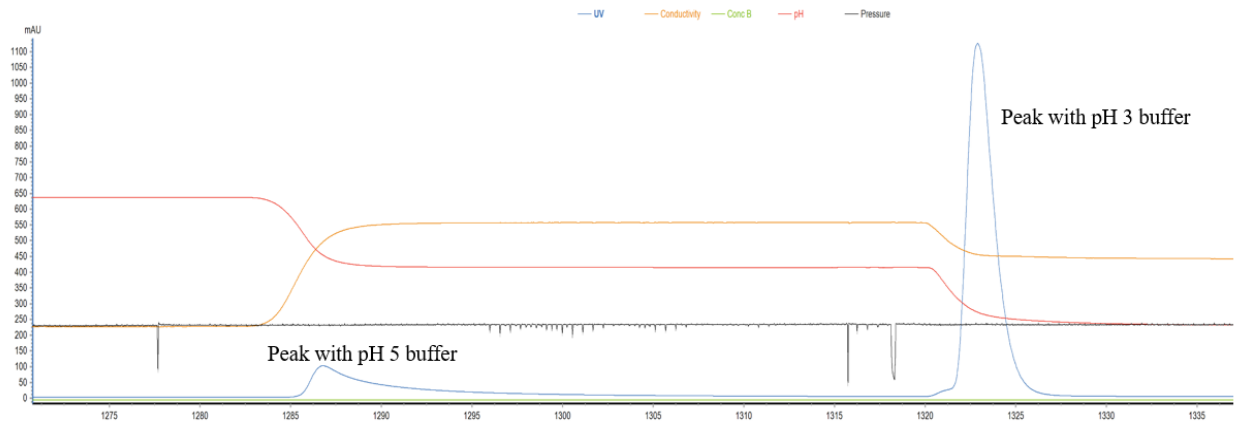

Fig. 4.9. Chromatogram of DIA 12.3 elution by Protein A Affinity Chromatography. *After the column washing, two elution steps were performed: pH 5 buffer containing 0.1M sodium citrate with 2% (v/v) glycerol and 5mM EDTA was used to separate the non-specific mAbs contained in the supernatant from DIA 12.3 antibody. This latter was eluted with 0.1 M sodium citrate, 2% (v/v) glycerol and 5mM EDTA at pH 3.*

4.4 Characterization of the subclone #12.3

In order to confirm the homogeneity of DIA 12.3 antibody-producing cell line, the subclone #12.3 was subjected to the limiting dilution and plated in three 96-multiwell plates under the pressure of the selective antibiotic G418 for two weeks. The grown clones were then tested in ELISA to evaluate the presence of non-antibody producing cell subpopulations. All the clones were positive to the binding to CEACAM1 antigen, suggesting that the cell line was exclusively composed of antibody producing cells (Fig. 4.10). The heterogeneity in the various absorbance values could reflect the different growth rate among the clones. In fact, the low values of absorbance were recorded for the small-size clones.

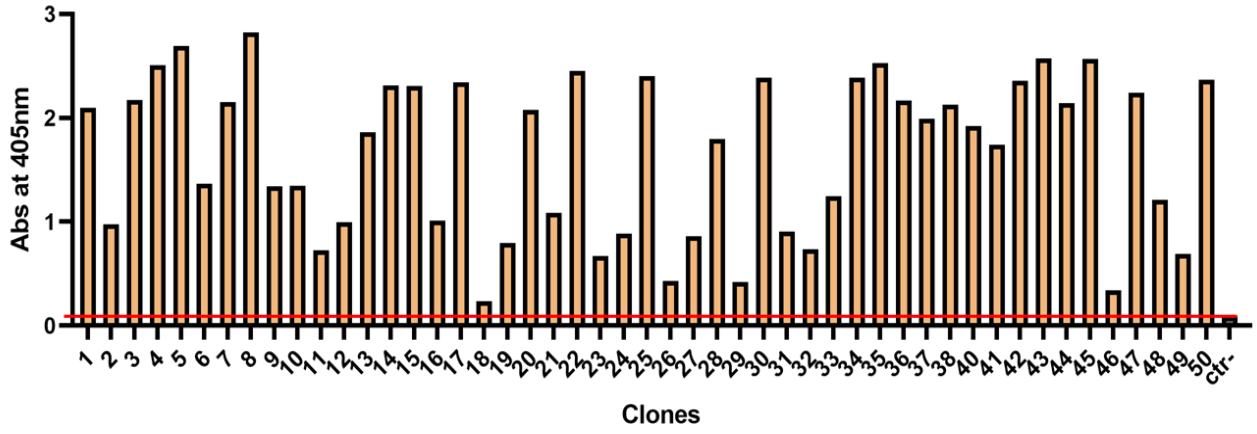

Fig. 4.10. Evaluation of the monoclonality of the subclone #12.3 by ELISA assay. The graph shows the absorbance values of the 50 clones grown 15 days after subjecting the subclone #12.3 to the limiting dilution. All the values are higher than the blank (red line).

Furthermore, the stability of the cell line for the antibody expression was also evaluated over prolonged periods of culture in absence of the selective antibiotic. The single cell clone method was applied and ELISA assays were performed on the grown clones, 15 days after each day of the limiting dilution, at 20th, 40th and 60th day (Fig. 4.11). All the grown clones produced the antibody at all the tested time points, leading to the conclusion that there was not any onset of negative cells unable to produce the antibody during the 60 days of cell culture, despite the cells were not subjected to the antibiotic selective pressure.

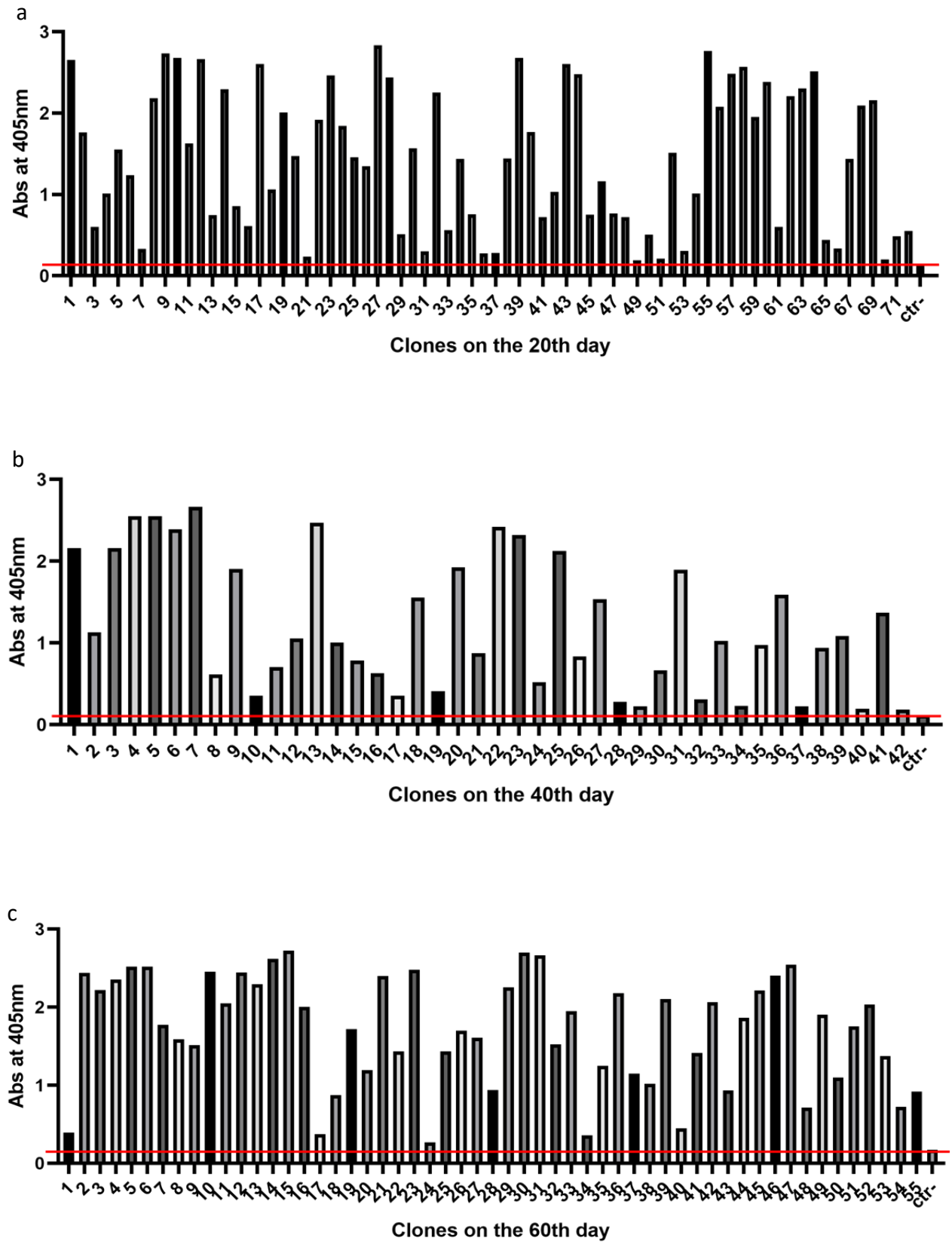

Fig. 4.11. Stability studies of antibody production from the subclone #12.3 by ELISA assay. The graphs report the absorbance values of the clones grown on the 20th (a), 40th (b) and on the 60th day (c) of culture without the pressure of the selective antibiotic. All the values are higher than the blank (red line).

4.5 Adaptation of the subclone #12.3 to the growth in suspension

The HEK293 cells of the subclone #12.3 grow in adhesion and, thus, they require the Fetal Serum Bovine (FBS) in the culture medium (191). In fact, the FBS provides attachment factors, besides nutrients and hormones for mammalian cells (191). However, the presence of the FBS has several disadvantages. Therefore, the subclone cells were adapted to the growth in suspension in CDM4HEK medium, a chemically defined medium devoid of FBS, for the following reasons:

- to reduce the intrinsic variability among different lots of the culture medium, aiming to guarantee the reproducibility in the processes and results;
- to obtain a final product for safe therapeutic applications with no collateral reactions due to the presence of components of animal origin in the medium;
- to scale up the production process enabling the increase in the protein yield;
- to reduce the antibody production costs.

The cells were adapted to serum-free suspension through the sequential adaptation protocol, which consists in culturing the cells with a progressive reduction of the medium with the FBS while increasing the FBS-free medium, until reaching the 100% of FBS-free medium. During this procedure, cell morphology, growth rate, viability and antibody titer were monitored (Fig. 4.12).

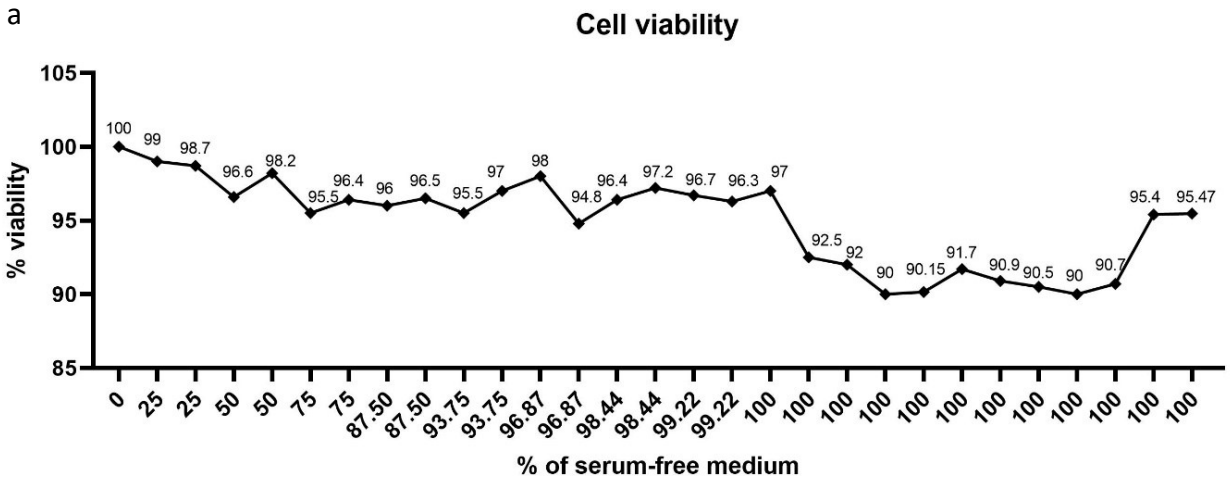

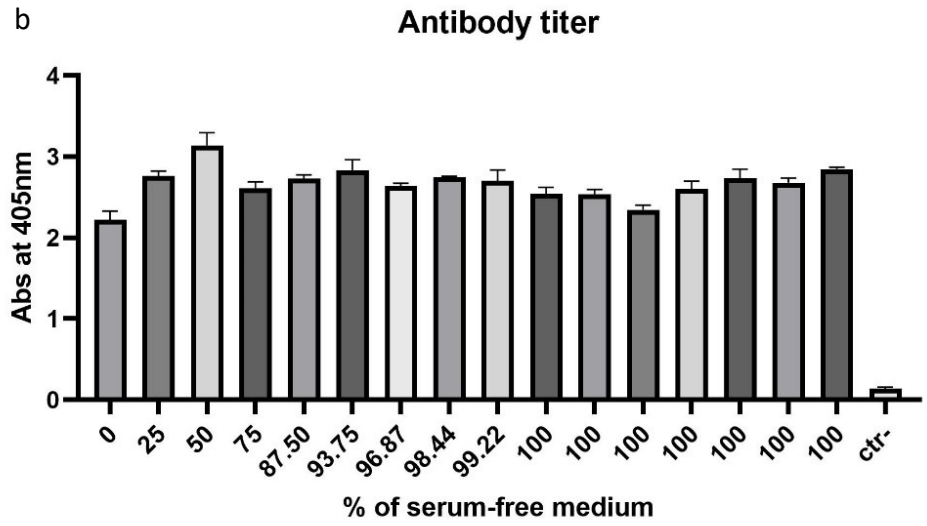

Fig. 4.12. Cell adaptation to the suspension growth: *monitoring of the cell viability (a) and antibody titer (b) during the various steps of the adaptation protocol to the suspension growth. Cell viability was assessed by Trypan Blue Exclusion method. To evaluate the antibody titer, 100µl of surnatant collected from the cell culture at each step of the adaptation process, were tested on a 1 µg/ml CEACAM1 antigen-coated 96-well plate by ELISA assay. Absorbance values are presented as mean +/- S.D. of measures in triplicate.*

In particular, the cell growth was not affected by the adaptation process, as highlighted by the recorded viability values which are higher than 90% at each step (Fig. 4.12a). A slight reduction in the cell viability was observed during the last adaptation steps but it was recovered in 100% serum-free medium. Furthermore, ELISA assays on the supernatants collected during each step of the adaptation process, confirmed that the antibody production was not affected, as similar values of the antibody titer were recorded during the overall process (Fig. 4.12b).

One of the critical steps of the adaptation process is the difficulty in culturing the suspension adapted cells once they have been thawed. In order to evaluate if the subclone #12.3 cells were successfully adapted to grow in suspension, the cell growth and the viability were monitored every day after thawing the cellular stock. The recorded values of the cell viabilty were higher than 90% from the day 1 after thawing, while a slight decrease in the viability was recorded from day 9 (end of the stationary phase and beginning of the death phase). These observations confirmed the success of the adaptation process (Fig. 4.13).

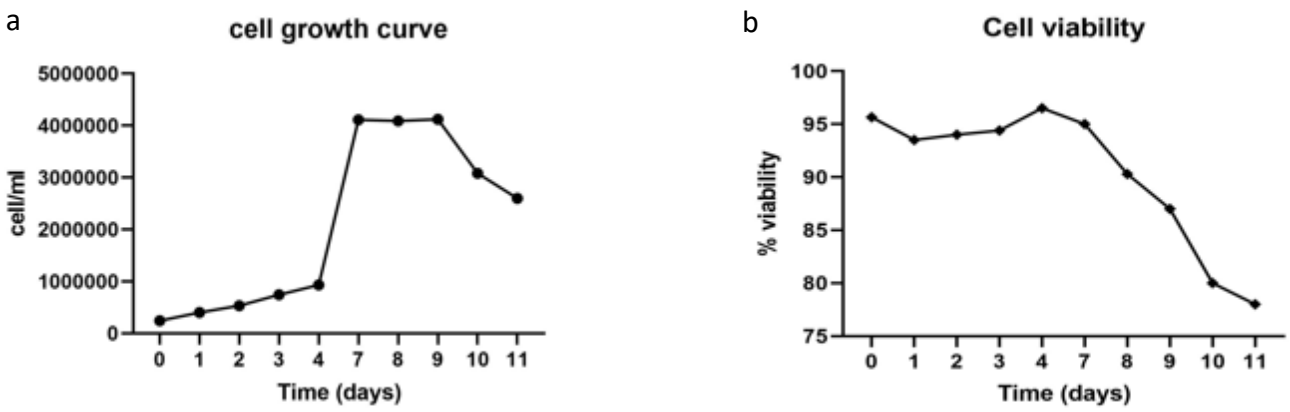

Fig. 4.13. Confirmation of the successful adaptation process: evaluation of the cell growth (a) and viability (b) of the subclone #12.3 cells upon thawing to confirm the adaptation to the suspension growth. Cell density and viability were assessed everyday by trypan blue exclusion staining.

In addition, the suspension adapted cells integrated the antibody expression cassette in their genome as shown by the agarose gel after PCR (Fig. 4.14a), and they produced DIA 12.3 antibody at the similar level recorded for the adherent cells (Fig. 4.14b).

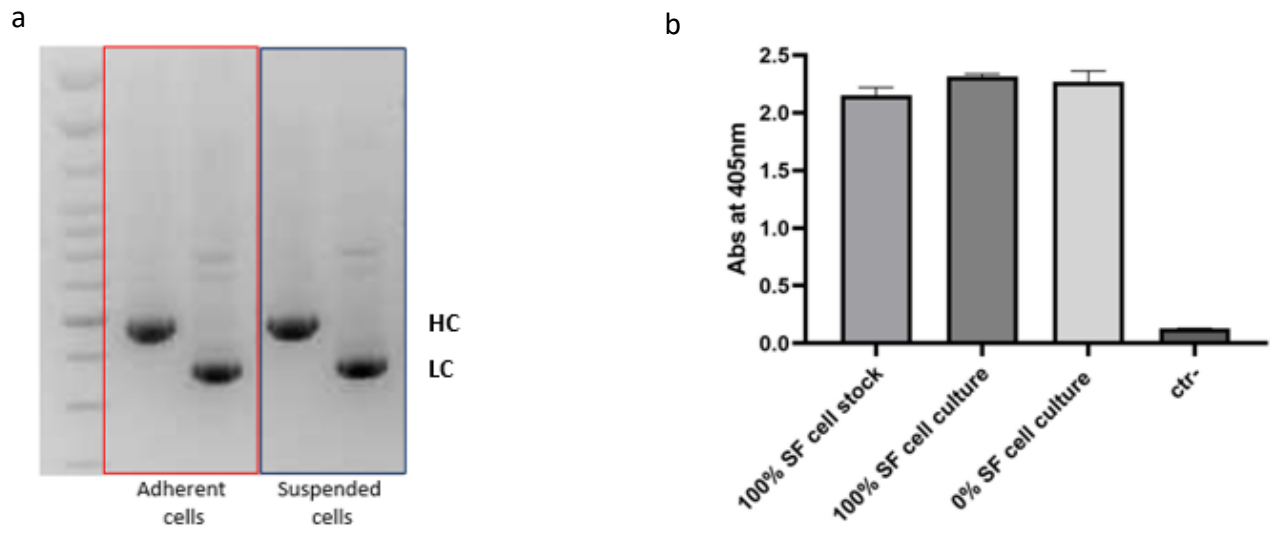

Fig. 4.14. Evaluation of the antibody expression and production: the 100% suspended subclone #12.3 cells integrated the antibody expression cassette (a) and did not alter the titer of the antibody production (b).

To determine the protein yield, the adapted subclone #12.3 cells were cultured for 9 days in CDM4HEK medium on the shaker at 100 rpm. The cell growth and viability were daily evaluated up to the day of collection of 1L of supernatant. DIA 12.3 antibody was purified by Protein A Affinity Chromatography, obtaining a protein yield equal to 16 mg of antibody per 1L of supernatant. The previous yield recorded by purifying the antibody from the adherent subclone #12.3 cells was equal to 10 mg (Table 4.1). Therefore, the adaptation to the growth in suspension allowed to increase the protein yield by 1.6 fold. A further increase could be obtained by improving the cell proliferation with the addition of cell boosters to the serum-free medium in feed-batch cultures.

mAb	Cells	Growth conditions	Yield (mg/L)
IgG1	Adherent subclone #12.3 cells	2 days at 37°C + 7 days at 30°C	10
	Suspended subclone #12.3 cells	9 days at 37°C on the shaker at 100 rpm	16

Table 4.1. Comparison of the protein yield between the adherent subclone #12.3 cells and the 100% serum-free adapted cells.

4.6 DIA 12.3: *in vitro* efficacy studies

4.6.1 Evaluation of DIA 12.3 binding on tumor cells

We investigated the ability of DIA 12.3 antibody to bind CEACAM1 antigen on a wider panel of tumor cell lines, including metastatic melanoma, bladder cancer and adenocarcinoma colon cancer cell lines. In fact, CEACAM1 is known to have an oncogenic role at the metastatic stages of these tumors, and its overexpression positively correlates with tumor progression, metastasis development and overall survival. Flow cytometry results confirmed the dose-dependent immunoreactivity of DIA 12.3 to CEACAM1 antigen at the cell surface level of the analyzed tumors (Fig. 4.15).

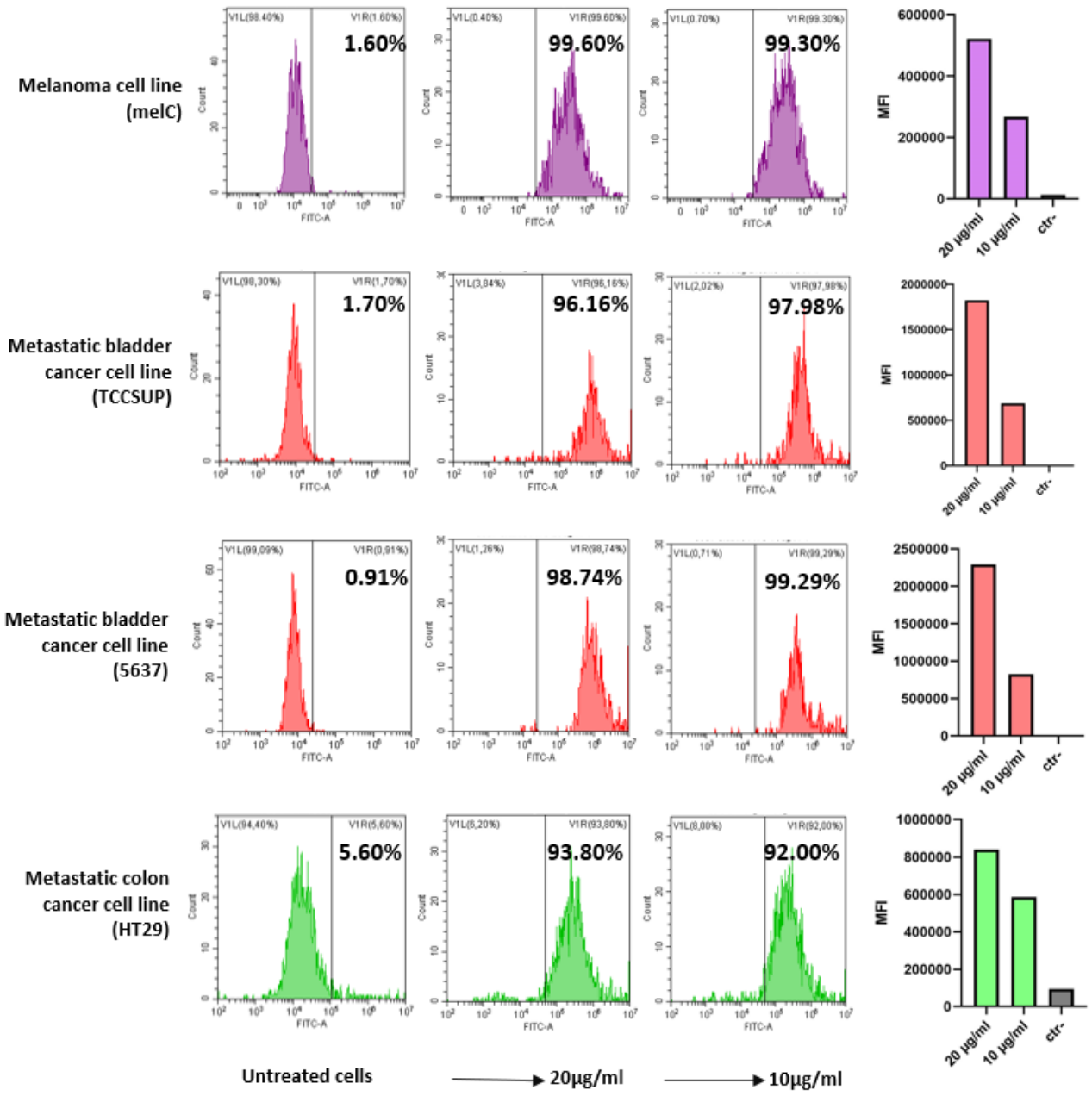

Fig. 4.15. *Assessment of DIA 12.3 binding on tumor cells by flow analysis:* *MelC, TCCSUP, 5637 and HT29 cells were treated with or without 20 and 10 µg/ml of DIA 12.3 antibody. The graphs showing the MFI values are reported on the right.*

4.6.2 Antibody effects on NK cell-mediated killing of tumor cells

As previously mentioned in the Introduction Chapter, tumor cells exploit the homophilic interactions via N-terminal domain which involves CEACAM1 on tumor cells and CEACAM1 on NK cells to escape from NK cell–mediated killing (49). Thus, the ability of the antibody to block the homophilic interactions and to rescue the NK cytotoxic activity against melanoma cells was evaluated as

mechanism of action. Antibody Dependent Cellular Cytotoxicity (ADCC) assays based on the bioluminescence method were performed by quantifying the LDH enzymatic activity in the cell culture supernatants. Upon 30 minutes of treatment with 20 or 10 µg/ml of DIA 12.3 antibody, melanoma cells were co-incubated with NK cells at different effector:target cell ratios, ranging from 10:1 to 1:1, for 4 hours at 37°C. The luminescence values recorded at each effector:target cell ratio were higher upon treatment of melanoma cells with the antibody compared to the untreated cells (Fig. 4.16 a). In fact, results showed that DIA 12.3 antibody was able to enhance the NK cell-mediated cytotoxicity, at each E:T cell ratio tested (Fig. 4.16b). Furthermore, DIA 12.3 treatment demonstrated to render also bladder, colon and head&neck tumor cells more vulnerable to NK-cell mediated killing (Fig. 4.17).

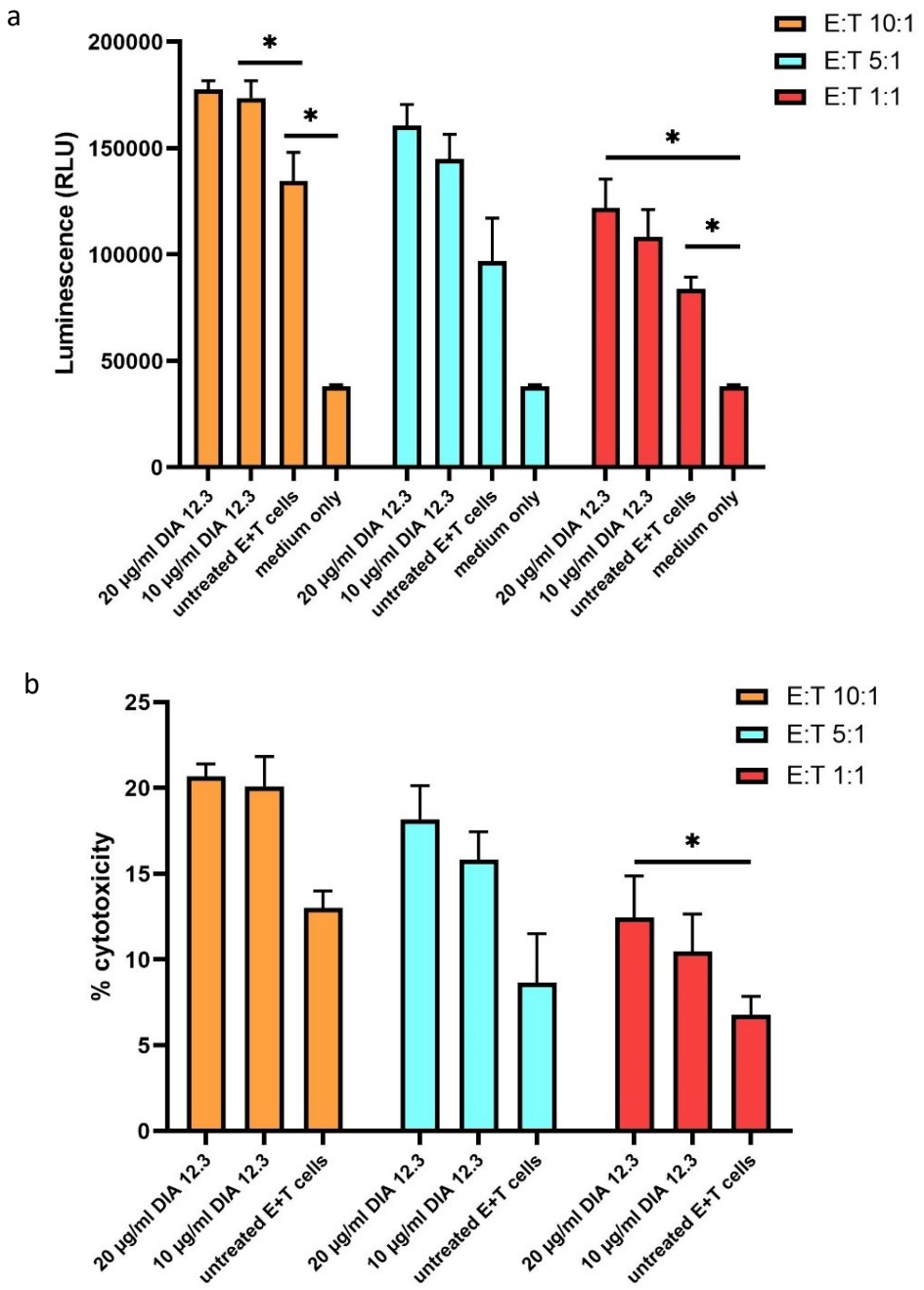

Figure 4.16. Cytotoxicity assay. MelC cells treated with or without 20 or 10 µg/ml DIA 12.3 antibody were co-incubated with NK cells at effector:target cell ratios ranging from 10:1 to 1:1. Luminescence was recorded after 30 minutes incubation at RT. A) Plot of the Relative Luminescence Units (RLU) values recorded for each E:T cell ratio. B) Plot showing the % of NK cell mediated cytotoxicity calculated upon antibody treatment in comparison with the basal NK cytotoxic activity against melanoma cells. The % of cytotoxicity was calculated as follows:
100 × (Experimental LDH Release – Medium Background)/(Maximum LDH Release Control – Medium Background).

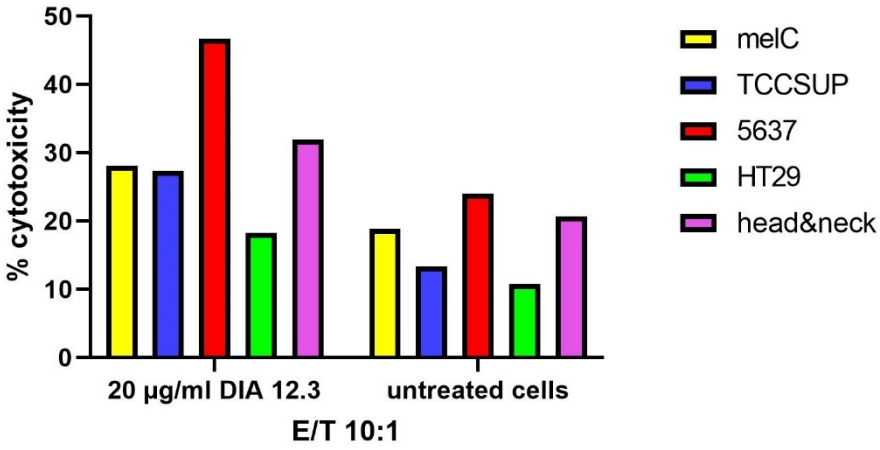

Figure 4.17. Cytotoxicity assay. MelC, TCCSUP, 5637, HT29 and head&neck cancer cells were treated with or without 20 µg/ml of DIA 12.3 antibody, and then co-incubated with NK cells at 10:1 effector:target cell ratio. Luminescence was recorded after 60 minutes of incubation at RT. The plot shows the % of NK cell-mediated cytotoxicity calculated upon antibody treatment in comparison with the basal NK cytotoxic activity against melanoma cells. The % of cytotoxicity was calculated as follows:
100 × (Experimental LDH Release – Medium Background)/(Maximum LDH Release Control – Medium Background).

Although their clinical success, many antibody-based therapies are often effective only in subsets of patients. Considerable efforts has been made to achieve efficacy in larger patient populations. Modulating the ability of antibodies to interact with the immune system cellular components by the Fc engineering represents one area of interest (192). For cases where mAbs are intended to bind target expressed not only on tumor cells, but also on immune cells, it may be desiderable to reduce the effector functions in order to prevent the death of target expressing immune cells and an enhanced cytotoxic response (192). The IgG binding to FcγRs can be affected by several modifications. The N297A mutation was among the first substitutions to be observed to reduce the FcγR-binding (175). This mutation eliminates the glycosylation site at N297, resulting in the reduction of effector functions, such as CDC and ADCC (175).

For these reasons, *in situ* site directed mutagenesis of DIA 12.3 was performed to obtain the mutated N297A DIA 12.3 antibody. Binding studies by ELISA and flow cytometry assays revealed that the N297A mutation did not affect the antibody binding activity to the N-terminal + A1 domain of human CEACAM1 antigen (Fig. 4.18). By contrast, LDH assay confirmed that the N297A mutation negatively affected the ability of the antibody to enhance the effector functions, as a reduction in the NK cell-mediated cytotoxicity was recorded upon cell treatment with mtN297A DIA 12.3 with respect to DIA 12.3 antibody, at all the E:T cell ratios (Fig. 4.19).

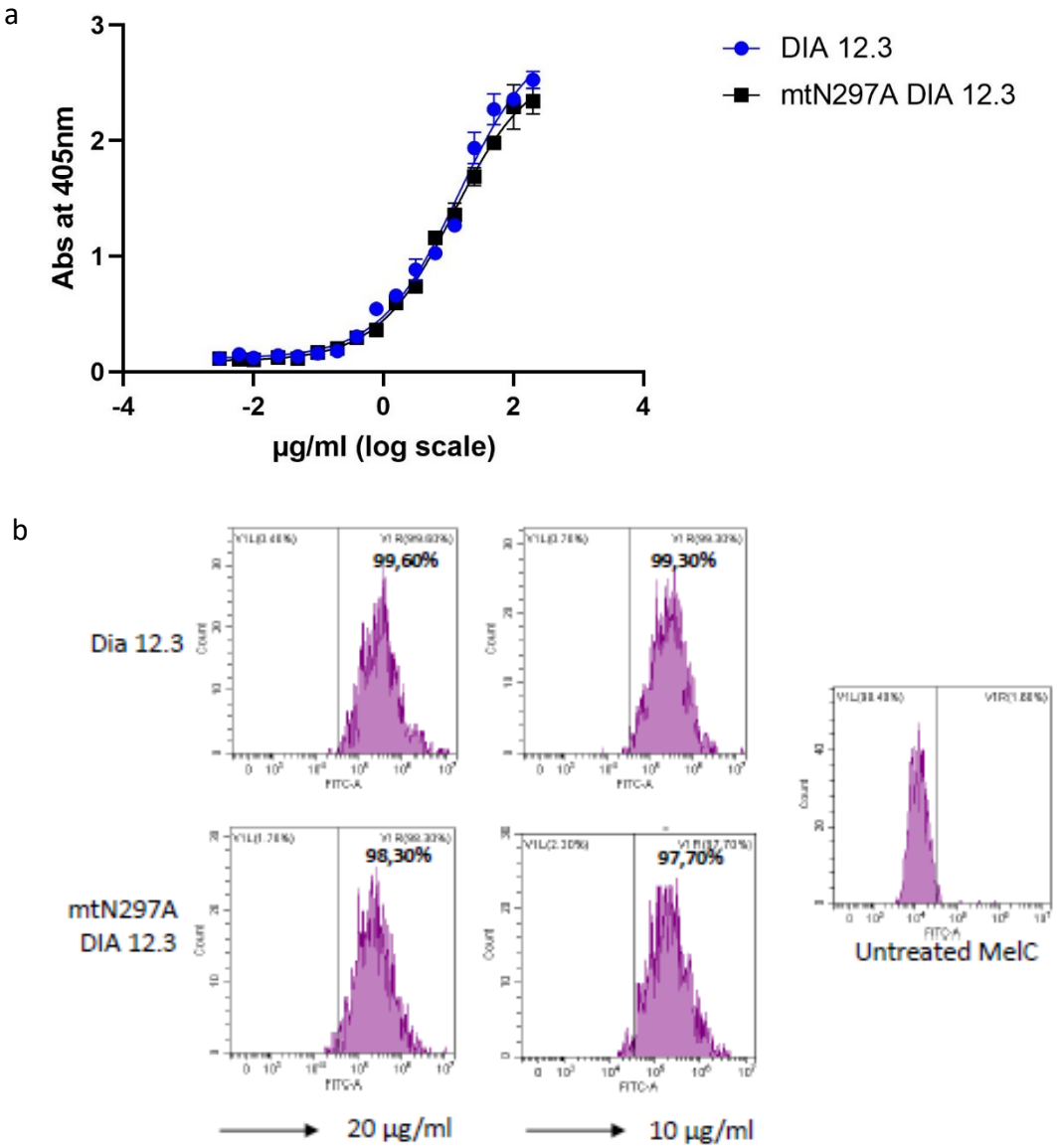

Fig. 4.18. Comparison of the binding activity between DIA 12.3 and mtN297A DIA 12.3 antibodies. *The binding activity of DIA 12.3 and its mutated form was assessed by ELISA titration assay (a). Absorbance values are presented as mean +/- S.D of measures in triplicate. FACS analysis were carried out on melC cells treated with 20 or 10µg/ml of DIA 12.3 or mtN297A DIA 12.3 antibodies (b).*

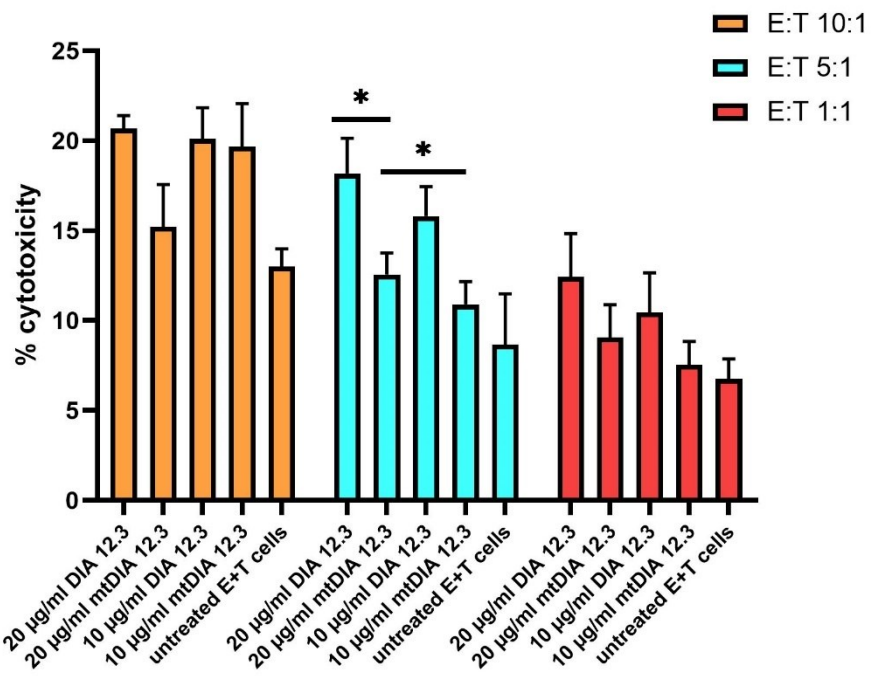

Fig. 4.19. Comparison of the effector functions between DIA 12.3 and mtN297A DIA 12.3. *MelC cells treated with or without 20 or 10 µg/ml of DIA 12.3 or mtN297A DIA 12.3 antibodies were co-incubated with NK cells at effector/target cell ratio ranging from 10:1 to 1:1. Luminescence was recorded after 30 minutes incubation at RT. The plot shows the % of NK cell mediated cytotoxicity calculated following antibody treatment with respect to the basal NK cytotoxic activity against melanoma cells.*

4.6.3 Neutrophil enrichment

In addition to NK cells, we investigated the effects of DIA 12.3 on neutrophil-mediated antitumor response. In fact, besides being the most abundant circulating immune cells, neutrophils are the first line of defense against infection and cancer (59). Among the anti-cancer cytotoxic effects, ADCC is one mechanism by which neutrophils kill cancer cells (69, 70).

Flow cytometric analyses that assess the purity of neutrophils isolated from healthy donors' fresh blood after the enrichment procedure are shown in Fig. 4.20. Staining with anti-CD66b antibody used as surface marker for neutrophil identification revealed the high purity of the neutrophil cell suspension. Results also showed that DIA 12.3 as well as mtN297A DIA antibodies strongly recognized and bound CEACAM1 antigen expressed on cell surface of more than 96% of the neutrophil population, similar to the commercial anti-CEACAM1 antibody (Fig. 4.20 d,e).

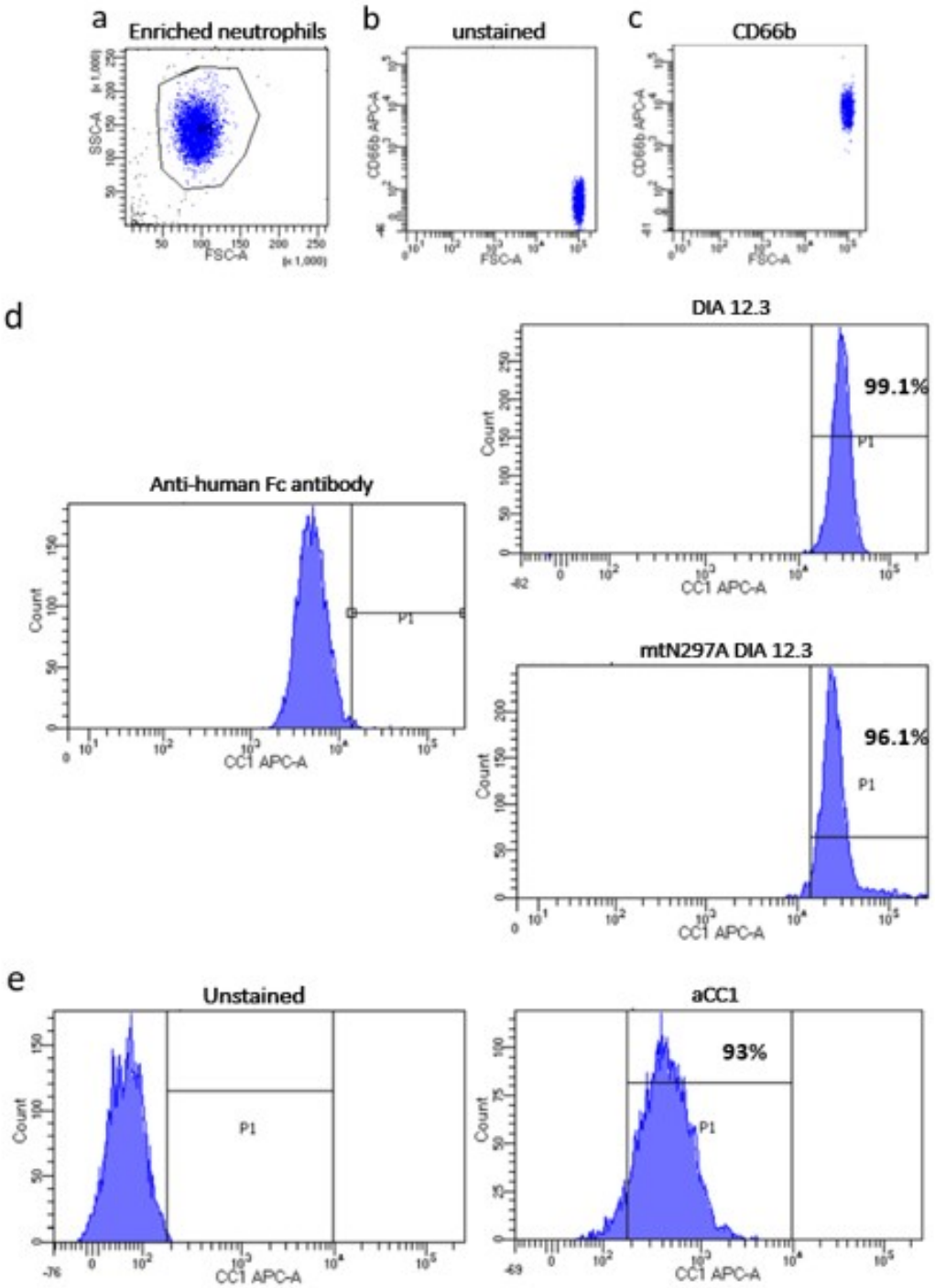

Fig. 4.20. Neutrophil staining and binding analysis by flow cytometry. Dot plot of freshly isolated neutrophils after the enrichment protocol (a). Unstained (b) and CD66b-stained (c) neutrophils. Binding profiles of DIA 12.3 and mtN297A DIA antibodies (10 µg/ml) on neutrophils (d) in comparison with the commercial anti-CEACAM1 antibody (e).

4.6.4 Evaluation of neutrophil apoptosis and NO production after antibody treatment

To test the potential toxicity of DIA 12.3 antibody on neutrophils, the spontaneous neutrophil apoptosis was evaluated at 0, 1, 2, 16, 18 and 20 hours after the treatment with or without DIA 12.3 (Fig. 4.21). The cell surface expression of phosphatidylserine (PS) is an early marker for apoptosis and it can be detected by staining with FITC annexin V. Propidium Iodide (PI) staining can discriminate between early apoptotic (annexin V-positive, PI-negative) and late apoptotic (annexin V-positive, PI-positive) cells (193). Double-staining revealed that the majority of neutrophils were early apoptotic cells after 16 hours of incubation at 37°C (Fig. 4.21 a). The % of late apoptotic cells also increased after this period, concomitantly with the reduction of cell viability (Fig 4.21 b, c). Notably, a higher number of late apoptotic cells at time 0 compared to the following time points was observed, suggesting that the incubation of neutrophils in RPMI medium at 37°C might exert a positive effect on the viability of enriched neutrophils.
Importantly, results also showed that the rate of living, as well as apoptotic cells, was not altered after the treatment with DIA 12.3 antibody compared with the untreated samples, suggesting that the antibody reacts with neutrophils without interfering with general cellular processes such as apoptosis.

a

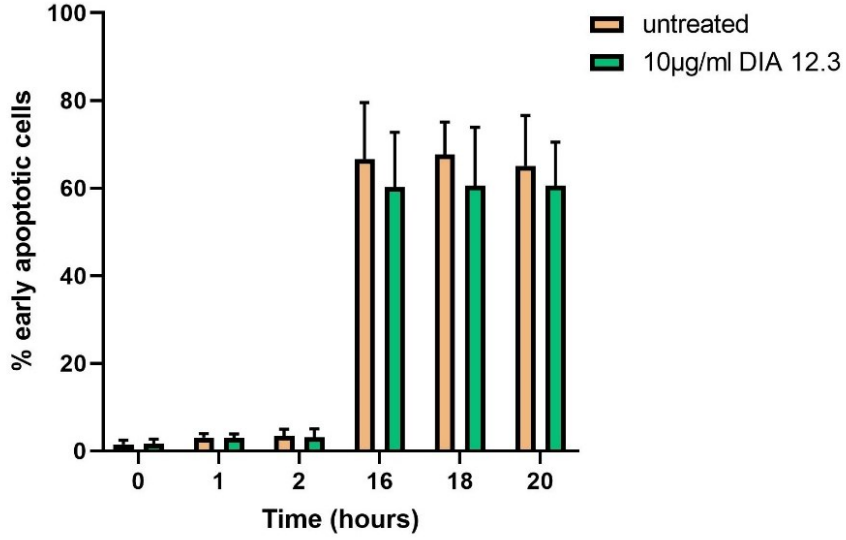

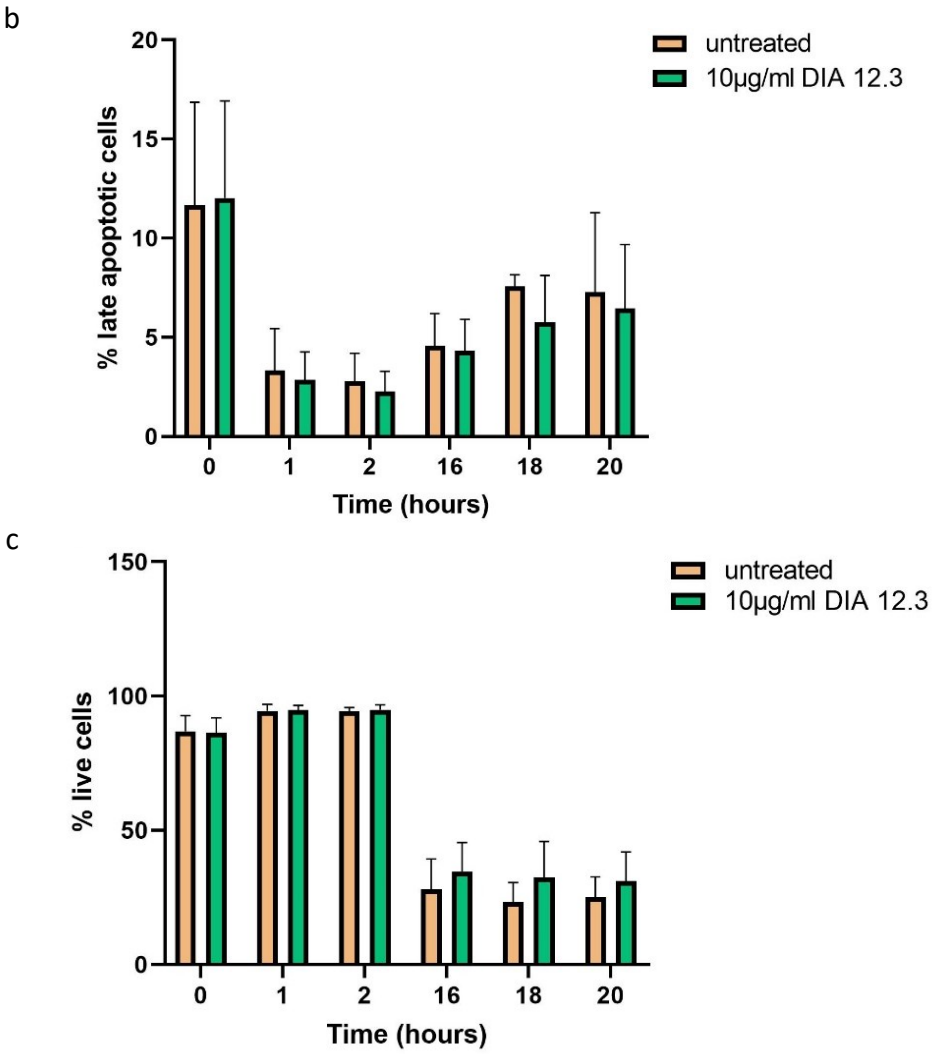

Fig. 4.21. Detection of spontaneous apoptosis in human neutrophils. Neutrophils were cultured for 0, 1, 2, 16, 18 and 20 hours in RPMI medium with or without 10 µg/ml of DIA 12.3 antibody at 37°C. At the end of each time point, neutrophils were double stained for FITC-annexin V and PI. The graphs show the % of early apoptotic (a), late apoptotic (b) and living cells (c) of three independent experiments. Bars are representative of the mean of triplicate values +/- SD.

A well studied neutrophil-mediated mechanism to limit tumor progression is through the production of reactive oxygen and nitrogen species (ROS and RNS) (194, 195). Among the RNS, nitric oxide (NO) is an important signaling molecule released by the activated neutrophils.

To assess if DIA 12.3 antibody triggers NO production, antibody treatments were performed on neutrophils co-cultured with CEACAM1-expressing breast tumor MDA-MB-231 cells at different effector:target cell ratios (Fig. 4.22). Neutrophil-produced NO was indirectly evaluated by measuring the concentration of nitrite (NO_2^-), a stable and nonvolatile product of NO released by neutrophils in the supernatants, according to the Griess reaction.

No statistically significant differences in the absorbance values were observed between the untreated neutrophils and the negative control (only medium) for none of the tested effector:target cell ratios, confirming the lack of NO production by unactivated neutrophils. Furthermore, no

alteration in the absorbance levels following the incubation with the antibody was observed, suggesting that DIA 12.3 antibody does not induce neutrophil-mediated NO production. These findings are in line with what observed from neutrophil staining with antibody against CD66b, a well known marker for neutrophil activation (196). Neutrophils were CD66b positive soon after the enrichment protocol (t=0, Fig. 4.23a) and at 1, 2 and 18 hours after the incubation with or without the antibody, suggesting that the steps during isolation and enrichment procedures might activate neutrophils (Fig.4.23b, c). However, treatment of neutrophils with DIA 12.3 did not lead to an increased activation compared with the untreated samples (Fig. 4.23d), confirming that the antibody does not interfere with the physiological cellular processes of neutrophils. Interestingly, an increased level of activation was observed after 1 and 2 hours of incubation in the culture medium at 37°C, regardeless the antibody treatment, in concordance with the previously observed reduction of the % of late apoptotic cells. Thus, in addition to the increase of cell viability, incubation of neutrophils in cell culture medium at 37°C also contributes to promote neutrophil activation.

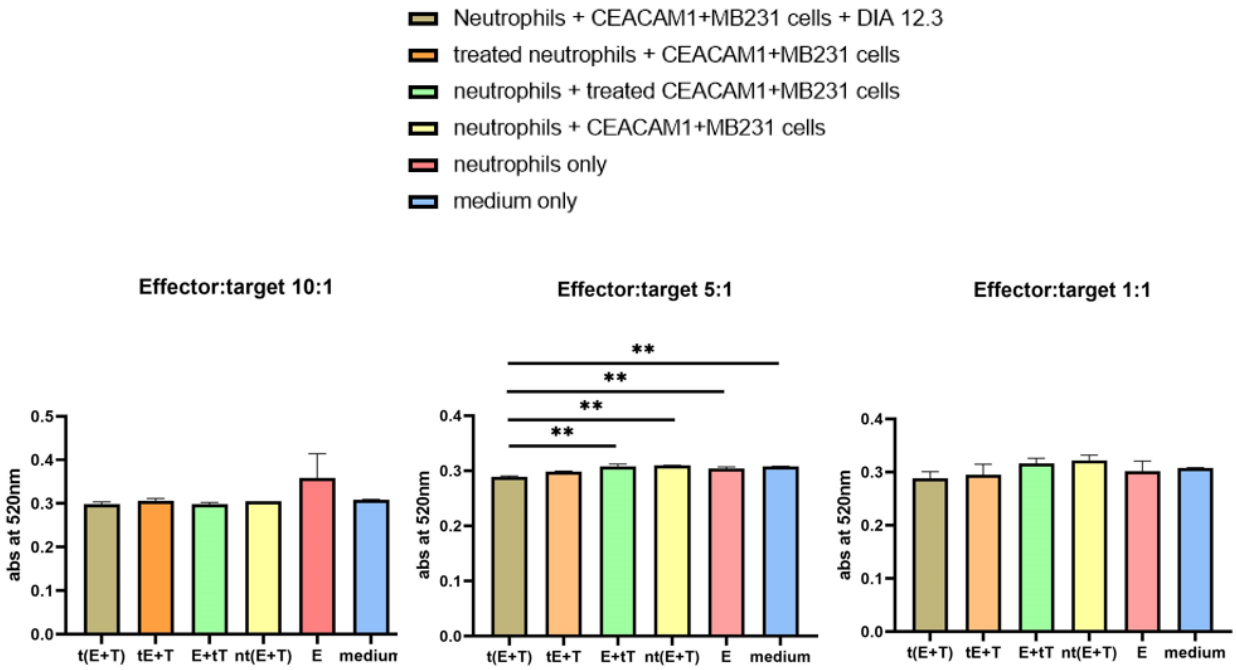

Fig. 4.22. Analysis of NO levels released by neutrophils in culture supernatants. Neutrophils were co-cultured with CEACAM1+ MDA-MB-231 cells at 10:1, 5:1 and 1:1 effector:target ratios. For each effector:target cell ratio, three different treatment conditions were tested: 1) neutrophils or 2) tumor cells alone pre-treated with or without 10 µg/ml of DIA 12.3 for 30 minutes at 37°C and then co-incubated 4 hours at 37°C with tumor cells or neutrophils, respectively; neutrophils and tumor cells co-treated with or without 10 µg/ml of DIA 12.3 for 4 hours at 37°C. Then the supernatants were subjected to nitrite assay according to the Griess reagent system. Bars are representative of duplicate values +/- SD.

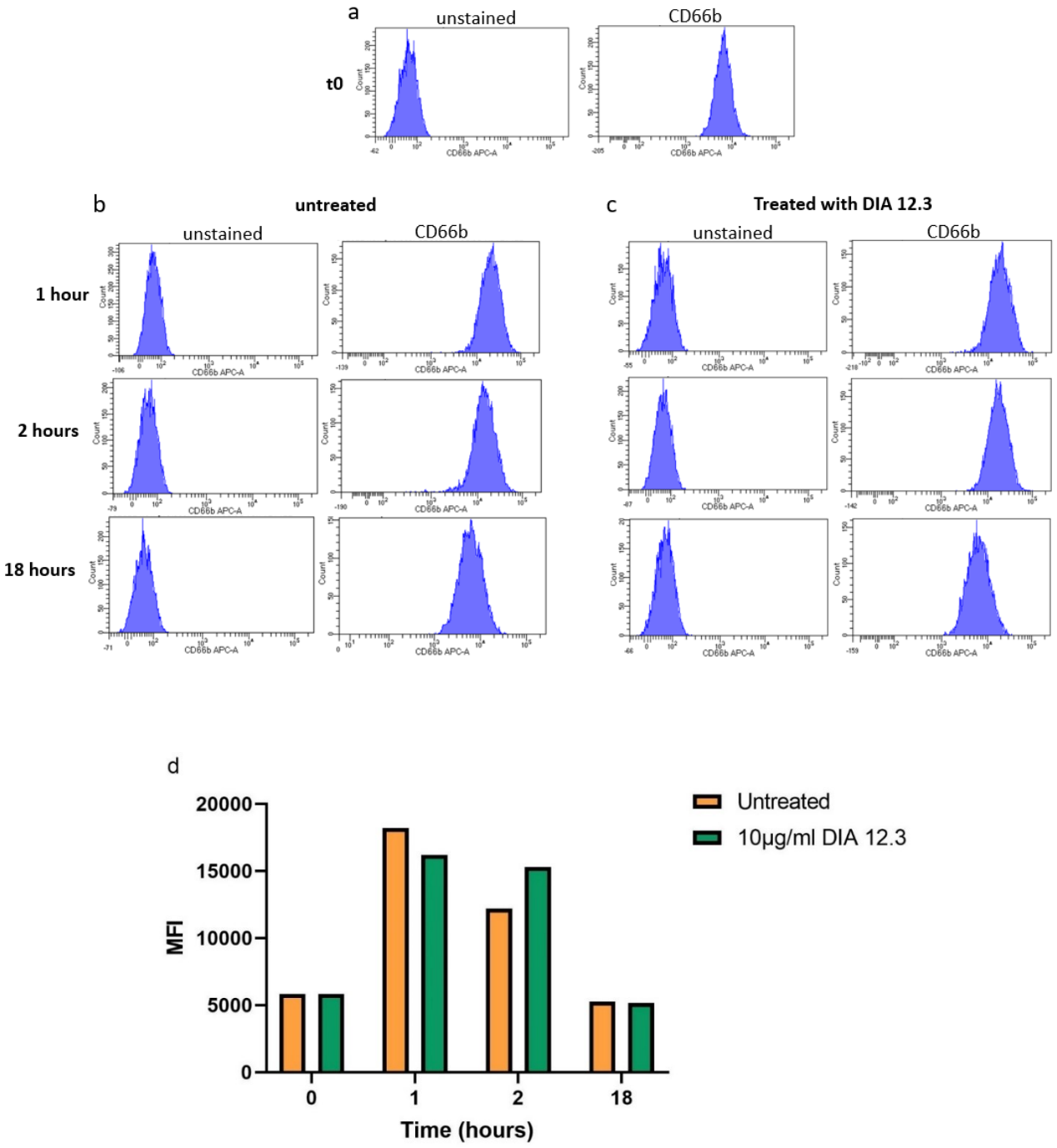

Fig. 4.23. Evaluation of DIA 12.3 antibody effects on neutrophil activation. Isolated and enriched human neutrophils were incubated for 1, 2 and 18 hours in RPMI medium at 37°C in absence (b) or presence (c) of 10 µg/ml of DIA 12.3 antibody. Following each time point, neutrophils were then stained with anti-CD66b antibody. Comparison of MFI values related to CD66b+ cells after treatment with or without DIA 12.3 is shown (d).

4.7 *In vivo* Imaging

4.7.1 DIA 12.3 DOTAylation and binding to hCEACAM1 and hCEA antigens in tumor cells

In order to radiolabel DIA 12.3 with the positron emitter ^{64}Cu, the antibody was conjugated to the chelate DOTA as previously described (186). Instant thin layer chromatogram (ITLC) showed that the efficiency of DOTA conjugation was higher than 96% (Fig. 4.24). In order to confirm that the DOTAylation did not affect the binding ability of the antibody, DIA 12.3 and DOTAylated-DIA 12.3 were tested on hCEACAM1 and hCEA-expressing MDA-MB-231 cells. Results showed overlapped binding profiles of the antibody to hCEACAM1 as well as hCEA antigens, in which the % of tumor cells bound to DIA 12.3 or DOTAylated-DIA 12.3 were similar to that recorded for anti-CEACAM1 and anti-CEA commercial antibodies (Fig. 4.25).

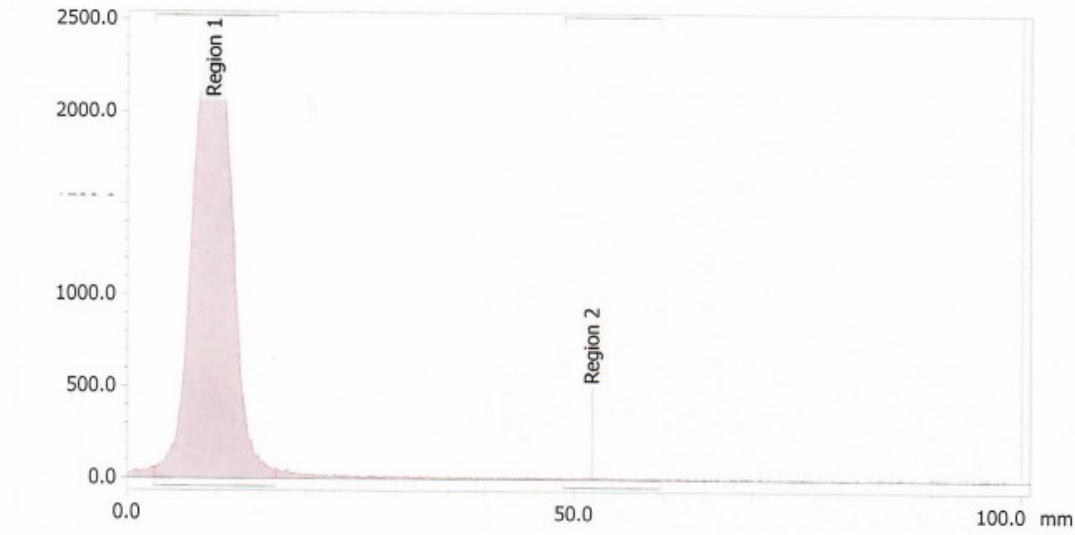

Regions: Cu-64 Detector: PMT

Name	Start (mm)	End (mm)	Retention (RF)	Area (Counts)	%ROI (%)	%Total (%)
Region 1	3.0	16.6	0.096	62500.0	99.71	96.32
Region 2	48.8	59.6	0.520	180.0	0.29	0.28
2 Peaks				62680.0	100.00	96.59

Fig. 4.24. Instant thin layer chromatogram (ITLC) analysis of DOTAylated-DIA 12.3 antibody. *Chromatogram from ITLC analysis of DOTAylabeled antibody revealed the presence of two peaks, region 1 and region 2, corresponding to DOTAylated-DIA 12.3 and unconjugated DIA 12.3 antibodies, respectively. The table indicates the % of each peak.*

a

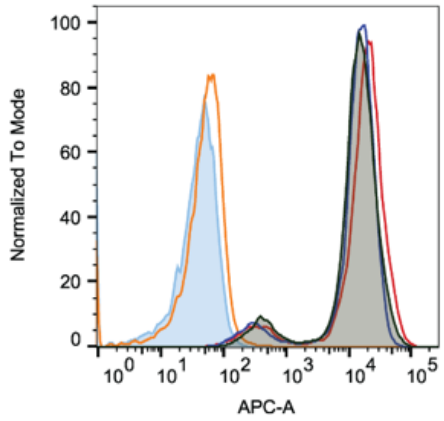

antibody	%
aCC1	91.2
DIA 12.3	91.3
DOTA-DIA 12.3	91.1
Anti-Fc	0.08
Unstained	0.01

b

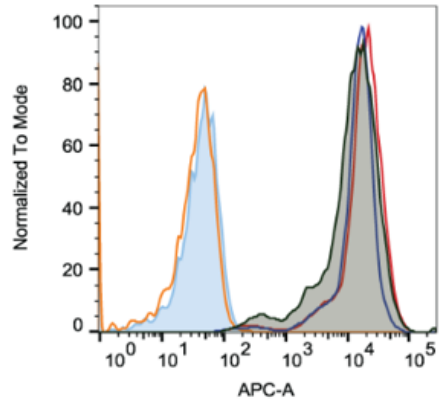

antibody	%
aCEA	94.4
DIA 12.3	97
DOTA-DIA 12.3	97
Anti-Fc	0.02
Unstained	0.01

Fig. 4.25. Binding profiles of DIA 12.3 and DOTAylated-DIA 12.3 antibodies on MDA-MB-231 cell lines. *hCEACAM1 (a) and hCEA (b)-expressing MDA-MB-231 cells were incubated with or without 10 µg/ml of DIA 12.3 and DOTAylated-DIA 12.3 antibodies, anti-CEACAM1(a) or anti-CEA (b) commercial antibodies.*

4.7.2 Studies in NSG mice

4.7.2.1 Radiolabeling and PET Imaging of ^{64}Cu-DOTAylated-DIA 12.3 in female NSG mice bearing breast tumor xenografts

Radiolabeling of DOTAylated-DIA 12.3 antibody gave a product that was 60% labeled with ^{64}Cu radioisotope (Fig. 4.26). To evaluate the antibody tumor-targeting, antigen-negative (Parental), hCEACAM1- and hCEA-positive human breast orthotopic tumor xenografts were established in mammary fat pads of female NSG mice. Because of technical issues encountered during the PET scan procedure, we were not able to obtain reliable images (data not shown). However, results from biodistribution analysis 46 hours post-injection showed uptake levels of almost 10% of antibody injected (ID) dose/g in hCEACAM-positive tumors (Fig. 4.27). At the same time point, the % ID/g in

hCEA-positive tumors was similar to the value recorded in the parental tumors, suggesting the higher *in vivo* binding specificity of the antibody to hCEACAM1 than hCEA antigen. Furthermore, the uptake of ^{64}Cu-DOTAylated-DIA 12.3 antibody by the CEACAM1-positive tumor was higher than in normal organs, with the exception of the lung and kidneys.

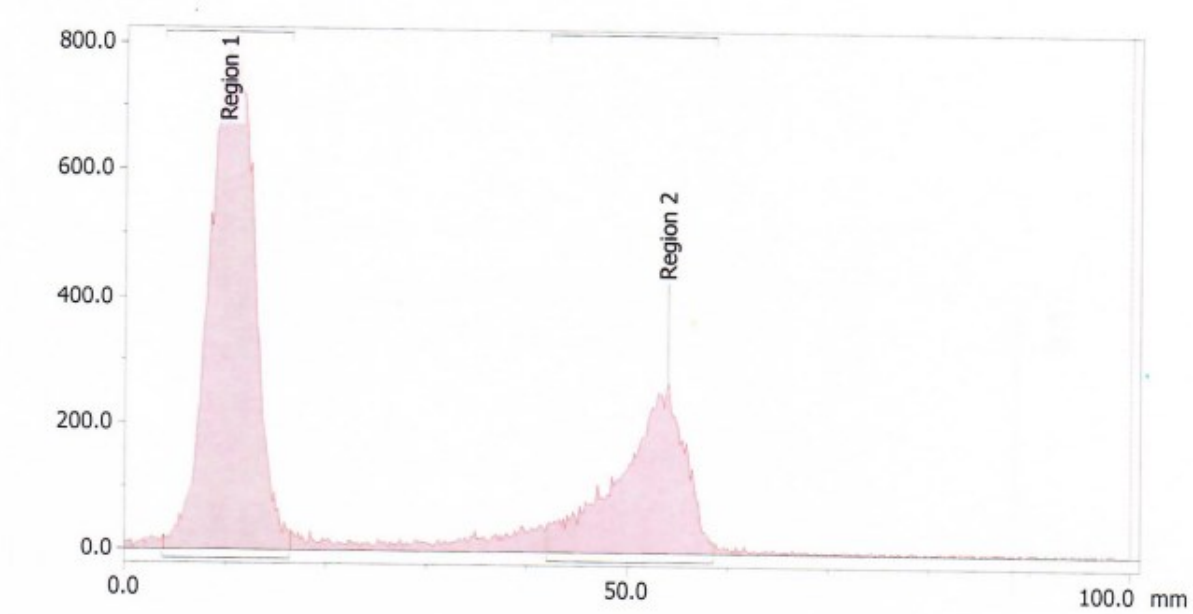

Regions: Cu-64 Detector: PMT

Name	Start (mm)	End (mm)	Retention (RF)	Area (Counts)	%ROI (%)	%Total (%)
Region 1	3.8	16.4	0.102	20682.0	67.22	61.05
Region 2	42.0	58.6	0.540	10086.0	32.78	29.77
2 Peaks				30768.0	100.00	90.82

Fig. 4.26. ITLC analysis of ^{64}Cu-DOTAylated-DIA 12.3 antibody. *Chromatogram from ITLC analysis of radiolabeled antibody revealed the presence of two peaks, region 1 and region 2, corresponding to ^{64}Cu DOTAylated-DIA 12.3 and unlabeled DOTAylated-DIA 12.3 antibodies, respectively. The table indicates the % of each peak.*

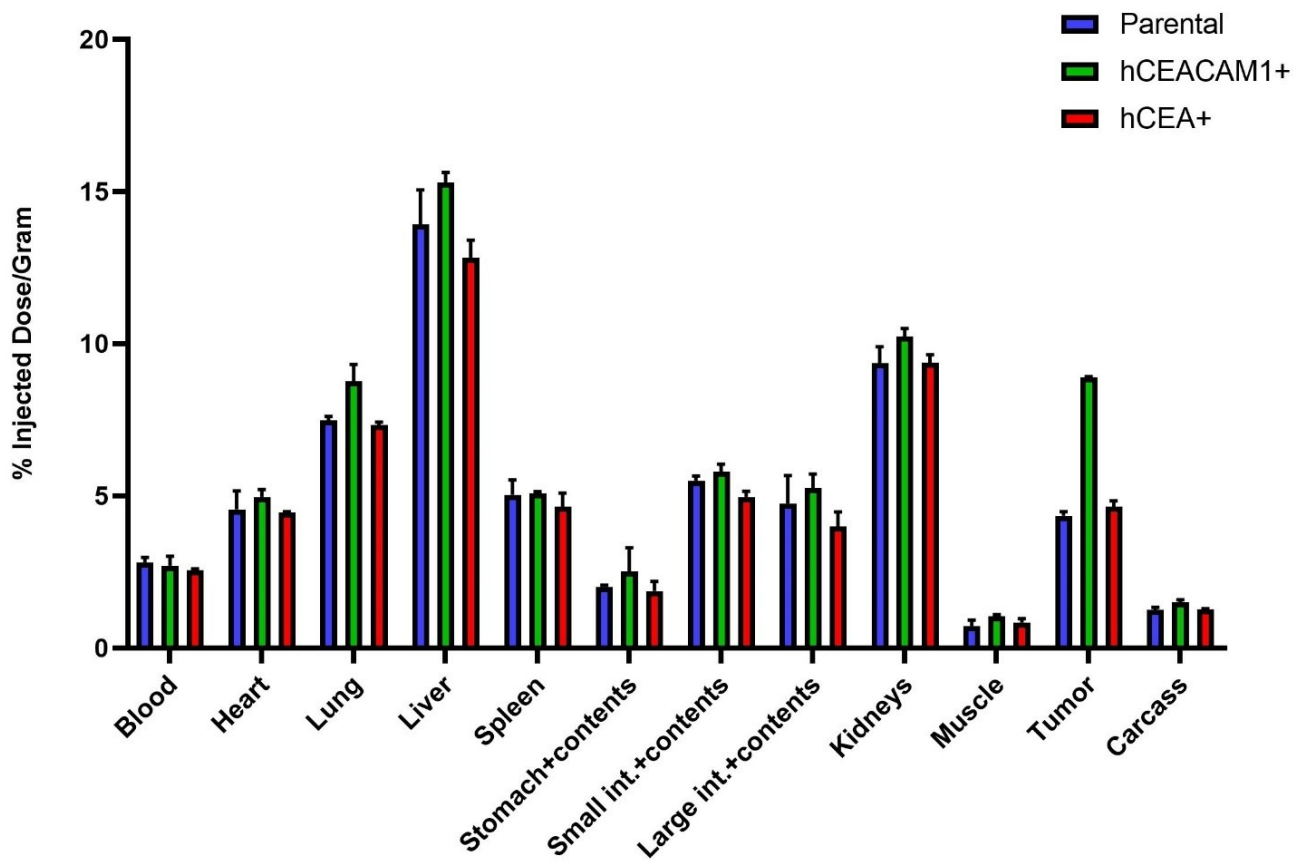

Fig. 4.27. Antibody biodistribution analysis of NSG mice bearing breast tumor xenografts. Organs and tumors from female NSG mice bearing parental, hCEACAM1- or hCEA-positive human breast tumor xenografts were assayed for radioactivity 46 hours after the via tail vein injection of 6,4 µg/mouse of ^{64}Cu-DOTAylated-DIA 12.3 antibody. Bars represent the mean +/- S.D. of the percentage of the antibody injected dose per gram of tissue (% ID/g) in various organs and tumors from mice injected with each cell line (n=2 mice per cell line).

Efficiency of the radiolabeling of DOTAylated-DIA 12.3 antibody for the second PET experiment was higher than the first one, resulting in 95% of radiolabeled antibody (Fig. 4.28).
However, results from the previously described PET with NSG mice underlined the need to increase the dose of the injected antibody in order to enhance the antibody tumor uptake. For the same reason, the protocol was optimized by increasing the specific radioactivity of the labeled antibody from 1 mCi to 10 mCi of $^{64}CuCl_2$ per 100 µg of DOTA-DIA 12.3. Therefore, 30 µg/mouse of unlabeled DIA 12.3 were injected in addition to 6,4 µg/mouse of ^{64}Cu-DOTA-labeled DIA 12.3 with 100 µCi of product per 10 µg. Differently from the previous PET experiment, PET images of mice at 46 hours post-injection showed a clear enhancement in the uptake levels of the antibody in the antigen-positive tumors compared to the parental tumor (Fig. 4.29a). Furthermore, results from biodistribution analysis displayed that the % ID/g in hCEACAM1-positive tumors was about 13% compared to 8% reached in the hCEA-expressing tumors at the same time point (Fig. 4.29b), confirming the DIA 12.3 specificity in the *in vivo* targeting of hCEACAM1-positive tumors.

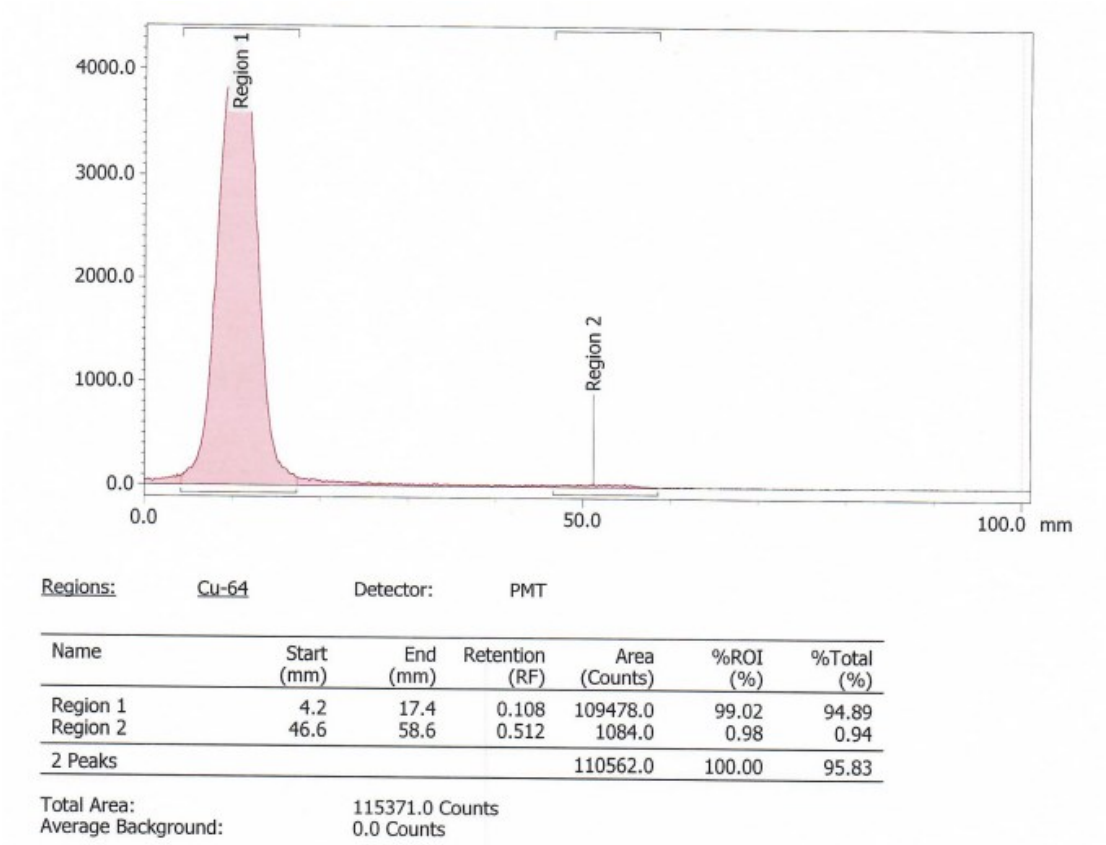

Fig. 4.28. ITLC analysis of ^{64}Cu-DOTAylated-DIA 12.3 antibody. Chromatogram from ITLC analysis of radiolabeled antibody revealed the presence of two peaks, region 1 and region 2, corresponding to ^{64}Cu DOTAylated-DIA 12.3 and unlabeled DOTAylated-DIA 12.3 antibodies, respectively. The table indicates the % of each peak.

a

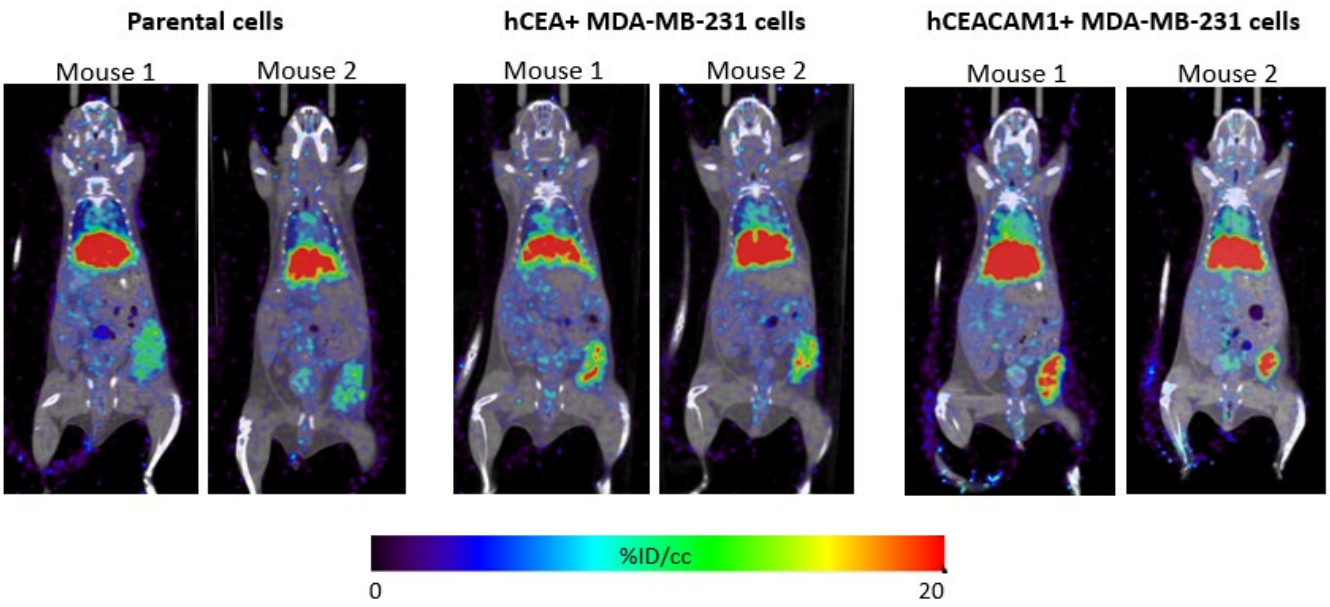

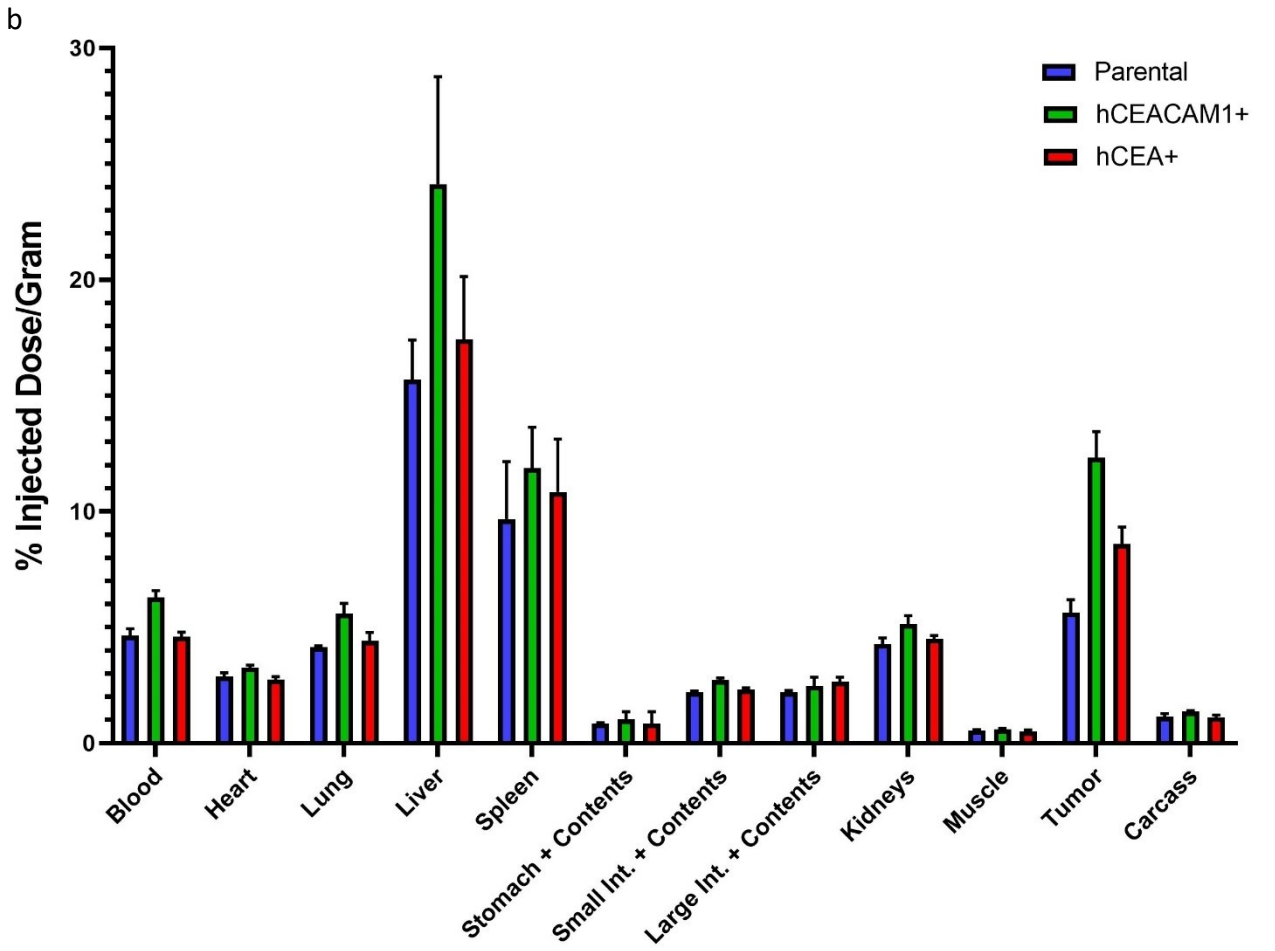

Fig. 4.29. PET imaging of female NSG mice bearing parental, hCEACAM1 and hCEA-positive human breast tumor xenografts. Mice bearing parental, hCEACAM1 or hCEA-positive human breast tumor MDA-MB-231 cells were imaged 46 hours after the via tail vein injection of 6,4 µg/mouse of ^{64}Cu-DOTAylated-DIA 12.3 antibody + 30 µg/mouse of unlabeled DIA 12.3 (a). Biodistribution analysis of the antibody 46 hours post-injection (b). Bars represent the mean +/- S.D. of the % ID/g in various organs and tumors from mice injected with each cell line (n=3 mice per cell line).

4.7.3 Studies in transgenic mice

4.7.3.1 Development of stable hCEACAM1- or hCEA-expressing murine bladder cancer and breast cancer cell lines for imaging studies in transgenic mice

To study DIA 12.3 antibody tumor targeting in syngeneic and immunocompetent mice, we generated two mouse cell lines expressing hCEACAM1 or hCEA antigens. After two weeks of cell culture under the antibiotic selective pressure, MB49 cellular pools with the highest % of hCEACAM1 and hCEA-positive cells were identified (Fig. 4.30a,e) and selectively sorted to high purity. Firstly, cell debris were excluded from the whole cell population by creating a gate using forward and side scatter parameters, which serve as indicators of relative particle size and complexity. Then doublets were excluded from the sort by examining the relative signal height vs. signal area of cells in this gate. Live single cells positive to the hCEACAM1 and hCEA staining were gated for sorting (Fig. 4.30 b,f). Each

sorted population was greater than 99% pure (Fig. 4.30 c,g) and confirmed the antigen expression two weeks after the expansion (Fig. 4.30 d,h).

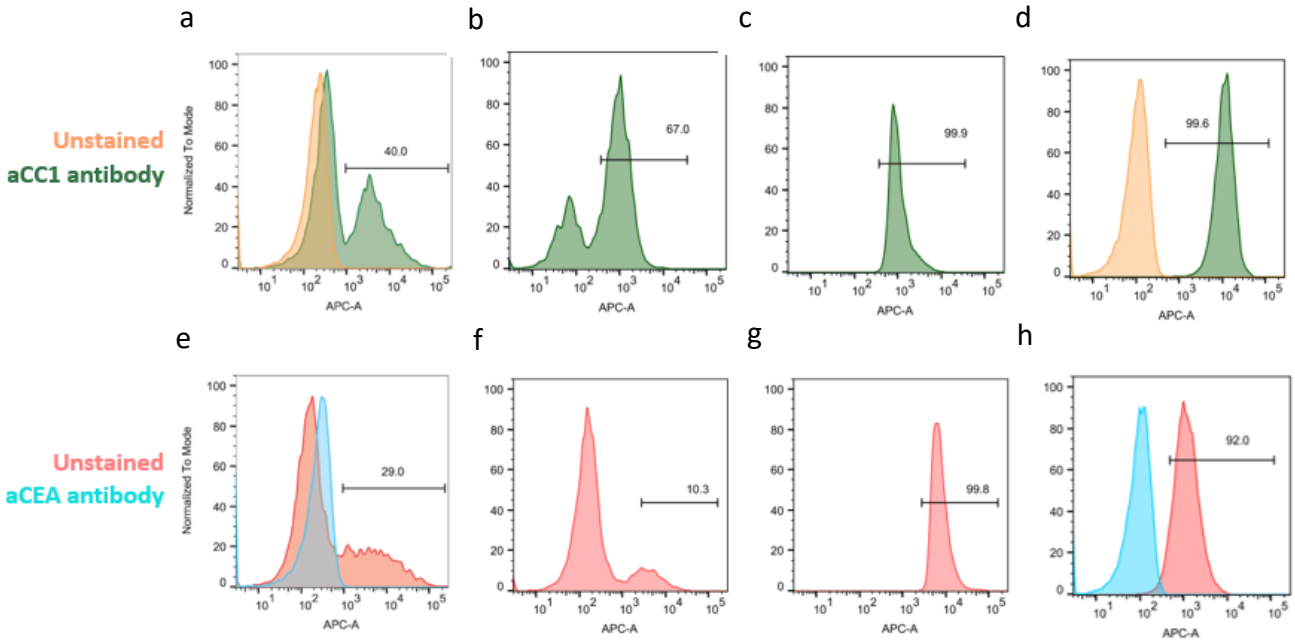

Fig. 4.30. Strategy to develop hCEACAM1 or hCEA-expressing MB49 cell lines. *The selected cellular pools (a, e) were subjected to cell sorting using the sorting channel to isolate only the positive cell subpopulations (b, f). A small amount of each sorted sample was re-analyzed in order to assess the purity (c, g). The expression of hCEACAM1 and hCEA antigens was evaluated two weeks after the expansion of the sorted cell populations (d, h).*

The transfected pool of hCEACAM1-expressing E0771 cells was not sorted, since 99.0% of the cells expressed hCEACAM1 after two weeks of antibiotic selection (Fig. 4.31a). In addition, almost 100% of cells kept the expression of hCEACAM1 antigen during the following weeks (Fig. 4.31b).

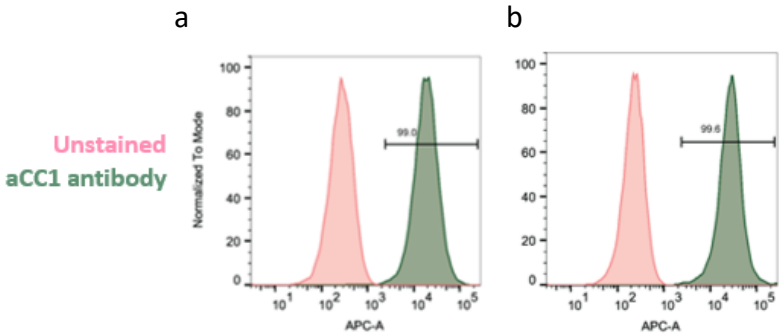

Fig. 4.31. Strategy to develop hCEACAM1 murine breast cancer cell lines (E0771). *Results from flow cytometry analysis on hCEACAM1-transfected E0771 cells stained with or without anti-CEACAM1 commercial antibody (a). The hCEACAM1 antigen expression was assessed after two weeks of cell culture (b).*

4.7.3.2 DIA 12.3 binding to hCEACAM1 and hCEA antigens in murine bladder cancer cells

The previously transfected murine bladder cancer MB49 cells were used for PET studies described below. Firstly, flow cytometry analyses were performed in order to assess the antibody binding activity to hCEACAM1 and hCEA antigens expressed by MB49 cells. Results confirmed that the parental cells do not express neither of the antigens (Fig. 4.32a). More than 99% of the hCEACAM1-expressing cells were bound to DIA 12.3 and commercial anti-CEACAM1 antibodies (Fig. 4.32b). Furthermore, DIA 12.3 bound hCEA-positive cells with a higher % than the aCEA commercial antibody (Fig. 4.32c).

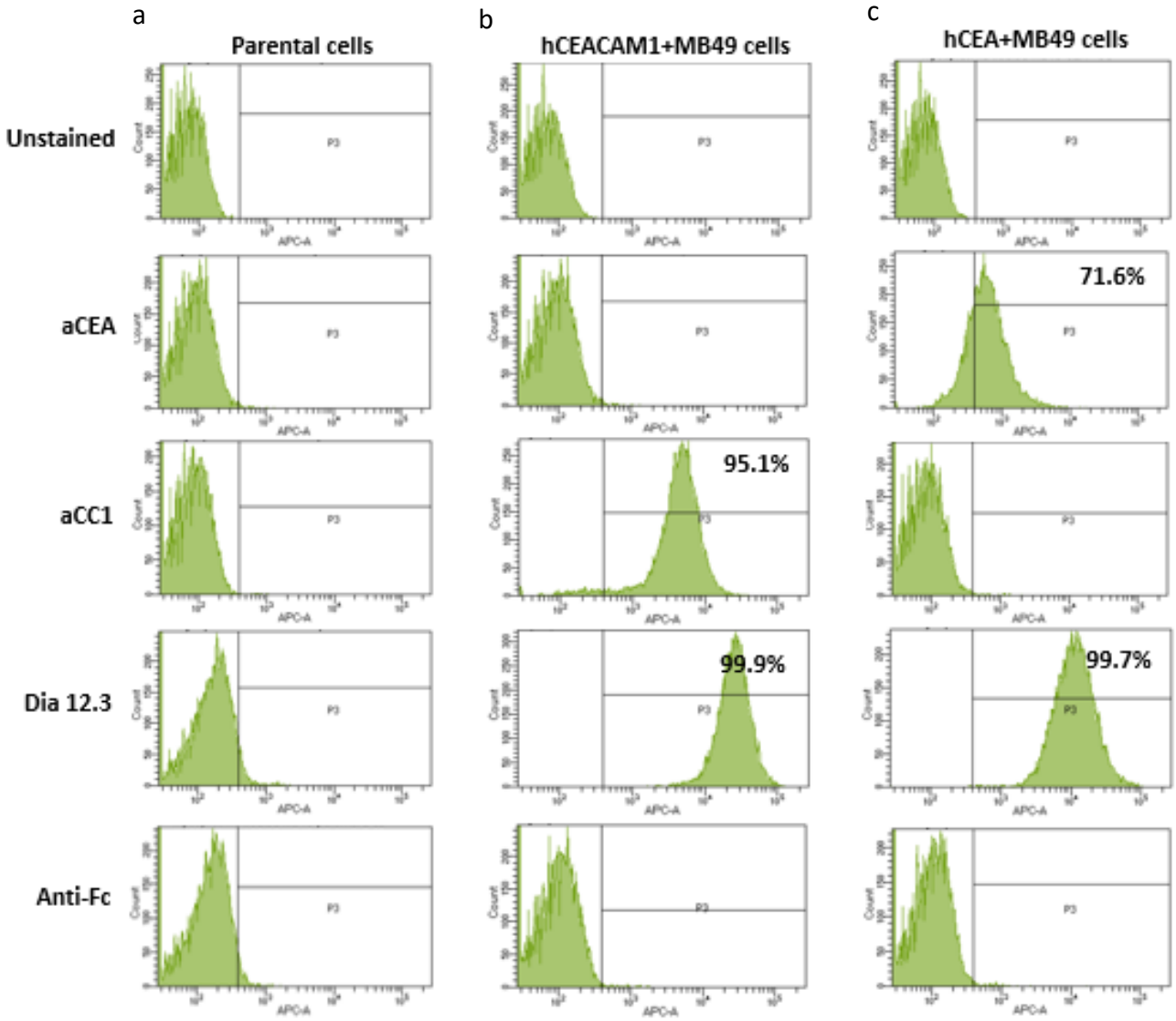

Fig. 4.32. Evaluation of hCEACAM1 and hCEA expression on parental and transfected MB49 cell lines. *Parental, hCEACAM1 and hCEA-expressing murine MB46 cell lines were stained with or without 10 µg/ml of DIA 12.3 antibody, aCC1 and aCEA commercial antibodies.*

4.7.3.3 Evaluation of hCEACAM1 expression and DIA 12.3 reactivity to murine immune cells from Tg(hCEACAM1) - Tg(hCEA) and CEACAM1 KO mice

Immune cells were isolated from the spleen and the blood collected from CEACAM1 knockout (KO) mice and Tg (hCEACAM1) - Tg(hCEA) mice developed by professor Shively and his group (185). The expression levels of hCEACAM1 antigen on T cells, B cells, neutrophils and myeloid cells were determined by staining with DIA 12.3 and the commercial anti-CEACAM1 antibody as control. In parallel with the spleen and the blood-derived immune cells, expression studies were performed on the neutrophil-enriched sample obtained from the collected whole blood. Results shown in Fig. 4.33 confirmed that the immune cells from the knockout mouse do not express hCEACAM1 antigen (Fig. 4.33a, b, c). By contrast, neutrophils derived from the transgenic mouse are the immune cells expressing the highest levels of hCEACAM1 in all the analyzed samples (Fig. 4.33d, e, f). However, a differential CEACAM1 expression can be observed between neutrophils derived from the spleen, blood and neutrophil-enriched samples. In fact, more than 60% of splenic neutrophils were positive stained cells, while blood-derived and enriched neutrophils showed 25% and 35% of positivity, respectively. Considering that CEACAM1 expression is lower on resting neutrophils, these findings are in line with the observation that blood-circulating neutrophils are activated to a lesser extent than the splenic neutrophils (197). The staining also showed that DIA 12.3 antibody specifically recognized hCEACAM1 expressed on the neutrophil cell surface, but with lower affinity than the commercial antibody, despite the previously described results. Taken all together, these preliminar results suggest that the Tg(hCEACAM1) - Tg(hCEA) mice represent a valuable animal model to study the effects of the antibody treatment on the crosstalk between tumor and immune cells.

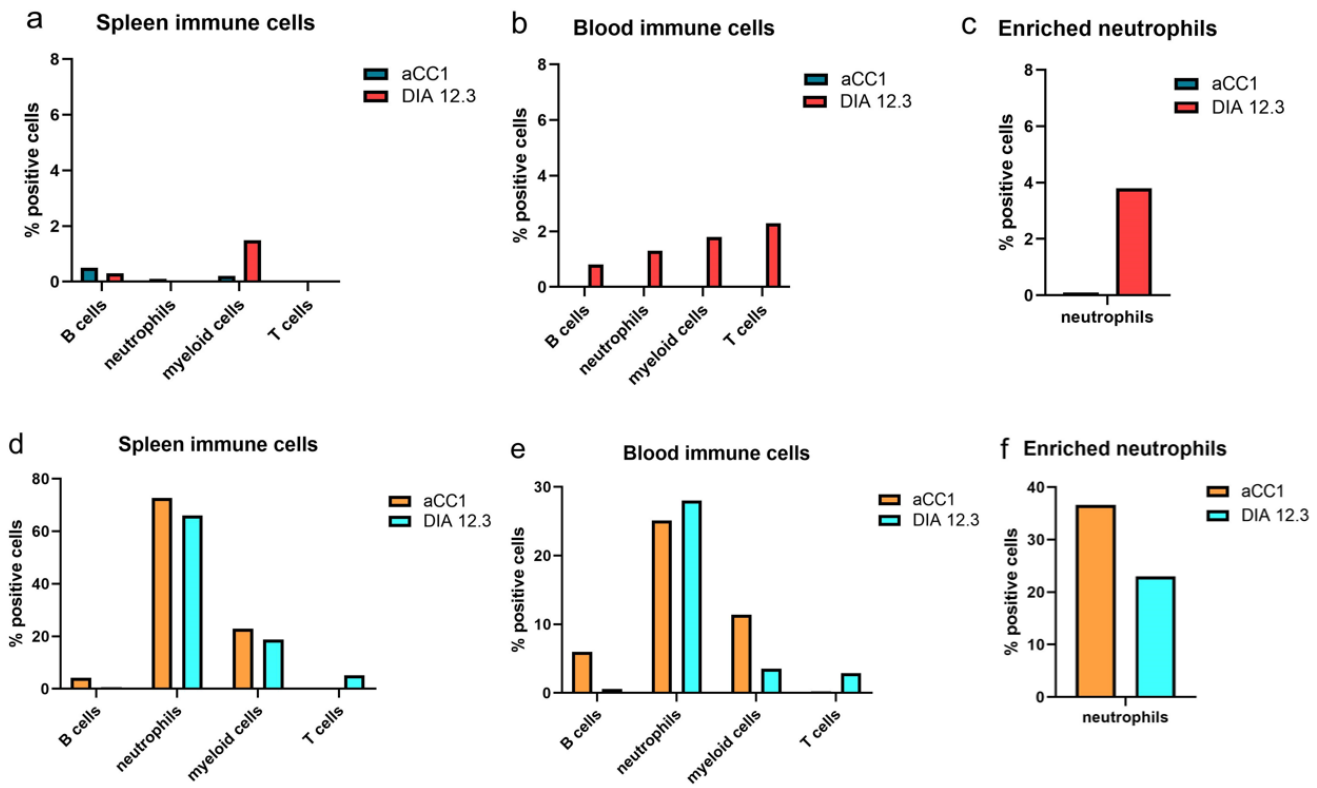

Fig. 4.33. CEACAM1 expression pattern on murine immune cells. Spleen and blood-derived immune cells and the enriched neutrophil suspension from the whole blood, all derived from hCEACAM1 KO (a) and Tg (hCEACAM1) (b), were stained with 10 µg/mL of DIA 12.3 or anti-CEACAM1 commercial antibodies. Samples were processed to assess the antibody binding pattern profiles by flow cytometry studies.

4.7.3.4 Radiolabeling and PET imaging of DOTAylated-DIA 12.3 antibody in male Tg (hCEACAM1) – Tg(hCEA) mice bearing murine bladder xenografts

Radiolabeling of DOTAylated-DIA 12.3 antibody resulted in a final product 95.23% labeled with ^{64}Cu (Fig. 4.34). Considering the better antibody tumor uptake observed in the last PET experiment with NSG mice, and given the high efficiency obtained from the antibody radiolabeling, the injected dose of DIA 12.3 antibody was increased by adding 30 µg/mouse of unlabeled DIA 12.3 to 6,4 µg/mouse of ^{64}Cu DOTAylated-DIA 12.3 antibody also in the transgenic mice. However, no significant differences in the % of the antibody ID/g were observed between the parental and the hCEA or hCEACAM1-positive tumors at 46 hours post-injection (Fig. 4.35), suggesting that the "cold" antibody might have played a blocking effect by preventing the binding of the radiolabeled antibody to hCEACAM1 and hCEA antigens. These results are in contrast with the previously discussed *in vitro* binding activity of DIA 12.3 antibody on antigen-negative and hCEACAM1 as well as hCEA-positive MB49 cells used for the injection. Furthermore, the recorded values of 6-8% of the antibody ID/g into the antigen-negative as well as positive tumors, suggest that the Enhanced Permeability Retention (EPR) effect might have been the only component that contributed to the antibody tumor uptake in this case. In fact, macromolecular compounds can be trapped into the tumor mass for a prolongued period of time due to the high permeability of the tumor vessels (198), resulting in a background % of antibody tumor uptake of approximately 5%, depending on the type of solid tumor.
Taken together, these results indicate that the dose of the radiolabeled antibody, the radiolabeled/unlabeled antibody ratio and the radioactivity of the ^{64}Cu, may represent all possible parameters to be optimized in order to achieve the best imaging conditions of DIA 12.3 antibody with the human CEACAM1 and CEA double transgenic mouse model.

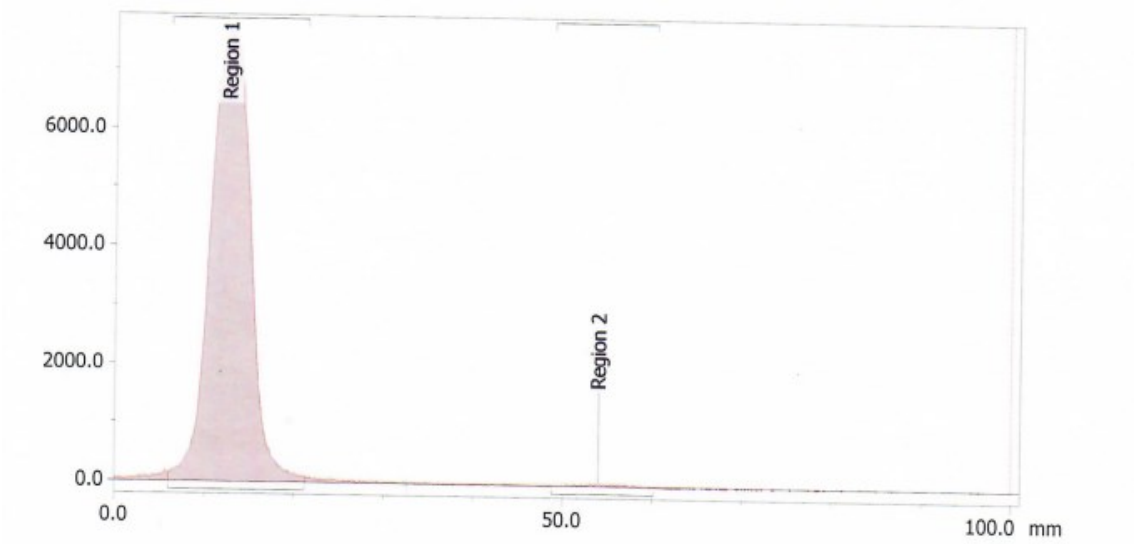

Regions: Cu-64 Detector: PMT

Name	Start (mm)	End (mm)	Retention (RF)	Area (Counts)	%ROI (%)	%Total (%)
Region 1	6.0	21.2	0.126	199400.0	99.04	95.23
Region 2	48.8	60.2	0.540	1925.0	0.96	0.92
2 Peaks				201325.0	100.00	96.15

Fig. 4.34: ITLC analysis of ^{64}Cu-DOTAylated-DIA 12.3. Chromatogram revealed the presence of two peaks, region 1 and region 2, corresponding to ^{64}Cu DOTAylated-DIA 12.3 and unlabeled DOTAylated DIA 12.3 antibodies, respectively. The table indicates the % of each peak.

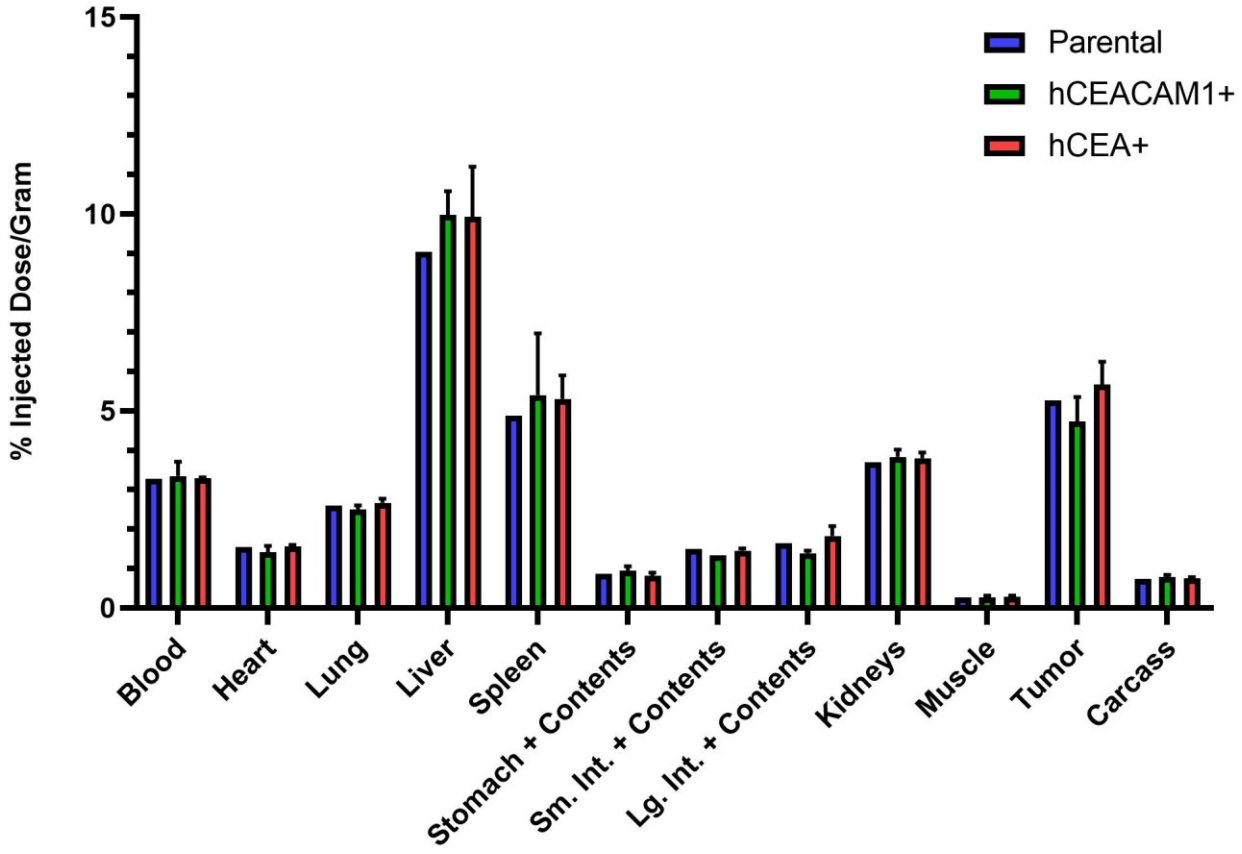

Fig. 4.35. Antibody biodistribution analysis in Tg (hCEA) - Tg (hCEACAM1) mice bearing murine bladder tumor xenografts. Organs and tumors from transgenic mice injected with parental, hCEACAM1 or hCEA-positive murine bladder tumor MB49 cells were assayed for radioactivity 46 hours after the via tail vein injection of 6,4 µg/mouse of ^{64}Cu-DOTAylated-DIA 12.3 antibody + 30 µg/mouse of unlabeled DIA 12.3 antibody. Bars represent the mean +/- S.D. of the %ID/g in various organs and tumors from mice injected with each cell line (n=2 mice for hCEA or hCEACAM1 cell lines and n=1 mouse for the parental)

5. CONCLUSION AND FUTURE PERSPECTIVES

Cancer Immunotherapy is a promising therapeutic approach that has revolutionized cancer treatment and improved the patient's quality of life in the last decades. Differently from the traditional cancer treatments, Immunotherapy relies on tumor-targeting immune cells which can reach distant area from the primary tumor site, allowing the long term control of cancer with reduced side effects (131).

Monoclonal antibody (mAb)-based cancer therapy represents the most successfully Immunotherapy approach for an increasing number of hematologic as well as solid tumors in the last decades. Indeed, mAbs have become one of the largest classes of approved pharmaceuticals for cancer treatment (142). High antibody affinity and specificity against the tumor-specific antigens (TSAa) and tumor-associated antigens (TAAs) are the main reasons at the core of the success of monoclonal antibodies as cancer therapeutics. Besides the antibody capability to spare healthy tissues, antibody engineering that relies on the structural and functional flexibility makes antibodies suitable therapeutic agents with broad therapeutic uses in cancer (199).

CEACAM1, a unique member of the CEA family, is an attractive target for cancer immunotherapy because of its involvement in tumor progression and metastasis development. Overexpression of CEACAM1 was observed in the advanced stages of several solid tumors, such as melanoma, bladder cancer, thyroid cancer, pancreatic cancer and colon cancer (200). CEACAM1 overexpression in these malignancies positively correlates with tumor progression and metastasis development, highlighting its role as tumor marker (93).

In addition, CEACAM1 has been established as an emerging immune checkpoint inhibitor expressed on activated immune cells, such as T cells, NK cells and neutrophils, by mediating the downregulation of the immune responses (93).

On NK cells, CEACAM1 is a negative co-receptor which mediates inhibitory signaling independently from the MHC complexes (45). The binding between the activating receptors on NK cells and the activating ligands on tumor cells, triggers the NK-mediated cytotoxic activity, leading to cell lysis. However, following the homophilic interactions between CEACAM1 expressed by NK cells and CEACAM1 on tumor cells via N-domain, CEACAM1 on NK cell surface dimerizes and physically associates with the NKG2D activating receptor, resulting in the inhibition of NKG2D-mediated cytolysis of CEACAM1-expressing tumor cells (56).

DIATHIS1 is a fully human anti-CEACAM1 antibody developed in the scFv format in GMP setting by DIATHEVA s.r.l. in collaboration with the Istituto Superiore della Sanità (177). Immunofluorescence and flow cytometry studies revealed that DIATHIS strongly bound to CEACAM1 antigen expressed on the surface of melanoma cells (177). Furthermore, DIATHIS1 was found to enhance the NK-cell mediated cytotoxicity against melanoma cells in co-incubation experiments at different effector:target cell ratios (180).

However, despite the scFv antibody fragments show better penetration into solid tumors than intact antibodies, the lack of the Fc domain and their reduced size are responsible for several drawbacks. With respect to full size antibodies, the lower stability, higher tendency to aggregate, shorter half-life and faster renal clearance of scFv antibody fragments, may result in the therapeutic requirement of higher and continuous antibody doses to reach the desired effects (181, 182). In order to overcome the limits of scFv fragment format and to make DIATHIS1's properties more suitable for therapeutic applications, the current project was focused on the convertion and characterization of the full size anti-CEACAM1 antibody format.
In the present study, the bicistronic vectors for the expression of IgG1 or IgG4 anti-CEACAM1 antibodies were created and used to develope stable antibody-producing clones in HEK293 cells. Antibody purification by Protein A Affinity Chromatography allowed to obtain IgG1 with a higher yield than IgG4 antibody. SEC-HPLC analyses revealed that the two antibodies were high-pure monomers of 150kDa. However, the observation of incompleted forms of IgG1 and IgG4 antibodies by non-reducing SDS-PAGE analyses highlighted the need to optimize the purification protocol. For istance, the introduction of further purification steps following the Protein A affinity chromatography might increase the purity of the final purified product.

Analyses of the purified antibodies after eight months of storage at 4°C revealed the higher structural stability of IgG1 than IgG4 antibody. In fact, contrarily from IgG4, precipitated aggregates and other bands besides the ones corresponding to the heavy chain and the light chains were not observed. These findings are in line with the observations that IgG4 is less stable and more prone to aggregate than IgG1, mainly because of the differences in the length, flexibility and amino acidic sequence of the hinge region (187, 188). Furthermore, despite IgG4 contained the S228P mutation in the hinge region that is known to abolish the Fab-arm exchange, it appeared to be insufficient to stabilize the antibody and prevent its aggregation, making the IgG4 production and manufacturing difficult.

Antibody functional characterization by ELISA and flow cytometry assays revealed that despite both the subclasses had a good and linear binding activity to human CEACAM1 antigen, IgG1 showed higher immunoreactivity than IgG4 at equal tested doses. Importantly, the binding profile of IgG1 as well as IgG4 antibodies was not altered eight months after the purification, confirming the antibody stability during the storage at 4°C. Taken all together, these preliminar results demonstrated the better performances of IgG1 antibody, termed DIA 12.3 from its producing cell subclone, than IgG4, and thus it was selected as therapeutic agent for the pre-clinical studies of the current project.

Characterization of the antibody expression by the final subclone #12.3 highlighted the homogeneity of the subclone, since it was exclusively composed of antibody-producing cell subpopulations. Furthermore, the subclone showed stability in the antibody expression up to 60 days in the absence of the antibiotic for the selective pressure in the culture medium. In order to circumvent the drawbacks due to the presence of FBS in the culture medium, the subclone #12.3 was successfully adapted to the suspension growth in a serum-free chemically defined medium, enabling also to increase the final protein yield. Although cell growth and viability were not negatively affected during the adaptation process, supplementing the cell culture medium with cell boosts that contain nutrient

elements may be a valuable approach to support the manufacturing process and further increase the final product yield.

Concerning the *in vitro* antibody efficacy, DIA 12.3 showed the ability to bind to CEACAM1 antigen on metastatic melanoma cells, bladder and colon cancer cells in dose-dependent manner. However, further *in vitro* studies are needed to add to our understanding of the antibody binding properties. To this end, Immunofluorescence analysis might provide evidences of the antibody localization on tumor target cells. In addition, Immunohistochemistry studies would be required to assess the cross-reactivity of the antibody on normal samples and the specificity on a larger panel of solid tumors, including head&neck, prostate, pancreatic and non-small cell lung (NSCLC) cancers. These studies will be of considerable interest to define all the possible target tumors for which DIA 12.3 might act as effective therapeutic agent. Coinciding with this purpose, positive results were observed by LDH cytotoxic assays. In fact, NK cells exhibited higher killing activity following antibody treatment of melanoma cells, compared to the cytotoxicity observed against untreated melanoma cells. However, in order to prevent excessive cytotoxic response also due to the killing of CEACAM1-expressing immune cells in addition to tumor cells (198), an anti-CEACAM1 antibody with reduced effector functions was developed by introducing the N297A substitution in the Fc fragment of DIA 12.3 antibody. Although the binding activity to CEACAM1 remained unalterated, the mutated antibody showed reduced ability to improve NK-cell mediated killing of melanoma cells, as expected.
It was shown that TIM3 and PD-1 are heterophilic ligands that cooperate with CEACAM1 to induce T cell exhaustion and function inhibition, by heterodimeric interactions with CEACAM1 on tumor cells (40, 41). Therefore, it would be interesting to evaluate whether combinatorial treatments of tumor cells with DIA 12.3 and TIM3 or PD-1 inhibitors induce synergistic effects in cancer cell killing, with a greater success rate than the antibody monotherapy.
In addition to NK cells, this project investigated the possibility to exploit the potential of neutrophils as effector cells with tumor suppression functions. Besides being the most abundant circulating immune cells and the first line of defense against infections (59), the attention to neutrophils has increased in recent years due to their controversial but undeniable dual role in suppressing and promoting cancer (68). Among the anti-cancer cytotoxic effects, ADCC is one mechanism by which neutrophils kill cancer cells (69, 70). Differently from resting neutrophils, CEACAM1 was expressed on neutrophil cell surface upon their activation and it was recognized by DIA 12.3 and mtN297A DIA antibodies. Investigation of the spontaneous neutrophil apoptosis and the activation following antibody treatment, confirmed the safe applications of the antibody with neutrophils. In fact, no toxic effects, alteration of neutrophil activation or neutrophil-mediated NO production were observed upon treatment with DIA 12.3 antibody. Furthermore, in line with their well known short half-life, these results confirmed that *in vitro* experiments with neutrophils have to be performed within the first hours after neutrophil isolation and enrichment, and not later than 16 hours, because of the drammatic drop of cell viability. In addition, these results showed that neutrophil incubation in culture medium at 37°C for 1 or 2 hours contributed to enhance cell viability and, as consequence, neutrophil activation. Working with neutrophils implies efforts, because of their known sensitivity, inhability to proliferate and limited lifespan. Therefore, all these preliminar results are useful considerations to take into account to perform the next *in vitro* efficacy experiments, which will be

aimed to test the efficay of DIA 12.3 antibody to alter the neutrophil-mediated killing of tumor cells in a CEACAM1 antigen-restricted manner.

DIA 12.3 antibody was successfully DOTAylated for *in vivo* tumor imaging purposes, without affecting the antibody binding activity. The first PET imaging was performed on NSG mice bearing breast tumor xenografts to evaluate the tumor-targeting of the radiolabeled ^{64}Cu-DOTAylated-DIA 12.3 antibody. To optimize the protocol based on the first results, in the second PET experiment a higher doses of antibody was used, by injecting unlabeled DIA 12.3 in addition to the ^{64}Cu-DOTAylated DIA 12.3 antibody, together with the increased radioactivity of this latter. The higher tumor uptake of DIA 12.3 into the CEACAM1-positive tumor compared to the parental and the CEA-positive tumors 46 hours post-injection suggested the *in vivo* binding specificity of DIA 12.3 to CEACAM antigen.

The *in vivo* tumor targeting of the antibody was investigated also in fully immunocompetent double transgenic mice expressing hCEACAM1 and hCEA antigens from Dr. Shively's lab at the Beckman Research Institute (City of Hope, Duarte, Ca) (185). However, in contrast with the strong antibody binding activity observed *in vitro* on antigen negative and hCEACAM1- or hCEA-positive murine MB49 cells, results from *in vivo* imaging with the same cell lines revealed a similar uptake of the antibody in the parental compared to the hCEACAM1- or hCEA- expressing tumours. This discrepancy might be probably due to the blocking effect of the unlabeled antibody that competed with ^{64}Cu-DOTAylated-DIA 12.3 to bind the target antigens. Furthermore, in all the tumors the antibody uptake was not higher than the backgroung % of the ID/g that is due to the EPR effect. Therefore, optimization of the imaging protocol will be required to better use this valuable Tg(hCEACAM1) - Tg(hCEA) mouse model. In fact, it would be extremely interesting to study in the future the effects of DIA 12.3 antibody on the *in vivo* cross talk between the tumor and the immune compartment.

6. BIBLIOGRAPHY

1) R.Kammerrer, V. Zimmermann, Co-evolution of activating and inhibitory receptors within mammalian carcinoembryonic antigen family, BMC Biol. 8 (2010)

2) CEA Gene Family. In: Schwab, M. (eds) Encyclopedia of Cancer. Springer, Berlin, Heidelberg. https://doi.org/10.1007/978-3-642-16483-5_969

3) Kuespert K, Pils S, Hauck CR. CEACAMs: their role in physiology and pathophysiology. Curr Opin Cell Biol. 2006 Oct;18(5):565-71. doi: 10.1016/j.ceb.2006.08.008. Epub 2006 Aug 17. PMID: 16919437; PMCID: PMC7127089.

4) The carcinoembryonic antigen CEA family: structures, suggested functions and expression in normal and malignant tissues

5) Hauck C.R., Agerer F., Muenzner P., Schmitter T. Cellular adhesion molecules as targets for bacterial infection. Eur J Cell Biol.

6) Obrink B: CEA adhesion molecules: multifunctional proteins with signal-regulatory properties. Curr Opin Cell Biol. 1997, 9: 616-626. 10.1016/S0955-0674(97)80114-7

7) Zebhauser, R. et al. Identification of a novel group of evolutionarily conserved members within the rapidly diverging murine CEA family. Genomics 86, 566–580 (2005)

8) Prall, F. et al. CD66a (BGP), an adhesion molecule of the carcinoembryonic antigen family, is expressed in epithelium, endothelium, and myeloid cells in a wide range of normal human tissues. J. Histochem. Cytochem. 44, 35–41 (1996).

9) Walter M. KimYu-Hwa HuangAmit GandhiRichard S. Blumberg, CEACAM1 structure and function in immunity and its therapeutic implications. Seminars in Immunology 42 (2019) 101296

10) Schumann, D., Chen, C. J., Kaplan, B. & Shively, J. E. Carcinoembryonic antigen cell adhesion molecule 1 directly associates with cytoskeleton proteins actin and tropomyosin. J. Biol. Chem. 276, 47421–47433 (2001)

11) Singer, B. B., Scheffrahn, I. & Öbrink, B. The tumor growth-inhibiting cell adhesion molecule CEACAM1 (C-CAM) is differently expressed in proliferating and quiescent epithelial cells and regulates cell proliferation. Cancer Res. 60, 1236–1244 (2000).

12) Fedarovich A, Tomberg J, Nicholas RA, Davies C, Structure of the N-terminal domain of human CEACAM1: binding target of the opacity proteins during invasion of Neisseria meningitidis and N. gonorrhoeae., *Acta Crystallogr. D. Biol. Crystallogr* 62 (2006) 971–9. doi: 10.1107/S0907444906020737

13) Bentley GA, Boulot G, Karjalainen K, Mariuzza RA, Crystal structure of the beta chain of a T cell antigen receptor, *Science (80-.)* 267 (1995) 1984 LP–1987. doi: 10.1126/science.7701320.

14) Gandhi AK, Kim WM, Sun ZJ, Huang Y, Bonsor DA, Sundberg EJ, Kondo Y, Wagner G, Kuchroo VK, Petsko G, Blumberg RS, High resolution X-ray and NMR structural study of human T-cell immunoglobulin and mucin domain containing protein-3, *Sci. Rep* (2018) 1–13. doi: 10.1038/s41598-018-35754-0

15) Lin DY-W, Tanaka Y, Iwasaki M, Gittis AG, Su H-P, Mikami B, Okazaki T, Honjo T, Minato N, Garboczi DN, The PD-1/PD-L1 complex resembles the antigen-binding Fv domains of antibodies and T cell receptors, *Proc. Natl. Acad. Sci. U. S. A* 105 (2008) 3011–3016. doi: 10.1073/pnas.0712278105

16) Watt SM, Homophilic adhesion of human CEACAM1 involves N-terminal domain interactions: structural analysis of the binding site, *Blood* 98 (2001) 1469–1479. doi: 10.1182/blood.V98.5.1469
17) Markel G, Gruda R, Achdout H, Katz G, Blumberg RS, Kammerer R, *The Critical Role of Residues 43 R and 44 Q of Carcinoembryonic Antigen Cell Adhesion Molecules-1 in the Protection from Killing by Human NK Cells*, (2019). doi: 10.4049/jimmunol.173.6.3732.
18) Hunter, I., Sawa, H., Edlund, M. & Öbrink, B. Evidence for regulated dimerization of cell-cell adhesion molecule (C-CAM) in epithelial cells. Biochem. J. 320, 847–853 (1996)
19) Öbrink, B. et al. Computational analysis of isoform specific signal regulation by CEACAM1 — a cell adhesion molecule expressed in PC12 cells. Ann. N Y Acad. Sci. 971, 597–607 (2002).
20) Gray-Owen, S., Blumberg, R. CEACAM1: contact-dependent control of immunity. *Nat Rev Immunol* 6, 433–446 (2006). https://doi.org/10.1038/nri1864
21) Öbrink, B. CEA adhesion molecules: multifunctional proteins with signal-regulatory properties. Curr. Opin. Cell Biol. 9, 616–626 (1997).
22) Hunter, I., Sawa, H., Edlund, M. & Öbrink, B. Evidence for regulated dimerization of cell-cell adhesion molecule (C-CAM) in epithelial cells. Biochem. J. 320, 847–853 (1996).
23) Watt, S. M. et al. Homophilic adhesion of human CEACAM1 involves N-terminal domain interactions: structural analysis of the binding site. Blood 98, 1469–1479 (2001).
24) Sundberg, U., Beauchemin, N. & Öbrink, B. The cytoplasmic domain of CEACAM1-L controls its lateral localization and the organization of desmosomes in polarized epithelial cells. J. Cell Sci. 117, 1091–1104 (2004).
25) Bonsor DA, Günther S, Beadenkopf R, Beckett D, Sundberg EJ, Diverse oligomeric states of CEACAM IgV domains, 112 (2015) 13561–13566. doi: 10.1073/pnas.1509511112
26) Markel G, Gruda R, Achdout H, Katz G, Blumberg RS, Kammerer R, The Critical Role of Residues 43 R and 44 Q of Carcinoembryonic Antigen Cell Adhesion Molecules-1 in the Protection from Killing by Human NK Cells, (2019). doi: 10.4049/jimmunol.173.6.3732
27) Dankner M, Gray-Owen SD, Huang YH, Blumberg RS, Beauchemin N. CEACAM1 as a multi-purpose target for cancer immunotherapy. Oncoimmunology. 2017 May 16;6(7):e1328336. doi: 10.1080/2162402X.2017.1328336. PMID: 28811966; PMCID: PMC5543821.
28) 23Gray-Owen SD, Blumberg RS. CEACAM1: contact-dependent control of immunity. *Nat Rev Immunol*. 2006;6(6):433-446
29) Khairnar, V. et al. CEACAM1 induces B-cell survival and is essential for protective antiviral antibody production. Nat. Commun. 6:6217 doi: 10.1038/ncomms7217 (2015).
30) Pan H, Shively JE. Carcinoembryonic antigen-related cell adhesion molecule-1 regulates granulopoiesis by inhibition of granulocyte colony-stimulating factor receptor. Immunity. 2010 Oct 29;33(4):620-31
31) Kammerer R, Hahn S, Singer BB, Luo JS, von Kleist S. Biliary glycoprotein (CD66a), a cell adhesion molecule of the immunoglobulin superfamily, on human lymphocytes: structure, expression and involvement in T cell activation. *Eur J Immunol* 1998; 28:3664-74; PMID:9842909
32) Chen L, Chen Z, Baker K, Halvorsen EM, da Cunha AP, Flak MB, Gerber G, Huang YH, Hosomi S, Arthur JC et al.. The short isoform of the CEACAM1 receptor in intestinal T cells regulates mucosal immunity and homeostasis via Tfh cell induction. *Immunity* 2012; 37:930-46; PMID:23123061

33) Chen D, Iijima H, Nagaishi T, Nakajima A, Russell S, Raychowdhury R, Morales V, Rudd CE, Utku N, Blumberg RS. Carcinoembryonic antigen-related cellular adhesion molecule 1 isoforms alternatively inhibit and costimulate human T cell function. *J Immunol (Baltimore, Md.: 1950)* 2004; 172:3535-43; PMID:15004154; https://doi.org/ 10.4049/jimmunol.172.6.3535
34) Morales VM, Christ A, Watt SM, Kim HS, Johnson KW, Utku N, Texieira AM, Mizoguchi A, Mizoguchi E, Russell GJ et al.. Regulation of human intestinal intraepithelial lymphocyte cytolytic function by biliary glycoprotein (CD66a). *J Immunol (Baltimore, Md.: 1950)* 1999; 163:1363-70
35) Staub E, Rosenthal A, Hinzmann B. Systematic identification of immunoreceptor tyrosine-based inhibitory motifs in the human proteome. *Cell Signal* 2004; 16:435-56; PMID:14709333
36) Chen Z, Chen L, Qiao SW, Nagaishi T, Blumberg RS. Carcinoembryonic antigen-related cell adhesion molecule 1 inhibits proximal TCR signaling by targeting ZAP-70. *J Immunol (Baltimore, Md.: 1950)* 2008; 180:6085-93; PMID:18424730; https://doi.org/ 10.4049/jimmunol.180.9.6085
37) Chen Z, Chen L, Qiao S-WW, Nagaishi T, Blumberg RS, Carcinoembryonic antigen-related cell adhesion molecule 1 inhibits proximal TCR signaling by targeting ZAP-70, *J. Immunol. (Baltimore, Md 1950)* 180 (2008) 6085–6093. doi:180/9/6085 [pii].
38) Lee HS, Ostrowski MA, Gray-Owen SD. CEACAM1 dynamics during *Neisseria gonorrhoeae* suppression of CD4+ T lymphocyte activation. *J Immunol (Baltimore, Md.: 1950)* 2008; 180:6827-35; PMID:18453603; https://doi.org/ 10.4049/jimmunol.180.10.6827
39) 43. Huang YH, Zhu C, Kondo Y, Anderson AC, Gandhi A, Russell A, Dougan SK, Petersen BS, Melum E, Pertel T et al.. Corrigendum: CEACAM1 regulates TIM-3-mediated tolerance and exhaustion. *Nature* 2016; 536:359; PMID:26982724; https://doi.org/ 10.1038/nature17421
40) Anderson AC, Joller N, Kuchroo VK. Lag-3, Tim-3, and TIGIT: co-inhibitory receptors with specialized functions in immune regulation. *Immunity* 2016; 44:989-1004; PMID:27192565
41) 5. Huang YH, Zhu C, Kondo Y, Anderson AC, Gandhi A, Russell A, Dougan SK, Petersen BS, Melum E, Pertel T et al.. CEACAM1 regulates TIM-3-mediated tolerance and exhaustion. *Nature* 2015; 517:386-90; PMID:25363763; https://doi.org/ 10.1038/nature13848
42) Zhang Y, Cai P, Li L, Shi L, Chang P, Liang T, Yang Q, Liu Y, Wang L, Hu L. Co-expression of TIM-3 and CEACAM1 promotes T cell exhaustion in colorectal cancer patients. *Int Immunopharmacol* 2016; 43:210-8; PMID:28038383; https://doi.org/ 10.1016/j.intimp.2016.12.024
43) Morvan MG, Lanier LL, NK cells and cancer: You can teach innate cells new tricks, Nat. Rev. Cancer 16 (2016) 7–19. doi: 10.1038/nrc.2015.5
44) Vivier E, Raulet DH, Moretta A, Caligiuri MA, Zitvogel L, Lanier LL, Yokoyama WM, Ugolini S, Vivier E, Raulet D, Moretta A, Caligiuri M. Innate or adaptive immunity? The example of natural killer cells, *Science (80-.)* 331 (2011) 44–49. doi: 10.1126/science.1198687.Innate
45) Markel G, Lieberman N, Katz G, Arnon TI, Lotem M, Drize O, Blumberg RS, Bar-haim E, Mader R, Eisenbach L, Mandelboim O, CD66a Interactions Between Human Melanoma and NK Cells: A Novel Class I MHC-Independent Inhibitory Mechanism of Cytotoxicity, J. Immunol. (Baltimore, Md 1950) 168 (2002) 2803 LP–2810. doi: 10.4049/jimmunol.168.6.2803
46) Agaugue S., Marcenaro E., Ferranti B., Moretta L., Moretta A. Human natural killer cells exposed to IL-2, IL-12, IL-18, or IL-4 differently modulate priming of naive T cells by monocyte-derived dendritic cells. *Blood.* 2008;112:1776–1783. doi: 10.1182/blood-2008-02-135871

47) Markel G, Mussaffi H, Ling KL, Salio M, Gadola S, Steuer G, Blau H, Achdout H, De Miguel M, Gonen-Gross T, Hanna J, Arnon TI, Qimron U, Volovitz I, Eisenbach L, Blumberg RS, Porgador A, Cerundolo V, Mandelboim O, The mechanisms controlling NK cell autoreactivity in TAP2-deficient patients, Blood 103 (2004) 1770–1778. doi: 10.1182/blood-2003-06-2114
48) Markel G, Achdout H, Katz G, Ling KL, Salio M, Gruda R, Gazit R, Mizrahi S, Hanna J, Gonen-Gross T et al.. Biological function of the soluble CEACAM1 protein and implications in TAP2-deficient patients. Euro J Immunol 2004; 34:2138-48; PMID:15259011; https://doi.org/ 10.1002/eji.200425021
49) Stern N, Markel G, Arnon TI, Gruda R, Wong H, Gray-Owen SD, Mandelboim O, Carcinoembryonic Antigen (CEA) Inhibits NK Killing via Interaction with CEA-Related Cell Adhesion Molecule 1, J. Immunol 174 (2005) 6692 LP–6701. doi: 10.4049/jimmunol.174.11.6692
50) Markel G, Gruda R, Achdout H, Katz G, Blumberg RS, Kammerer R, The Critical Role of Residues 43 R and 44 Q of Carcinoembryonic Antigen Cell Adhesion Molecules-1 in the Protection from Killing by Human NK Cells, (2019). doi: 10.4049/jimmunol.173.6.3732
51) Lanier LL. Up on the tightrope: natural killer cell activation and inhibition. *Nat Immunol.* 2008;9:495–502
52) Diefenbach A, Tomasello E, Lucas M, Jamieson AM, Hsia JK, Vivier E, Raulet DH. Selective associations with signaling proteins determine stimulatory versus costimulatory activity of NKG2D. *Nat Immunol.* 2002;3:1142–1149.
53) Zompi S, Hamerman JA, Ogasawara K, Schweighoffer E, Tybulewicz VL, Di Santo JP, Lanier LL, et al. NKG2D triggers cytotoxicity in mouse NK cells lacking DAP12 or Syk family kinases. Nat Immunol. 2003;4:565–572
54) Hosomi S, Chen Z, Baker K, Chen L, Huang YH, Olszak T, Zeissig S, Wang JH, Mandelboim O, Beauchemin N, Lanier LL, Blumberg RS, CEACAM1 on activated NK cells inhibits NKG2D-mediated cytolytic function and signaling, *Eur. J. Immunol* 43 (2013) 2473–2483. doi: 10.1002/eji.201242676.
55) Helfrich I, Singer BB. Size Matters: The Functional Role of the CEACAM1 Isoform Signature and Its Impact for NK Cell-Mediated Killing in Melanoma. Cancers (Basel). 2019 Mar 13;11(3):356. doi: 10.3390/cancers11030356. PMID: 30871206; PMCID: PMC6468645
56) Chen Z, Chen L, Baker K, Olszak T, Zeissig S, Huang Y, Kuo TT, Mandelboim O, Beauchemin N, Lanier LL, Blumberg RS, CEACAM1 dampens antitumor immunity by down-regulating NKG2D ligand expression on tumor cells, *J. Exp. Med* 208 (2011) 2633–2640. doi: 10.1084/jem.20102575
57) Markel G, Seidman R, Cohen Y, et al. Dynamic expression of protective CEACAM1 on melanoma cells during specific immune attack. Immunology. 2009;126:186–200.
58) Huang Y, Zhu C, Kondo Y, et al. CEACAM1 regulates TIM-3-mediated tolerance and exhaustion. *Nature*. 2015;517:386–390.
59) Cytokine production by human neutrophils: Revisiting the “dark side of the moon”
60) Ducker TP, Skubitz KM. Subcellular localization of CD66, CD67, and NCA in human neutrophils. *J Leukoc Biol* 1992; 52:11-6; PMID:1640165
61) 78. Sarantis H, Gray-Owen SD. Defining the roles of human carcinoembryonic antigen-related cellular adhesion molecules during neutrophil responses to *Neisseria gonorrhoeae*. *Infect Immun* 2012; 80:345-58; PMID:22064717; https://doi.org/ 10.1128/IAI.05702-11

62) Antibody ligation of CEACAM1, CEACAM3, and CEACAM6, differentially enhance the cytokine release of human neutrophils in responses to Candida albicans
63) Sintsova A, Sarantis H, Islam EA, Sun CX, Amin M, Chan CH, Stanners CP, Glogauer M, Gray-Owen SD. Global analysis of neutrophil responses to *Neisseria gonorrhoeae* reveals a self-propagating inflammatory program. *PLoS Pathog* 2014; 10:e1004341; PMID:25188454; https://doi.org/ 10.1371/journal.ppat.1004341
64) Rowe HA, Griffiths NJ, Hill DJ, Virji M (2007) Co-ordinate action of bacterial adhesins and human carcinoembryonic antigen receptors in enhanced cellular invasion by capsulate serum resistant Neisseria meningitidis. Cell Microbiol 9: 154–168.
65) 80. Singer BB, Klaile E, Scheffrahn I, Muller MM, Kammerer R, Reutter W, Obrink B, Lucka L. CEACAM1 (CD66a) mediates delay of spontaneous and Fas ligand-induced apoptosis in granulocytes. *Eur J Immunol* 2005; 35:1949-59; PMID:15909305; https://doi.org/ 10.1002/eji.200425691
66) Pan H, Shively JE. Carcinoembryonic antigen-related cell adhesion molecule-1 regulates granulopoiesis by inhibition of granulocyte colony-stimulating factor receptor. *Immunity*. 2010;33(4):620-631.
67) Lu R, Pan H, Shively JE. CEACAM1 negatively regulates IL-1β production in LPS activated neutrophils by recruiting SHP-1 to a SYK-TLR4-CEACAM1 complex. PLoS Pathog. 2012;8(4):e1002597. doi: 10.1371/journal.ppat.1002597. Epub 2012 Apr 5. PMID: 22496641; PMCID: PMC3320586.
68) Xiong, S., Dong, L. & Cheng, L. Neutrophils in cancer carcinogenesis and metastasis. *J Hematol Oncol* 14, 173 (2021). https://doi.org/10.1186/s13045-021-01187-y
69) (d) Matlung HL, Babes L, Zhao XW, van Houdt M, Treffers LW, van Rees DJ, Franke K, Schornagel K, Verkuijlen P, Janssen H, et al. Neutrophils kill antibody-opsonized cancer cells by trogoptosis. Cell Rep. 2018;23(13):3946-3959.e3946.
70) Hubert P, Heitzmann A, Viel S, Nicolas A, Sastre-Garau X, Oppezzo P, Pritsch O, Osinaga E, Amigorena S. Antibody-dependent cell cytotoxicity synapses form in mice during tumor-specific antibody immunotherapy. Can Res. 2011;71(15):5134–43.
71) van Egmond M, Bakema JE. Neutrophils as effector cells for antibody based Immunotherapy of cancer. Semin Cancer Biol. 2013;23(3):190–9.
72) Zhang X, Shi H, Yuan X, Jiang P, Qian H, Xu W. Tumor-derived exosomes induce N2 polarization of neutrophils to promote gastric cancer cell migration. Mol Cancer. 2018;17(1):146.
73) Vono M, Lin A, Norrby-Teglund A, Koup RA, Liang F, Loré K. Neutrophils acquire the capacity for antigen presentation to memory CD4(+) T cells in vitro and ex vivo. Blood. 2017;129(14):1991–2001.
74) Granot Z, Henke E, Comen EA, King TA, Norton L, Benezra R. Tumor entrained neutrophils inhibit seeding in the premetastatic lung. Cancer Cell. 2011;20(3):300–14
75) Li P, Lu M, Shi J, Hua L, Gong Z, Li Q, Shultz LD, Ren G. Dual roles of neutrophils in metastatic colonization are governed by the host NK cell status. Nat Commun. 2020;11(1):4387.
76) Wculek SK, Malanchi I. Neutrophils support lung colonization of metastasis-initiating breast cancer cells. Nature. 2015;528(7582):413–7. 127.
77) Liu Y, Gu Y, Han Y, Zhang Q, Jiang Z, Zhang X, Huang B, Xu X, Zheng J, Cao X. Tumor exosomal RNAs promote lung pre-metastatic niche formation by activating alveolar epithelial TLR3 to recruit neutrophils. Cancer Cell. 2016;30(2):243–56. 128.

78) Shen M, Hu P, Donskov F, Wang G, Liu Q, and Du J. 2014 Tumor-associated neutrophils as a new prognostic factor in cancer: a systematic review and meta-analysis. PLoS One 9: e98259. [PubMed: 24906014] 3.
79) Liang W, Ferrara N. The complex role of neutrophils in tumor angiogenesis and metastasis. *Cancer Immunol Res* 2016; 4:83-91; PMID:26839309; https://doi.org/ 10.1158/2326-6066.CIR-15-0313
80) Campregher C, Luciani MG, Gasche C. Activated neutrophils induce an hMSH2-dependent G2/M checkpoint arrest and replication errors at a (CA)13-repeat in colon epithelial cells. Gut. 2008;57(6):780–7.
81) Romano A, Parrinello NL, Vetro C, Tibullo D, Giallongo C, La Cava P, Chiarenza A, Motta G, Caruso AL, Villari L, et al. The prognostic value of the myeloid-mediated immunosuppression marker Arginase-1 in classic Hodgkin lymphoma. Oncotarget. 2016;7(41):67333–46.
82) Grieshaber-Bouyer R, Radtke FA, Cunin P, Stifano G, Levescot A, Vijaykumar B, Nelson-Maney N, Blaustein RB, Monach PA, Nigrovic PA. The neutrotime transcriptional signature defines a single continuum of neutrophils across biological compartments. Nat Commun. 2021;12(1):2856.
83) Lee W, Ko SY, Mohamed MS, Kenny HA, Lengyel E, Naora H. Neutrophils facilitate ovarian cancer premetastatic niche formation in the omentum. J Exp Med. 2019;216(1):176–94.
84) Christoffersson G, Vågesjö E, Vandooren J, Lidén M, Massena S, Reinert RB, Brissova M, Powers AC, Opdenakker G, Phillipson M. VEGF-A recruits a proangiogenic MMP-9-delivering neutrophil subset that induces angiogenesis in transplanted hypoxic tissue. Blood. 2012;120(23):4653–62.
85) . Morimoto-Kamata R, Yui S. Insulin-like growth factor-1 signaling is responsible for cathepsin G-induced aggregation of breast cancer MCF-7 cells. Cancer Sci. 2017;108(8):1574–83
86) Papayannopoulos V. Neutrophil extracellular traps in immunity and disease. Nat Rev Immunol. 2018;18(2):134–47
87) Cools-Lartigue J, Spicer J, McDonald B, Gowing S, Chow S, Giannias B, Bourdeau F, Kubes P, Ferri L. Neutrophil extracellular traps sequester circulating tumor cells and promote metastasis. J Clin Investig. 2013;123(8):3446–58.
88) Cools-Lartigue J, Spicer J, McDonald B, Gowing S, Chow S, Giannias B, Bourdeau F, Kubes P, Ferri L. Neutrophil extracellular traps sequester circulating tumor cells and promote metastasis. J Clin Investig. 2013;123(8):3446–58.
89) Szczerba BM, Castro-Giner F, Vetter M, Krol I, Gkountela S, Landin J, Scheidmann MC, Donato C, Scherrer R, Singer J, et al. Neutrophils escort circulating tumour cells to enable cell cycle progression. Nature. 2019;566(7745):553–7
90) . McDowell SAC, Luo RBE, Arabzadeh A, Doré S, Bennett NC, Breton V, Karimi E, Rezanejad M, Yang RR, Lach KD, et al. Neutrophil oxidative stress mediates obesity-associated vascular dysfunction and metastatic transmigration. Nat Cancer. 2021;2(5):545–62.
91) Saini M, Szczerba BM, Aceto N. Circulating tumor cell-neutrophil tango along the metastatic process. Can Res. 2019;79(24):6067–73.
92) Neutrophil Extracellular Trap–Associated CEACAM1 as a Putative Therapeutic Target to Prevent Metastatic Progression of Colon Carcinoma
93) Dankner M, Gray-Owen SD, Huang YH, Blumberg RS, Beauchemin N. CEACAM1 as a multi-purpose target for cancer immunotherapy. Oncoimmunology. 2017 May 16;6(7):e1328336. doi: 10.1080/2162402X.2017.1328336. PMID: 28811966; PMCID: PMC5543821.

94) Thies A, Moll I, Berger J, Wagener C, Brummer J, Schulze HJ, Brunner G, Schumacher U. CEACAM1 expression in cutaneous malignant melanoma predicts the development of metastatic disease. *J Clin Oncol* 2002; 20:2530-6;
95) Tilki D, Singer BB, Shariat SF, Behrend A, Fernando M, Irmak S, Buchner A, Hooper AT, Stief CG, Reich O, Ergün S. CEACAM1: a novel urinary marker for bladder cancer detection. Eur Urol. 2010 Apr;57(4):648-54. doi: 10.1016/j.eururo.2009.05.040. Epub 2009 May 28. PMID: 19487071
96) Simeone DM, Ji B, Banerjee M, Arumugam T, Li D, Anderson MA, Bamberger AM, Greenson J, Brand RE, Ramachandran V, Logsdon CD. CEACAM1, a novel serum biomarker for pancreatic cancer. Pancreas. 2007 May;34(4):436-43. doi: 10.1097/MPA.0b013e3180333ae3. PMID: 17446843.
97) Hollandsworth HM, Amirfakhri S, Filemoni F, Schmitt V, Wennemuth G, Schmidt A, Hoffman RM, Singer BB, Bouvet M. Anti-carcinoembryonic antigen-related cell adhesion molecule antibody for fluorescence visualization of primary colon cancer and metastases in patient-derived orthotopic xenograft mouse models. Oncotarget. 2020 Jan 28;11(4):429-439. doi: 10.18632/oncotarget.27446. PMID: 32064046; PMCID: PMC6996915.
98) Sienel W, Dango S, Woelfle U, Morresi-Hauf A, Wagener C, Brümmer J, Mutschler W, Passlick B, Pantel K. Elevated expression of carcinoembryonic antigen-related cell adhesion molecule 1 promotes progression of non-small cell lung cancer. Clin Cancer Res. 2003 Jun;9(6):2260-6. PMID: 12796394.
99) Chen Z., Chen L., Baker K., et al. CEACAM1 dampens antitumor immunity by down-regulating NKG2D ligand expression on tumor cells. Journal of Experimental Medicine. 2011;208(13):2633–2640. doi: 10.1084/jem.20102575.
100) Ebrahimnejad A., Streichert T., Nollau P., et al. CEACAM1 enhances invasion and migration of melanocytic and melanoma cells. The American Journal of Pathology.
101) Egawa K., Honda Y., Kuroki M., Ono T. The carcinoembryonic antigen (CEA) family (CD66) expressed in melanocytic naevi is not expressed in blue naevuscell naevi in dendritic type. Journal of Cutaneous Pathology.
102) Gambichler T., Grothe S., Rotterdam S., Altmeyer P., Kreuter A. Protein expression of carcinoembryonic antigen cell adhesion molecules in benign and malignant melanocytic skin lesions. American Journal of Clinical Pathology.
103) Ortenberg R., Galore-Haskel G., Greenberg I., et al. CEACAM1 promotes melanoma cell growth through Sox-2. Neoplasia.
104) Thies A, Moll I, Berger J, Wagener C, Brummer J, Schulze HJ, Brunner G, Schumacher U. CEACAM1 expression in cutaneous malignant melanoma predicts the development of metastatic disease. J Clin Oncol 2002; 20:2530-6; PMID:12011132; https://doi.org/ 10.1200/JCO.2002.05.033
105) Sivan S, Suzan F, Rona O, Tamar H, Vivian B, Tamar P, Jacob S, Gal M, Michal L. Serum CEACAM1 correlates with disease progression and survival in malignant melanoma patients. Clin Dev Immunol 2012; 2012:290536; PMID:22291846; https://doi.org/ 10.1155/2012/290536
106) Markel G., Ortenberg R., Seidman R., et al. Systemic dysregulation of CEACAM1 in melanoma patients. Cancer Immunology, Immunotherapy. 2010;59(2):215–230. doi: 10.1007/s00262-009-0740-5.
107) Ullrich N, Heinemann A, Nilewski E, Scheffrahn I, Klode J, Scherag A, Schadendorf D, Singer BB, Helfrich I. CEACAM1-3S drives melanoma cells into NK cell-mediated cytolysis and enhances patient

survival. Cancer Res 2015; 75:1897-907; PMID:25744717; https://doi.org/ 10.1158/0008-5472.CAN-14-1752
108) Markel G., Seidman R., Stern N., et al. Inhibition of human tumor-infiltrating lymphocyte effector functions by the homophilic carcinoembryonic cell adhesion molecule 1 interactions. The Journal of Immunology. 2006;177(9):6062–6071. doi: 10.4049/jimmunol.177.9.6062
109) Ortenberg R, Sapir Y, Raz L, Hershkovitz L, Ben Arav A, Sapoznik S, Barshack I, Avivi C, Berkun Y, Besser MJ, Ben-Moshe T, Schachter J, Markel G. Novel immunotherapy for malignant melanoma with a monoclonal antibody that blocks CEACAM1 homophilic interactions. Mol Cancer Ther. 2012 Jun;11(6):1300-10. doi: 10.1158/1535-7163.MCT-11-0526. Epub 2012 Mar 30. PMID: 22466331.
110) Gold P, Freedman SO. Specific carcinoembryonic antigens of the human digestive system. J Exp Med 1965; 122:467-81; PMID:4953873; https://doi.org/ 10.1084/jem.122.3.467
111) Neumaier M, Paululat S, Chan A, Matthaes P, Wagener C. Biliary glycoprotein, a potential human cell adhesion molecule, is down-regulated in colorectal carcinomas. Proc Natl Acad Sci U S A 1993; 90:10744-8; PMID:7504281; https://doi.org/ 10.1073/pnas.90.22.10744
112) Zhang L., Zhou W., Velculescu V. E., et al. Gene expression profiles in normal and cancer cells.
113) Kang W.-Y., Chen W.-T., Wu M.-T., Chai C.-Y. The expression of CD66a and possible roles in colorectal adenoma and adenocarcinoma. International Journal of Colorectal Disease.
114) Yeatman TJ, Mao W, Karl RC. Biliary glycoprotein is overexpressed in human colon cancer cells with high metastatic potential
115) Arabzadeh A, Dupaul-Chicoine J, Breton V, Haftchenary S, Yumeen S, Turbide C, Saleh M, McGregor K, Greenwood CM, Akavia UD et al.. Carcinoembryonic Antigen Cell Adhesion Molecule 1 long isoform modulates malignancy of poorly differentiated colon cancer cells. Gut 2016; 65:821-9
116) Huang YH, Zhu C, Kondo Y, Anderson AC, Gandhi A, Russell A, Dougan SK, Petersen BS, Melum E, Pertel T et al. CEACAM1 regulates TIM-3-mediated tolerance and exhaustion. Nature 2015; 517:386-90
117) Zhang Y, Cai P, Li L, Shi L, Chang P, Liang T, Yang Q, Liu Y, Wang L, Hu L. Co-expression of TIM-3 and CEACAM1 promotes T cell exhaustion in colorectal cancer patients. Int Immunopharmacol 2016; 43:210-8
118) A Novel Anti-CEACAM5 Monoclonal Antibody, CC4, Suppresses Colorectal Tumor Growth and Enhances NK Cells-MediatedTumorImmunityZheng C, Feng J, Lu D, Wang P, Xing S, et al. (2011) A Novel Anti-CEACAM5 Monoclonal Antibody, CC4, Suppresses Colorectal Tumor Growth and Enhances NK Cells-Mediated Tumor Immunity. PLOS ONE 6(6): e21146. https://doi.org/10.1371/journal.pone.0021146
119) Jin Liu, Guohu Di, Chu-Tse Wu, Xianwen Hu, Haifeng Duan, Development and evaluation of a novel anti-colorectal cancer monoclonal antibody, WL5, Biochemical and Biophysical Research Communications, Volume 432, Issue 2, 2013
120) Oliveira-Ferrer L, Tilki D, Ziegeler G, Hauschild J, Loges S, Irmak S, Kilic E, Huland H, Friedrich M, Ergun S. Dual role of carcinoembryonic antigen-related cell adhesion molecule 1 in angiogenesis and invasion of human urinary bladder cancer. Cancer Res 2004
121) Tilki D., Irmak S., Oliveira-Ferrer L., et al. CEA-related cell adhesion molecule-1 is involved in angiogenic switch in prostate cancer. Oncogene.

122) Ergün S., Kilic N., Ziegeler G., et al. CEA-related cell adhesion molecule 1: a potent angiogenic factor and a major effector of vascular endothelial growth factor. Molecular Cell.
123) Tilki D, Singer BB, Shariat SF, Behrend A, Fernando M, Irmak S, Buchner A, Hooper AT, Stief CG, Reich O et al.. CEACAM1: a novel urinary marker for bladder cancer detection. Euro Urol 2010
124) Oliveira-Ferrer L., Tilki D., Ziegeler G., et al. Dual role of carcinoembryonic antigen-related cell adhesion molecule 1 in angiogenesis and invasion of human urinary bladder cancer.
125) Kunath T., Ordoñez-Garcia C., Turbide C., Beauchemin N. Inhibition of colonic tumor cell growth by biliary glycoprotein. Oncogene.
126) Ergün S., Kilic N., Ziegeler G., et al. CEA-related cell adhesion molecule 1: a potent angiogenic factor and a major effector of vascular endothelial growth factor. Molecular Cell.
127) P. Sharma, S. Hu-Lieskovan, J.A. Wargo, A. Ribas, Primary, Adaptive, and Acquired Resistance to Cancer Immunotherapy, Cell 168 (4) (2017) 707–723.
128) Balachandran VP, Beatty GL and Dougan SK: Broadening the impact of immunotherapy to pancreatic cancer: Challenges and opportunities. Gastroenterology. 156:2056–2072. 2019
129) Waldman A.D., Fritz J.M., Lenardo M.J. A guide to cancer immunotherapy: From T cell basic science to clinical practice. *Nat. Rev. Immunol.* 2020;20:651–668. doi: 10.1038/s41577-020-0306-5.
130) Yang Y. Cancer immunotherapy: Harnessing the immune system to battle cancer. *J. Clin. Investig.* 2015;125:3335–3337. doi: 10.1172/JCI83871
131) Dimberu PM, Leonhardt RM (2011) Cancer immunotherapy takes a multi-faceted approach to kick the immune system into gear. Yale J Biol Med 84:371–380
132) Akkın, S.; Varan, G.; Bilensoy, E. A Review on Cancer Immunotherapy and Applications of Nanotechnology to Chemoimmunotherapy of Different Cancers. *Molecules* 2021, *26*, 3382. https://doi.org/10.3390/molecules26113382
133) June CH, Riddell SR, Schumacher TN. Adoptive cellular therapy: a race to the finish line. *Sci Transl Med.*
134) Schuster SJ, Bishop MR, Tam CS, et al.Tisagenlecleucel in adult relapsed or refractory diffuse large B-cell lymphoma. N Engl J Med Overseas Ed 2019;380:45–56
135) Farkona S, Diamandis EP, Blasutig IM (2016) Cancer immunotherapy: the beginning of the end of cancer? BMC Med. 14
136) Raman S.S., Hecht J.R., Chan E. Talimogene laherparepvec: Review of its mechanism of action and clinical efficacy and safety. *Immunotherapy.* 2019;11:705–723. doi: 10.2217/imt-2019-0033.
137) Melief CJ, van Hall T, Arens R, Ossendorp F, van der Burg SH. Therapeutic cancer vaccines. J Clin Invest. 2015 Sep;125(9):3401-12. doi: 10.1172/JCI80009. Epub 2015 Jul 27. PMID: 26214521; PMCID: PMC4588240.
138) Waldmann TA. Cytokines in Cancer Immunotherapy. Cold Spring Harb Perspect Biol. 2018 Dec 3;10(12):a028472. doi: 10.1101/cshperspect.a028472. PMID: 29101107; PMCID: PMC6280701.
139) Taefehshokr N, Baradaran B, Baghbanzadeh A, Taefehshokr S, Promising Approaches in Cancer Immunotherapy, Immunobiology (2019), doi: https://doi.org/10.1016/j.imbio.2019.11.010
140) Franzin R, Netti GS, Spadaccino F, Porta C, Gesualdo L, Stallone G, Castellano G, Ranieri E. The Use of Immune Checkpoint Inhibitors in Oncology and the Occurrence of AKI: Where Do We Stand? Front Immunol. 2020 Oct 8;11:574271. doi: 10.3389/fimmu.2020.574271. PMID: 33162990; PMCID: PMC7580288.

141) Antibody therapeutics approved or in regulatory review in the EU or US. The Antibody Society. Available at: https:// www.antibodysociety.org/resources/approved-antibodies/ (accessed 14 April 2020)
142) Zahavi D, Weiner L. Monoclonal Antibodies in Cancer Therapy. Antibodies (Basel). 2020 Jul 20;9(3):34. doi: 10.3390/antib9030034. PMID: 32698317; PMCID: PMC7551545
143) https://www.abcam.com/protocols/antibody-structure-and-isotypes
144) Kretschmer A, Schwanbeck R, Valerius T, Rösner T. Antibody Isotypes for Tumor Immunotherapy. Transfus Med Hemother. 2017 Sep;44(5):320-326. doi: 10.1159/000479240. Epub 2017 Sep 7. PMID: 29070977; PMCID: PMC5649311.
145) Kohler G, et al.Milstein C. Continuous cultures of fused cells secreting antibody of predefined specificity. *Nature.* 1975;256(5517):495–497. doi: 10.1038/256495a0.
146) Vukovic N, van Elsas A, Verbeek JS, Zaiss DMW. Isotype selection for antibody-based cancer therapy. Clin Exp Immunol. 2021 Mar;203(3):351-365. doi: 10.1111/cei.13545. Epub 2020 Nov 30. PMID: 33155272; PMCID: PMC7874837.
147) Adams, G, Weiner, L. Monoclonal antibody therapy of cancer. Nat Biotechnol 2005; 23: 1147–57.
148) Harris TJ, Drake CG (2013) Primer on tumor immunology and cancer immunotherapy. J Immunother Cancer
149) David Zahavi, Dalal AlDeghaither, Allison O'Connell, Louis M Weiner, Enhancing antibody-dependent cell-mediated cytotoxicity: a strategy for improving antibody-based immunotherapy, *Antibody Therapeutics*, Volume 1, Issue 1, June 2018, Pages 7–12, https://doi.org/10.1093/abt/tby002
150) Nimmerjahn, F, Ravetch, J. Fcγ receptors as regulators of immune responses. *Nat Rev Immunol*2008; 8: 34–47.
151) Wallace, P, Howell, A, Fanger, M. Role of Fcγ receptors in cancer and infectious disease. *J Leukoc Biol*1994; 55: 816–26.
152) Nimmerjahn, F. & Ravetch, J. V. Fcγ receptors: old friends and new family members. Immunity 24, 19–28 (2006).
153) Saint Basile, G, Ménasché, G, Fischer, A. Molecular mechanisms of biogenesis and exocytosis of cytotoxic granules. *Nat Rev Immunol*2010; 10: 568–79
154) an Erp EA, Luytjes W, Ferwerda G, van Kasteren PB. Fc-Mediated Antibody Effector Functions During Respiratory Syncytial Virus Infection and Disease. Front Immunol. 2019 Mar 22;10:548. doi: 10.3389/fimmu.2019.00548. PMID: 30967872; PMCID: PMC6438959.
155) Eischen, C, Leibson, P. Role for NK-cell-associated Fas ligand in cell-mediated cytotoxicity and apoptosis. *Res Immunol*1997; 148: 164–9.
156) Glassman PM, Balthasar JP (2014) Mechanistic considerations for the use of monoclonal antibodies for cancer therapy. Cancer Biol Med. https://doi.org/10.7497/j.issn.2095-3941.2014.01.002
157) Redman JM, Hill EM, AlDeghaither D, et al.Weiner LM. Mechanisms of action of therapeutic antibodies for cancer. *Mol Immunol.* 2015;67(2 Pt A):28–45. doi: 10.1016/j.molimm.2015.04.002.

158) Bennouna J, Sastre J, Arnold D, Osterlund P, Greil R, Van Cutsem E, et al.Investigators MLS. Continuation of bevacizumab after first progression in metastatic colorectal cancer (ML18147): a randomised phase 3 trial. *Lancet Oncol.* 2013;14(1):29–37. doi: 10.1016/S1470-2045(12)70477-1.
159) Ascierto PA, et al.Marincola FM. 2015: The Year of Anti-PD-1/PD-L1s Against Melanoma and Beyond. *EBioMedicine.* 2015;2(2):92–93. doi: 10.1016/j.ebiom.2015.01.011.
160) Chen L, et al.Flies DB. Molecular mechanisms of T cell co-stimulation and co-inhibition. *Nat Rev Immunol.* 2013;13(4):227–242. doi: 10.1038/nri3405.
161) Pardoll DM. The blockade of immune checkpoints in cancer immunotherapy. *Nat Rev Cancer.* 2012;12(4):252–264. doi: 10.1038/nrc3239.
162) Lohmueller J, Finn OJ. Current modalities in cancer immunotherapy: Immunomodulatory antibodies, CARs and vaccines. Pharmacol Ther. 2017 Oct;178:31-47. doi: 10.1016/j.pharmthera.2017.03.008. Epub 2017 Mar 16. PMID: 28322974; PMCID: PMC5600680.
163) Cooper MD. The early history of B cells. *Nat Rev Immunol.* 2015;15:191–197
164) Vukovic N, van Elsas A, Verbeek JS, Zaiss DMW. Isotype selection for antibody-based cancer therapy. Clin Exp Immunol. 2021 Mar;203(3):351-365. doi: 10.1111/cei.13545. Epub 2020 Nov 30. PMID: 33155272; PMCID: PMC7874837.
165) Kretschmer A, Schwanbeck R, Valerius T, Rösner T. Antibody Isotypes for Tumor Immunotherapy. Transfus Med Hemother. 2017 Sep;44(5):320-326. doi: 10.1159/000479240. Epub 2017 Sep 7. PMID: 29070977; PMCID: PMC5649311.
166) Beers SA, Glennie MJ, White AL. Influence of immunoglobulin isotype on therapeutic antibody function. *Blood.* 2016;127:1097–1101
167) Papaioannou NE, Beniata OV, Vitsos P, Tsitsilonis O, Samara P. Harnessing the immune system to improve cancer therapy. Ann Transl Med. 2016 Jul;4(14):261. doi: 10.21037/atm.2016.04.01. PMID: 27563648; PMCID: PMC4971375.
168) Yu, J., Song, Y. & Tian, W. How to select IgG subclasses in developing anti-tumor therapeutic antibodies. *J Hematol Oncol* 13, 45 (2020). https://doi.org/10.1186/s13045-020-00876-4
169) Brüggemann M, Williams GT, Bindon CI et al. Comparison of the effector functions of human immunoglobulins using a matched set of chimeric antibodies. J Exp Med 1987; 166:1351–61.
170) Vukovic N, van Elsas A, Verbeek JS, Zaiss DMW. Isotype selection for antibody-based cancer therapy. Clin Exp Immunol. 2021 Mar;203(3):351-365. doi: 10.1111/cei.13545. Epub 2020 Nov 30. PMID: 33155272; PMCID: PMC7874837.
171) Stewart R, Hammond SA, Oberst M, Wilkinson RW. The role of Fc gamma receptors in the activity of immunomodulatory antibodies for cancer. Journal for ImmunoTherapy of Cancer. 2014;2:29
172) Saunders KO. Conceptual approaches to modulating antibody effector functions and circulation half-life. Front Immunol 2019; 10:1296. https://doi.org/10.3389/fimmu.2019.01296.
173) Wurm FM. Production of recombinant protein therapeutics in cultivated mammalian cells. *Nat Biotechnol.* 2004;22:1393–1398.
174) Du X, Tang F, Liu M, Su J, Zhang Y, Wu W, et al. A reappraisal of CTLA-4 checkpoint blockade in cancer immunotherapy. Cell Res. 2018;28(4):416–32
175) Sazinsky SL, Ott RG, Silver NW, Tidor B, Ravetch JV, Wittrup KD. Aglycosylated immunoglobulin G1 variants productively engage activating Fc receptors. Proc Natl Acad Sci U S A. 2008 Dec

23;105(51):20167-72. doi: 10.1073/pnas.0809257105. Epub 2008 Dec 12. PMID: 19074274; PMCID: PMC2629253.
176) Chen W, Yuan Y, Jiang X. Antibody and antibody fragments for cancer immunotherapy. J Control Release. 2020 Dec 10;328:395-406. doi: 10.1016/j.jconrel.2020.08.021. Epub 2020 Aug 24. PMID: 32853733.
177) Moricoli D, Laguardia ME, Carbonella DC, Balducci MC, Dominici S, Fiori V, Serafini G, Flego M, Cianfriglia M, Magnani M. Isolation of a new human scFv antibody recognizing a cell surface binding site to CEACAM1. Large yield production, purification and characterization in E. coli expression system. Protein Expr Purif. 2014 Jan;93:38-45. doi: 10.1016/j.pep.2013.10.009. Epub 2013 Oct 30. PMID: 24184403.
178) F. Viti, F. Nilsson, S. Demartis, A. Huber, D. Neri, Design and use of phage display libraries for the selection of antibodies and enzymes, Methods Enzymol. 326 (2000) 480–505
179) D. Neri, H. Petrul, G. Winter, Y. Light, R. Marais, K.E. Britton, A.M. Creighton, Radioactive labeling of recombinant antibody fragments by phosphorylation using human casein kinase II and [gamma-32P] -ATP, Nat. Biotechnol. 14 (4) (1996) 485–490.
180) Dupuis ML, Fiori V, Soriani A, Ricci B, Dominici S, Moricoli D, Ascione A, Santoni A, Magnani M, Cianfriglia M. The human antibody fragment DIATHIS1 specific for CEACAM1 enhances natural killer cell cytotoxicity against melanoma cell lines in vitro. J Immunother. 2015 Nov-Dec;38(9):357-70. doi: 10.1097/CJI.0000000000000100. PMID: 26448580; PMCID: PMC4605278.
181) Nelson AL. Antibody fragments: hope and hype. MAbs. 2010 Jan-Feb;2(1):77-83. doi: 10.4161/mabs.2.1.10786. Epub 2010 Jan 27. PMID: 20093855; PMCID: PMC2828581.182) Andreas H. Laustsen, José María Gutiérrez, Cecilie Knudsen, Kristoffer H. Johansen, Erick Bermúdez-Méndez, Felipe A. Cerni, Jonas A. Jürgensen, Line Ledsgaard, Andrea Martos-Esteban, Mia Øhlenschlæger, Urska Pus, Mikael R. Andersen, Bruno Lomonte, Mikael Engmark, Manuela B. Pucca, Pros and cons of different therapeutic antibody formats for recombinant antivenom development, Toxicon, Volume 146, 2018
183) Roopenian DC, Akilesh S. FcRn: the neonatal Fc receptor comes of age. Nat Rev Immunol. 2007 Sep;7(9):715-25. doi: 10.1038/nri2155. Epub 2007 Aug 17. PMID: 17703228.
184) Chames, P., Van Regenmortel, M., Weiss, E. and Baty, D. (2009), Therapeutic antibodies: successes, limitations and hopes for the future. British Journal of Pharmacology, 157: 220-233. https://doi.org/10.1111/j.1476-5381.2009.00190.x
185) Gu A, Zhang Z, Zhang N, Tsark W, Shively JE. Generation of human CEACAM1 transgenic mice and binding of Neisseria Opa protein to their neutrophils. PLoS One. 2010 Apr 9;5(4):e10067. doi: 10.1371/journal.pone.0010067. PMID: 20404914; PMCID: PMC2852402.
186)Li L; Bading J; Yazaki PJ; Ahuja AH; Crow D; Colcher D; Williams LE; Wong JY; Raubitschek A; Shively JE, A versatile bifunctional chelate for radiolabeling humanized anti-CEA antibody with In-111 and Cu-64 at either thiol or amino groups: PET imaging of CEA-positive tumors with whole antibodies. Bioconjug Chem 2008, 19 (1), 89–96
187) Chang-Ai Xu, Andrew Z. Feng, Charan K. Ramineni, Matthew R. Wallace, Elizabeth K. Culyba, Kevin P. Guay, Kinjal Mehta, Robert Mabry, Stephen Farrand, Jin Xu & Jianwen Feng (2019): L445P mutation on heavy chain stabilizes IgG4 under acidic conditions, mAbs, DOI: 10.1080/19420862.2019.1631116

188) Lai PK, Ghag G, Yu Y, Juan V, Fayadat-Dilman L, Trout BL. Differences in human IgG1 and IgG4 S228P monoclonal antibodies viscosity and self-interactions: Experimental assessment and computational predictions of domain interactions. MAbs. 2021 Jan-Dec;13(1):1991256. doi: 10.1080/19420862.2021.1991256. PMID: 34747330; PMCID: PMC8583000.
189) Farhana A, Khan YS. Biochemistry, Lipopolysaccharide. [Updated 2022 Apr 21]. In: StatPearls [Internet]. Treasure Island (FL): StatPearls Publishing; 2022 Jan-. Available from: https://www.ncbi.nlm.nih.gov/books/NBK554414/
190)https://www.fda.gov/inspections-compliance-enforcement-and-criminal-investigations/inspection-technical-guides/bacterial-endotoxinspyrogens
191) Subbiahanadar Chelladurai K, Selvan Christyraj JD, Rajagopalan K, Yesudhason BV, Venkatachalam S, Mohan M, Chellathurai Vasantha N, Selvan Christyraj JRS. Alternative to FBS in animal cell culture - An overview and future perspective. Heliyon. 2021 Jul 28;7(8):e07686. doi: 10.1016/j.heliyon.2021.e07686. PMID: 34401573; PMCID: PMC8349753.
192) Wang, X., Mathieu, M. & Brezski, R.J. IgG Fc engineering to modulate antibody effector functions. *Protein Cell* 9, 63–73 (2018). https://doi.org/10.1007/s13238-017-0473-8
193)Singer BB, Klaile E, Scheffrahn I, Müller MM, Kammerer R, Reutter W, Obrink B, Lucka L. CEACAM1 (CD66a) mediates delay of spontaneous and Fas ligand-induced apoptosis in granulocytes. Eur J Immunol. 2005 Jun;35(6):1949-59. doi: 10.1002/eji.200425691. PMID: 15909305.
194)Hsu BE, Shen Y, Siegel PM. Neutrophils: Orchestrators of the Malignant Phenotype. Front Immunol. 2020 Aug 11;11:1778. doi: 10.3389/fimmu.2020.01778. PMID: 32849639; PMCID: PMC7433712.
195)Xiong, S., Dong, L. & Cheng, L. Neutrophils in cancer carcinogenesis and metastasis. J Hematol Oncol 14, 173 (2021). https://doi.org/10.1186/s13045-021-01187-y
196)Torsteinsdóttir I, Arvidson NG, Hällgren R, Håkansson L. Enhanced expression of integrins and CD66b on peripheral blood neutrophils and eosinophils in patients with rheumatoid arthritis, and the effect of glucocorticoids. Scand J Immunol. 1999 Oct;50(4):433-9. doi: 10.1046/j.1365-3083.1999.00602.x. PMID: 10520185.
197) Matsumoto H, Fujita Y, Onizawa M, Saito K, Sumichika Y, Yoshida S, Temmoku J, Matsuoka N, Yashiro-Furuya M, Asano T, Sato S, Suzuki E, Machida T, Watanabe H, Migita K. Increased CEACAM1 expression on peripheral blood neutrophils in patients with rheumatoid arthritis. Front Immunol. 2022 Dec 14;13:978435. doi: 10.3389/fimmu.2022.978435. PMID: 36591283; PMCID: PMC9794574.
198)Wu J. The Enhanced Permeability and Retention (EPR) Effect: The Significance of the Concept and Methods to Enhance Its Application. J Pers Med. 2021 Aug 6;11(8):771. doi: 10.3390/jpm11080771. PMID: 34442415; PMCID: PMC8402171.
199) Goydel RS, Rader C. Antibody-based cancer therapy. Oncogene. 2021 May;40(21):3655-3664. doi: 10.1038/s41388-021-01811-8. Epub 2021 May 4. PMID: 33947958; PMCID: PMC8357052.
200) (Fiori V, Magnani M, Cianfriglia M. The expression and modulation of CEACAM1 and tumor cell transformation. Ann Ist Super Sanità 2012, 48:161-71

7. ACKNOWLEDGEMENTS

I am sincerely indebted to my supervisor, Professor Magnani, for bringing his plentiful knowledge and experience to this project, making this work possible.

I am deeply gratful to Professor Shively, for his invaluable experience on the research subject. The significant completion of this project at City of Hope, one of the greatest experience of my life, could not have been possible without him.

A deep debt of gratitude is also owed to Dr. Fiori, for her continuous support, advice and patience during all these three years, to my amazing and supportive team-mates Dr. Di Mambro and Angelo, and all the Diatheva's group for the valuable help.

Moreover, I wish to extent my appreciation to Dr. Shively's lab team, and in particular to: Dr. Kujawski, Dr. Yazaki, Dr. Li, Dr. Wong, Dr. Williams, Dr. Hu and Dr. Aniogo for providing me helpful guidance in the final year of the project spent at City of Hope. Likewise, I thank the Small Animal Imaging Core of City of Hope for the precious *in vivo* Imaging studies, and the Radio Pharmacy Department at City of Hope for the crucial help in the antibody radiolabelling.

The financial supports of the University of Urbino, Regione Marche and the NIH Grant number P30CA033572 are gratefully acknowledged for making the concrete realization of this project possible.

Last but not least, I will be forever thankful to my caring and wonderful Family and to my boyfriend, who never gave up on me. To my lifelong friends and to the amazing people from all over the World I met during this incredible journey. I warmly thank you all.